Abstract

The quasiclassical theory of superconductivity is applied to diffusive nanowires connecting normal-metal and superconducting bulk materials. The diffusion equations for ferromagnetic junctions with spin-orbit coupling are generalized to include non-equilibrium phenomena. The main result of this thesis is an analytical method to calculate non-equilibrium quantities such as currents and differential electrical conductivity in systems with arbitrary spin structure at zero temperature. For more general systems that also include spin-orbit coupling, a numerical method is derived. It is shown that the rotation of the magnetization through the wire directly determines the long-range triplet density, reduces the Zeeman splitting of the zero-bias conductance peak in the differential conductivity spectrum. In systems with spin-orbit coupling it is found that both the triplet density and the position and height of peaks in the conductivity of the junction can be tuned by changing the relative orientation of the magnetization with respect to the wire.

Preface

This thesis concludes the two-year programme of the Master of Science in Physics at the Norwegian University of Science and Technology (Norges teknisk-naturvitenskapelige universitet). The project corresponds to 60 ECTS, or two semesters of credits, and has been worked on over a period of two years. To ensure that this thesis is both accessible and useful as an introductory text for future students, a large share of this time has been used on a detailed description and derivation of the theory and equations commonly used in the field of superconducting spintronics. A comparable amount of time has been used on the development of numerical methods to calculate the Green functions and the physical quantities derived from them in the systems considered. The main part of this thesis focuses on neither of these, but rather centres around the main results. The numerical material, in the form of scripts written for Matlab R2015b, is available upon request.

There are several people that have contributed to this thesis to varying degrees. First I would like to mention Jacob Linder, whom I thank for his guidance and motivation and who has been a great source of knowledge and insight during the past two years as my supervisor. I would like to thank Jabir Ali Ouassou for the many interesting discussions and his inspiring enthusiasm for our field. Alfredo Sánchez García, Ajender Rathore and Brage Bøe Svendsen were very helpful in proofreading and commenting on different parts of the thesis. Last but not least, I would like to mention Sjoerd Vogel, who with his passion for mathematics has helped me prove, derive and define different expressions more rigorously.

Tom Doekle Vethaak
Trondheim, Norway
November 7, 2016

Contents

Introduction

Since its discovery in 1911 by Heike Kamerlingh Onnes [1], superconductivity has grown from a curious abnormality to an irreplaceable part of modern technology, with applications ranging from electromagnets in MRI machines and particle accelerators to measuring instruments so precise that they are used to define SI units [2]. With ongoing research and development, it is not unreasonable to expect many more applications to follow. Quantum computing, possibly the natural successor of conventional computing, is benefiting heavily from the invention of several superconducting structures [3, 4]. In future, superconductors may even prove essential for the transition to carbon neutrality, with applications in both power generation [5] and energy transport [6]. More recently, there has been a growing effort to incorporate superconductors into the field of spintronics [7], a research area that has provided the world with indispensable technology from the first digital storage in the form of tape readers, to rapid access memory (RAM) and modern solid state drives (SSDs).

Besides its ability to transport current without energy loss, superconductors also have unique magnetic properties, as bulk superconducting materials expel magnetic fields from their interior, and currents in loops of superconducting wire can be used for perpetual magnetization. On smaller scales, comparable to the London penetration depth, the interplay of superconductors and ferromagnets allows for interesting spin behaviour. Some notable examples include triplet injection [8], superconducting spin valves [9, 10] and electric control of the superconducting critical temperature [11]. It is this fusion of ferromagnetism and superconductivity on small scales that we will concern us with in this thesis.

In superconductors, the electric current is carried by pairs of electrons with opposite momentum, and in the case of singlet pairs, also opposite spin [12]. As magnetic interactions, either exchange interaction with the magnetized material [13, 14] or external magnetic field, or orbital interaction with the magnetic vector potential [15, 16], break these pairs, superconductors and ferromagnets seem each other's natural foes. By clever engineering however, either by tuning the spin-orbit coupling [17], or by using inhomogeneous ferromagnets [18], it is

possible to create spin-triplet Cooper pairs that persist even in the presence of magnetic interactions [7, 19–22]. To better understand this interplay between magnetism and superconductivity, we focus in this thesis on non-equilibrium effects in nanowire junctions between normal metal and superconducting reservoirs, where we treat both wires with inhomogeneous magnetization and wires with intrinsic spin-orbit coupling. We describe two methods to calculate currents in superconducting junctions: one slow but generally applicable, and one very fast but with some limitations on what systems can be considered. Both methods are tested, and their results are compared to existing literature.

This thesis is divided into three main chapters. The different physical interactions and their energy contributions are described in chapter 1, where we also introduce the general equations of motion for junctions with proximity-induced superconductivity. The Usadel equation, which describes the diffusion of quasiparticles (such as Cooper pairs) in materials where impurity scattering is the leading energy term [23], is derived within the framework of the quasiclassical theory of superconductivity. The motion of the particles is treated classically by ignoring their oscillations on the scale of the Fermi wave length, and looking instead at behaviour on larger length scales by only considering interactions at the Fermi surface. The quantum nature of spin and particle-hole interactions do not permit a classical approach, which we will still treat quantum mechanically [24]. To keep th discussion in this chapter concise, the complete derivation of the central Usadel equation has been moved to appendix D. Chapter 2 covers the theory on non-equilibrium phenomena, and is supplemented with derivations in appendix E. In this chapter the main result of this thesis is presented: an analytical method to calculate non-equilibrium quantities, notably the differential conductivity, in composite structures of superconducting and ferromagnetic materials. A more general set of coupled differential equations is derived for the components of the distribution function. Chapter 3 applies the theory of the previous chapters to a range of systems. The dependence of various physical quantities on parameters such as system dimensions, boundary resistance, magnetics and spin-orbit coupling is calculated numerically. The validity of the analytical method derived in chapter 2 is demonstrated by reproducing numerical and experimental results from the literature.

Notation and units

Most notation in this text will be standard, such as the notation of vectors by boldface characters, for example $\boldsymbol{r}$ for the position and $\boldsymbol{p}$ for the momentum. Bra-kets $\langle\cdot|\cdot\rangle$ will be used for the quantum-mechanical expectation value, square braces with minus ($[\cdot,\cdot]_-$) and plus ($[\cdot,\cdot]_+$) signs will be used for commutators and anticommutators respectively, and asterisks (*) and daggers (†) for complex conjugation and conjugate transposition. Units will be related to the natural units c, $\hbar$ and k_B where possible, and to the properties of the system (such as the band gap Δ_0, system length L and coherence length ξ) otherwise, which will always be made explicit in the text.

Where this thesis is most likely to deviate from other works is the notation of different matrix structures. These are described more explicitly below.

Matrices

We will distinguish in notation between the matrix dimensions in Nambu (particle-hole) space and those in spin space. The structure in Nambu space will be indicated by marks over the characters, whereas the structure in spin space will be indicated by marks under the characters. For example, a retarded Green function describing the correlation between two spins σ and σ' would have 1×1 structure in both spin and Nambu space, and would be written as $G^R_{\sigma,\sigma'}$. Combining the four possible combinations of spins, we get a Green function with a 2×2 structure in spin space, but still a 1×1 structure in Nambu space,

$$\underline{G}^R = \begin{pmatrix} G^R_{\uparrow,\uparrow} & G^R_{\uparrow,\downarrow} \\ G^R_{\downarrow,\uparrow} & G^R_{\downarrow,\downarrow} \end{pmatrix}.$$

The 2×2 structure in Nambu space, which we see for example when we combine the regular and anomalous Green functions, is denoted by a hat over the function:

$$\underline{\hat{G}}^R = \begin{pmatrix} \underline{G}^R & \underline{F}^R \\ -\underline{\tilde{F}}^R & -\underline{\tilde{G}}^R \end{pmatrix}$$

The largest matrix structure we will consider in this thesis is 8×8, built up from a 2×2 structure in Keldysh space, crossed with a 2×2 structrure in Nambu space, and a 2×2 structure in spin space. An example of such a matrix is the following Green function combining the retarded, advanced and Keldysh Green functions in one:

$$\underline{\check{G}} = \begin{pmatrix} \underline{\hat{G}}^R & \underline{\hat{G}}^K \\ 0 & \underline{\hat{G}}^A \end{pmatrix}.$$

The Green functions themselves are discussed in appendix C.

Pauli matrices

In order to distinguish between Pauli matrices in spin space and those in Nambu space, we will use the symbol $\underline{\sigma}$ for spin space and the symbol $\hat{\tau}$ for Nambu space. Since we will only use the Pauli matrices in spin space when considering fermions with spin 1/2 (spin up and spin down), the only relevant structure in spin space is 2×2: $\underline{\sigma}$.

The Pauli matrices in 2×2 dimensions are given by

$$\hat{\tau}_0, \underline{\sigma}_0 = \begin{pmatrix} 1 & 0 \\ 0 & 1 \end{pmatrix}, \quad \hat{\tau}_1, \underline{\sigma}_1 = \begin{pmatrix} 0 & 1 \\ 1 & 0 \end{pmatrix},$$

$$\hat{\tau}_2, \underline{\sigma}_2 = \begin{pmatrix} 0 & -i \\ i & 0 \end{pmatrix}, \quad \text{and} \quad \hat{\tau}_3, \underline{\sigma}_3 = \begin{pmatrix} 1 & 0 \\ 0 & -1 \end{pmatrix}.$$

Since the Pauli matrices in Nambu spaces will generally be used in combination with those in spin space, the absence of any structure in the latter will be indicated by only a bar under the matrix. This means that the Pauli matrix in Nambu space is multiplied by the identity matrix in spin space,

$$\underline{\hat{\rho}}_i = \hat{\tau}_i \otimes \begin{pmatrix} 1 & 0 \\ 0 & 1 \end{pmatrix} = \hat{\tau}_i \otimes \underline{\sigma}_0,$$

where $i = 0, 1, 2, 3$.

Chapter 1

Equations of motion

The physics of nanowire junctions connecting normal metal and superconducting bulk materials will be described within the quasiclassical theory of superconductivity. In this framework, we describe the system with Green functions, which describe the correlations between field operators (introduced in section 1.1). The time evolution of these functions is determined by the energy contributions of the different interactions, introduced as Hamiltonians in sections 1.2 and 1.3. From the time evolution of the field operators we can derive in section 1.4 a diffusion equation for the quasiparticles formed in the superconducting state. It is this diffusion equation, and its boundary conditions provided in sections 1.5 and 1.6, that allows us to calculate different physical quantities for a variety of structures, as shown in section 1.7. The derivations of the equations presented in this chapter are provided in appendix D.

1.1 Field operators

Starting from the creation and annihilation operators for states in momentum-spin space, the field operators for the annihilation and creation of a particle are defined, respectively, as [25, 26]

$$\psi_\sigma(\boldsymbol{r},t) = \frac{1}{\sqrt{V}}\sum_{\boldsymbol{r}} e^{i\boldsymbol{k}\cdot\boldsymbol{r}}\, c_{\boldsymbol{k},\sigma}, \quad \psi^\dagger_\sigma(\boldsymbol{r},t) = \frac{1}{\sqrt{V}}\sum_{\boldsymbol{r}} e^{-i\boldsymbol{k}\cdot\boldsymbol{r}}\, c^\dagger_{\boldsymbol{k},\sigma}. \tag{1.1.1}$$

Here c, $c^\dagger$ are the annihilation and creation operators in momentum-spin space and V is a potential. The commutation relations for these field operators can be

taken directly from those for the regular annihilation and creation operators:

$$\begin{aligned}\left[c_i, c_j^\dagger\right]_\pm = \delta_{ij} \quad &\Rightarrow \quad \left[\psi_\sigma(\boldsymbol{r},t), \psi_{\sigma'}^\dagger(\boldsymbol{r}',t')\right]_\pm = \delta_{\sigma,\sigma'}\delta(\boldsymbol{r}-\boldsymbol{r}')\delta(t-t') \\ \left[c_i, c_j\right]_\pm = \left[c_i^\dagger, c_j^\dagger\right]_\pm = 0 \quad &\Rightarrow \quad \left[\psi_\sigma(\boldsymbol{r},t), \psi_{\sigma'}(\boldsymbol{r}',t')\right]_\pm = (\cdots)^\dagger = 0,\end{aligned} \tag{1.1.2}$$

where the commutators are for bosons and the anticommutators for fermions. A vector notation can be introduced where the Nambu vectors ψ and $\psi^\dagger$ are of the form [27]

$$\psi = \begin{pmatrix} \psi_\uparrow \\ \psi_\downarrow \\ \psi_\uparrow^\dagger \\ \psi_\downarrow^\dagger \end{pmatrix}, \qquad \psi^\dagger = \begin{pmatrix} \psi_\uparrow^\dagger & \psi_\downarrow^\dagger & \psi_\uparrow & \psi_\downarrow \end{pmatrix}. \tag{1.1.3}$$

This allows us to describe all field excitations — particles and holes, with both spin up and down — simultaneously with a single matrix expression, as will be shown in the next section.

1.2 The Hamiltonian of mesoscopic systems

To describe the time evolution of the Nambu vectors introduced in section 1.1, we will use the Heisenberg equations [26]

$$i\partial_t \psi_\sigma = \left[\psi_\sigma, \mathcal{H}\right]_-, \qquad i\partial_t \psi_\sigma^\dagger = \left[\psi_\sigma^\dagger, \mathcal{H}\right]_-. \tag{1.2.1}$$

The Hamiltonian $\mathcal{H}$ on the rhs of both expressions has multiple components describing different physical effects and interactions, as we will see in the next section.

1.2.1 Kinetic and electromagnetic terms

In the nearly free electron model we describe an electron as moving through a perfect lattice without impurities, including only the kinetic energy and the lattice potential $q\varphi$:[1]

$$H_0 = \frac{m\boldsymbol{v}^2}{2} + q\varphi. \tag{1.2.2}$$

[1] In this thesis we use q for the charge of the particle, which in the usual case of electrons is $-e$, with e being the elementary charge. Beware that in the literature e is sometimes used for the electron charge itself, resulting in a sign difference in some equations.

Writing this in terms of the canonical momentum $\boldsymbol{p} = -i\hbar\nabla_{\boldsymbol{r}} = m\boldsymbol{v} + q\boldsymbol{A}$, we get [17]

$$H_0 = \frac{(-i\hbar\nabla_{\boldsymbol{r}} - q\boldsymbol{A})^2}{2m} + q\varphi = -\frac{(\hbar\nabla_{\boldsymbol{r}} - iq\boldsymbol{A})^2}{2m} + q\varphi.$$

To assure gauge independence, we introduce the covariant derivative (see appendix B.1 for details)

$$\tilde{\nabla}_{\boldsymbol{r}} \equiv \nabla_{\boldsymbol{r}} + ie\boldsymbol{A} = \nabla_{\boldsymbol{r}} - iq\boldsymbol{A}, \tag{1.2.3}$$

which simplifies our Hamiltonian to

$$H_0 = -\frac{\hbar^2}{2m}\tilde{\nabla}^2_{\boldsymbol{r}} + q\varphi - \mu. \tag{1.2.4}$$

Writing this in second quantization and including the chemical potential μ for completeness, this becomes

$$\mathcal{H}_0 = \sum_\sigma \int d\boldsymbol{r}\, \psi^\dagger_\sigma(\boldsymbol{r},t) \left(-\frac{\hbar^2}{2m}\tilde{\nabla}^2_{\boldsymbol{r}} + q\varphi - \mu\right) \psi_\sigma(\boldsymbol{r},t). \tag{1.2.5}$$

1.2.2 Superconductivity

Superconductivity stems from an attractive electron-electron interaction between particles with opposite spin, which in second quantization can be written as[2] [12]

$$\mathcal{H}_{\text{BCS}} = \int d\boldsymbol{r} \int d\boldsymbol{r}'\, V_{\text{BCS}}(\boldsymbol{r},\boldsymbol{r}')\psi^\dagger_\downarrow(\boldsymbol{r},t)\psi^\dagger_\uparrow(\boldsymbol{r}',t)\psi_\uparrow(\boldsymbol{r}',t)\psi_\downarrow(\boldsymbol{r},t). \tag{1.2.6}$$

Assuming that the interaction is short-ranged, i.e. $V_{\text{BCS}} = \delta(\boldsymbol{r}-\boldsymbol{r}')\lambda(\boldsymbol{r})$, this simplifies to

$$\mathcal{H}_{\text{BCS}} = \int d\boldsymbol{r}\, \lambda(\boldsymbol{r})\psi^\dagger_\downarrow(\boldsymbol{r},t)\psi^\dagger_\uparrow(\boldsymbol{r},t)\psi_\uparrow(\boldsymbol{r},t)\psi_\downarrow(\boldsymbol{r},t). \tag{1.2.7}$$

Recognizing the spin-0 pair operators

$$A(\boldsymbol{r},t) = \psi_\downarrow(\boldsymbol{r},t)\psi_\uparrow(\boldsymbol{r},t) \qquad \text{and} \qquad A^\dagger(\boldsymbol{r},t) = \psi^\dagger_\uparrow(\boldsymbol{r},t)\psi^\dagger_\downarrow(\boldsymbol{r},t), \tag{1.2.8}$$

this can more clearly be written in terms of the number operator for electron pairs:

$$\mathcal{H}_{\text{BCS}} = \int d\boldsymbol{r}\, \lambda(\boldsymbol{r})A^\dagger(\boldsymbol{r},t)A(\boldsymbol{r},t). \tag{1.2.9}$$

[2] For a quick introduction to superconductivity, see the book *Superconductivity, Physics and Applications* by Fossheim and Sudbø [28]. The Hamiltonian we start with here can be found in section 4.1 (albeit in slightly different notation), with a similar derivation of the gap equation in the section after that. For a more complete phenomenological introduction, see *Introduction to Superconductivity* by Rose-Innes and Rhoderick [29].

The total number of electron pairs in the system will fluctuate around some value, the *mean field*. As the dynamics of the system only depend on the deviation from the average, it is useful to express the Hamiltonian in terms of this. Writing

$$\mu_A(\boldsymbol{r},t) = \big\langle A(\boldsymbol{r},t)\big\rangle \qquad \text{and} \qquad \mu_A^\dagger(\boldsymbol{r},t) = \big\langle A^\dagger(\boldsymbol{r},t)\big\rangle \tag{1.2.10}$$

for the mean field and

$$\delta_A(\boldsymbol{r},t) = A(\boldsymbol{r},t) - \mu_A(\boldsymbol{r},t), \qquad \delta_A^\dagger(\boldsymbol{r},t) = A^\dagger(\boldsymbol{r},t) - \mu_A^\dagger(\boldsymbol{r},t) \tag{1.2.11}$$

for the deviation from it, we can approximate the number operator in equation (1.2.9) as

$$A^\dagger A = (\mu_A^\dagger + \delta_A^\dagger)(\mu_A + \delta_A) = \mu_A^\dagger\mu_A + \mu_A^\dagger\delta_A + \delta_A^\dagger\mu_A + \delta_A^\dagger\delta_A. \tag{1.2.12}$$

The key to the mean field *approximation* is that we assume the deviation from the mean to be small, allowing us to neglect the last term:

$$A^\dagger A \approx \mu_A^\dagger\mu_A + \mu_A^\dagger\delta_A + \delta_A^\dagger\mu_A, \tag{1.2.13}$$

which by substitution of equation (1.2.11) becomes

$$A^\dagger A \approx \mu_A^\dagger A + A^\dagger\mu_A - \mu_A^\dagger\mu_A. \tag{1.2.14}$$

As we only care about the deviation from the mean field, we can ignore the last term here as well. Defining now the *gap function* or *order parameter*[3] $\Delta(\boldsymbol{r},t) = \lambda(\boldsymbol{r})\mu_A(\boldsymbol{r},t)$, the BCS Hamiltonian can be approximated as

$$\mathcal{H}_{\text{BCS}} = \int d\boldsymbol{r}\left(\Delta^*(\boldsymbol{r},t)A(\boldsymbol{r},t) + A^\dagger(\boldsymbol{r},t)\Delta(\boldsymbol{r},t)\right), \tag{1.2.15}$$

or in terms of ψ and $\psi^\dagger$ [20]:

$$\mathcal{H}_{\text{BCS}} = \int d\boldsymbol{r}\left(\Delta^*(\boldsymbol{r},t)\psi_\downarrow(\boldsymbol{r},t)\psi_\uparrow(\boldsymbol{r},t) + \Delta(\boldsymbol{r},t)\psi_\uparrow^\dagger(\boldsymbol{r},t)\psi_\downarrow^\dagger(\boldsymbol{r},t)\right). \tag{1.2.16}$$

1.2.3 Impurity scattering

We will distinguish between two types of impurities; those that leave the spin unaffected, and those that flip it. The first kind is a position-dependent potential $V_{\text{imp}}(\boldsymbol{r})$, the second a potential $V_{\text{sf}}(\boldsymbol{r})\,\underline{\boldsymbol{\sigma}}(\boldsymbol{r},t)\cdot\boldsymbol{s}(\boldsymbol{r},t)$ that depends on the position

[3]Throughout this thesis, we will consider the value of the band gap to be constant. To incorporate its variation under changing temperature, applied magnetic fields and spin-orbit coupling, the reader is referred to Refs. 12,21,30.

and spin of the particle as well as the spin field $\boldsymbol{s}(\boldsymbol{r},t)$ of the material. Writing both terms in second quantization, this gives us [20]

$$\mathcal{H}_{\text{imp}} = \sum_{\sigma} \int d\boldsymbol{r}\, \psi_{\sigma}^{\dagger}(\boldsymbol{r},t) V_{\text{imp}}(\boldsymbol{r}) \psi_{\sigma}(\boldsymbol{r},t) \tag{1.2.17}$$

and

$$\mathcal{H}_{\text{sf}} = \sum_{\sigma,\sigma'} \int d\boldsymbol{r}\, \psi_{\sigma}^{\dagger}(\boldsymbol{r},t) \left[\boldsymbol{\sigma}\cdot\boldsymbol{s}(\boldsymbol{r})\right]_{\sigma,\sigma'} V_{\text{sf}}(\boldsymbol{r}) \psi_{\sigma'}(\boldsymbol{r},t). \tag{1.2.18}$$

1.2.4 Ferromagnetism

The ferromagnetic term is very similar to the spin-flip scattering term, the inner product of the particle spin and the magnetic field [20]:

$$\mathcal{H}_{\mathbf{h}} = -\sum_{\sigma,\sigma'} \int d\boldsymbol{r}\, \psi_{\sigma}^{\dagger}(\boldsymbol{r},t) \left[\boldsymbol{\sigma}\cdot\boldsymbol{h}(\boldsymbol{r})\right]_{\sigma,\sigma'} \psi_{\sigma'}(\boldsymbol{r},t). \tag{1.2.19}$$

1.2.5 The full Hamiltonian

Combining all the terms derived in the previous sections, we arrive at the full Hamiltonian

$$\begin{aligned}
\mathcal{H} &= \mathcal{H}_0 + \mathcal{H}_{\text{BCS}} + \mathcal{H}_{\text{imp}} + \mathcal{H}_{\text{sf}} + \mathcal{H}_{\mathbf{h}} \\
&= \sum_{\sigma} \int d\boldsymbol{r}\, \psi_{\sigma}^{\dagger}(\boldsymbol{r},t) \left(-\frac{\hbar^2}{2m}\tilde{\nabla}_{\boldsymbol{r}}^2 + q\varphi - \mu + V_{\text{imp}}(\boldsymbol{r}) \right) \psi_{\sigma}(\boldsymbol{r},t) \\
&\quad + \sum_{\sigma,\sigma'} \int d\boldsymbol{r}\, \psi_{\sigma}^{\dagger}(\boldsymbol{r},t) \left\{ \boldsymbol{\sigma}\cdot\left[\boldsymbol{s}(\boldsymbol{r}) V_{\text{sf}}(\boldsymbol{r}) - \boldsymbol{h}(\boldsymbol{r})\right] \right\}_{\sigma,\sigma'} \psi_{\sigma'}(\boldsymbol{r},t) \\
&\quad + \int d\boldsymbol{r} \left(\Delta^*(\boldsymbol{r},t) \psi_{\downarrow}(\boldsymbol{r},t) \psi_{\uparrow}(\boldsymbol{r},t) + \Delta(\boldsymbol{r},t) \psi_{\uparrow}^{\dagger}(\boldsymbol{r},t) \psi_{\downarrow}^{\dagger}(\boldsymbol{r},t) \right).
\end{aligned} \tag{1.2.20}$$

1.3 Spin-orbit coupling

In nanowires, the finite thickness of the wire constricts the transverse movement of particles with a potential $V(x,y)$. This potential gives rise to an electric field, experienced by the moving electrons as an effective magnetic field, to which their spins couple. Hence the electron spin couples to its orbit, as the effective magnetic field's direction and magnitude are determined by the particle's motion. This

coupling is commonly referred to as Rashba coupling [31]. A similar coupling happens when the momentum is restricted not by the system's geometry, but by the crystal's structure, which is known as Dresselhaus coupling [32].

Spin-orbit coupling enters as a contribution to the vector potential, where we define [30, 33]

$$\underline{\boldsymbol{\mathcal{A}}} = q\underline{\boldsymbol{A}} + \underline{\boldsymbol{w}}\boldsymbol{\sigma}. \tag{1.3.1}$$

Here $\underline{\boldsymbol{w}}$ is a 3×3 matrix acting on the vector $\boldsymbol{\sigma}$, which we will derive for nanowires here. The covariant derivative in equation (1.2.3) can then be expanded to include this,

$$\tilde{\nabla}_{\boldsymbol{r}} \mapsto \nabla_{\boldsymbol{r}} - i\underline{\boldsymbol{\mathcal{A}}}, \tag{1.3.2}$$

leaving the notation for the Hamiltonian in equation (1.2.5) unchanged. In general, to include the vector potential, one just needs to replace [17]

$$\boxed{\nabla_{\boldsymbol{r}} \mapsto \nabla_{\boldsymbol{r}} - i\left[\hat{\underline{\boldsymbol{\mathcal{A}}}},\ \cdot\ \right]_- = \tilde{\nabla}_{\boldsymbol{r}},} \tag{1.3.3}$$

where $\hat{\underline{\boldsymbol{\mathcal{A}}}} = \operatorname{diag}(\underline{\boldsymbol{\mathcal{A}}}, -\underline{\boldsymbol{\mathcal{A}}}^{\star})$, as described in appendix B. With this we can also expand the covariant Laplacian as

$$\tilde{\nabla}^2_{\boldsymbol{r}}(\ \cdot\ ) = \nabla^2_{\boldsymbol{r}}(\ \cdot\ ) - 2i\left[\hat{\underline{\boldsymbol{\mathcal{A}}}}, \nabla_{\boldsymbol{r}}(\ \cdot\ )\right]_- - i\left[\nabla_{\boldsymbol{r}}\hat{\underline{\boldsymbol{\mathcal{A}}}},\ \cdot\ \right]_- - \left[\hat{\underline{\boldsymbol{\mathcal{A}}}}, \left[\hat{\underline{\boldsymbol{\mathcal{A}}}},\ \cdot\ \right]_-\right]_- . \tag{1.3.4}$$

1.3.1 Rashba and Dresselhaus Hamiltonians in nanowires

The spin-orbit Hamiltonian (combining Rashba and Dresselhaus coupling) can be defined in terms of the spin-orbit field [22, 30]:

$$\mathcal{H}_{\mathrm{R+D}} = -\frac{\boldsymbol{p}}{\hbar m^*}\cdot\boldsymbol{\mathcal{A}}_{\mathrm{SOC}} = -\frac{\boldsymbol{p}}{\hbar m^*}\cdot\underline{\boldsymbol{w}}\boldsymbol{\sigma}, \tag{1.3.5}$$

where m^* is the effective mass of the particle [11][4]. By assuming that the width of the wire in either direction is small compared to the Fermi wavelength, we can reduce the Rashba and Dresselhaus Hamiltonians to one dimension [35, 36]:

$$\begin{aligned} \mathcal{H}_{\mathrm{R}} &= \left(\alpha_y\underline{\sigma}_x - \alpha_x\underline{\sigma}_y\right)\frac{p_z}{\hbar m^*}, \\ \mathcal{H}_{\mathrm{D}} &= \beta\,\underline{\sigma}_z\,\frac{p_z}{\hbar m^*}. \end{aligned} \tag{1.3.6}$$

[4] By choosing this notation, the α and β introduced here have the property that $\alpha L/\hbar^2$ and $\beta L/\hbar^2$ (with L the with of the wire) are dimensionless. Experimental values for α/m^* range from $5\times 10^{-12}\,\mathrm{eV\,m}$ to $4\times 10^{-10}\,\mathrm{eV\,m}$ [31, 34], which for a system of 1–10nm correspond to $7\times 10^{-2} < \alpha L/\hbar^2 < 5\times 10^2$. In this thesis, we will use values up to $\alpha L/\hbar^2 = 5$.

Here the Rashba SO field $\underline{\boldsymbol{w}}_{\mathrm{R}}$ comes from the Lorentz force exerted on electrons by the effective magnetic field $\boldsymbol{B} \propto \boldsymbol{p} \times \boldsymbol{E}$ they perceive when moving through the confining electric fields $E_x = E_y = -\nabla V_{\mathrm{wire}}$ [34]. The Dresselhaus SO field is only nonzero in materials where the crystal structure has bulk inversion asymmetry [32], and as we will show below, only appears in nanowires that are rotationally asymmetric in the plane orthogonal to the wire.

The parameters α_k and β are defined as [36]

$$\begin{aligned} \alpha_k &= \frac{\gamma_{\mathrm{R}}}{m^*} \langle \partial_k V_k \rangle , \\ \beta &= \frac{\gamma_{\mathrm{D}}}{\hbar^2 m^*} (\langle p_x^2 \rangle - \langle p_y^2 \rangle). \end{aligned} \tag{1.3.7}$$

where γ_{R} and γ_{D} are the Rashba and Dresselhaus coupling strength parameters, and $L_{x,y}$ and $V_{x,y}$ are the dimensions of the system and their corresponding confining potentials in the x and y-direction. Writing this in terms of the SO field $\underline{\boldsymbol{w}}$,

$$\boxed{\underline{\boldsymbol{w}} = \begin{pmatrix} 0 & 0 & 0 \\ 0 & 0 & 0 \\ -\alpha_y & \alpha_x & -\beta \end{pmatrix}, \quad \underline{\boldsymbol{w}}\boldsymbol{\sigma} = (-\alpha_y \underline{\sigma}_x + \alpha_x \underline{\sigma}_y - \beta \underline{\sigma}_z)\hat{\boldsymbol{e}}_z.} \tag{1.3.8}$$

For a system that is rotationally symmetric around the wire, we can write

$$\alpha_x = \gamma_R \langle \partial_x V_x \rangle = \gamma_R \langle \partial_y V_y \rangle = \alpha_y = \alpha, \tag{1.3.9}$$

where $V_{x,y}$ are the confining potentials in the x and y directions and γ_R is the Rashba strength parameter. Another consequence of rotational symmetry in the x-y plane is that the Dresselhaus parameter becomes zero:

$$\beta \propto \langle p_x^2 \rangle - \langle p_y^2 \rangle = 0. \tag{1.3.10}$$

1.4 The Usadel equation

To avoid distracting the reader from the physics with superfluous mathematics, the full derivations of the equations mentioned in this section have been moved to appendix D. Here, in section D.1 it is shown that the time evolution of the creation and annihilation operators is described by the relations

$$i\hat{\underline{\rho}}_3 \partial_t \psi = \hat{\underline{\boldsymbol{H}}}\psi, \quad \text{and} \quad -i\partial_t \psi^\dagger \hat{\underline{\rho}}_3 = \psi^\dagger \hat{\underline{\boldsymbol{H}}}^\dagger, \tag{1.4.1}$$

where the components of the Hamiltonian in equation (1.2.20) are combined into the matrix

$$\underline{\hat{\boldsymbol{H}}} = \begin{pmatrix} H' + V_{\uparrow\uparrow} & V_{\uparrow\downarrow} & 0 & \Delta \\ V_{\downarrow\uparrow} & H' + V_{\downarrow\downarrow} & -\Delta & 0 \\ 0 & \Delta^* & H'^* + V^*_{\uparrow\uparrow} & V^*_{\downarrow\uparrow} \\ -\Delta^* & 0 & V^*_{\uparrow\downarrow} & H'^* + V^*_{\downarrow\downarrow} \end{pmatrix}. \tag{1.4.2}$$

This equation can be used to construct kinetic equations for the Green functions (see appendix C):

$$\begin{aligned} \left(i\check{\underline{\rho}}_3\partial_t - \check{\boldsymbol{H}}(\boldsymbol{r},t)\right)\check{\underline{G}} &= \delta(\boldsymbol{r}-\boldsymbol{r}')\delta(t-t'), \\ \check{\underline{G}}\left(i\check{\underline{\rho}}_3\partial_{t'} - \check{\boldsymbol{H}}(\boldsymbol{r}',t')\right)^\dagger &= \delta(\boldsymbol{r}-\boldsymbol{r}')\delta(t-t'). \end{aligned} \tag{1.4.3}$$

Appendix D.3 shows that by Fourier transforming and introducing the bullet product $\bullet$ (defined in appendix A.6), we can derive the Eilenberger equation

$$\begin{aligned} \frac{\hbar^2\boldsymbol{p}}{m}\cdot\tilde{\nabla}_{\boldsymbol{r}}\check{\underline{G}} = i\Big[\epsilon\check{\underline{\rho}}_3 - q\check{\underline{\varphi}} - \check{\underline{V}}_{\text{imp}} - \check{\underline{V}}_{\text{sf}} - \check{\underline{V}}_{\mathbf{h}} - \check{\underline{\Delta}}\,\bullet\,\check{\underline{G}}\Big]_- \\ - \frac{i\hbar^2e^2}{2m}\left[\check{\underline{\boldsymbol{A}}}^2\,\bullet\,\check{\underline{G}}\right]_- - \frac{\hbar^2 e}{4m}\left[\nabla_{\boldsymbol{r}}\cdot\check{\underline{\boldsymbol{A}}} + \check{\underline{\boldsymbol{A}}}\cdot\nabla_{\boldsymbol{r}}\,\bullet\,\check{\underline{G}}\right]_+. \end{aligned} \tag{1.4.4}$$

of which the components are defined in equations (D.3.6) and (D.3.7). In the quasiclassical approximation, the Green functions $\check{\underline{G}}$ are replaced by their quasiclassical counterparts $\check{\underline{g}}$ (see appendix D.3.1), and eq. (1.4.4) is simplified to

$$\frac{\hbar^2\boldsymbol{p}_F}{m}\cdot\tilde{\nabla}_{\boldsymbol{r}}\check{\underline{g}} = i\Big[\epsilon\check{\underline{\rho}}_3 - q\check{\underline{\varphi}} - \check{\underline{V}}_{\text{imp}} - \check{\underline{V}}_{\text{sf}} - \check{\underline{V}}_{\mathbf{h}} - \check{\underline{\Delta}}\circ\check{\underline{g}}\Big]_-. \tag{1.4.5}$$

In the diffusive or dirty limit (see details in appendix D.4), we can derive the Usadel equation, which describes the first term $\check{\underline{g}}_s$ in the spherical expansion fo $\check{\underline{g}}$:

$$\boxed{-D\tilde{\nabla}_{\boldsymbol{r}}\cdot(\check{\underline{g}}_s\circ\tilde{\nabla}_{\boldsymbol{r}}\check{\underline{g}}_s) = i\left[\epsilon\check{\underline{\rho}}_3 - q\check{\underline{\varphi}} + \frac{i}{2\tau_{\text{sf}}}\check{\underline{\rho}}_3\check{\underline{g}}_s\check{\underline{\rho}}_3 + \hat{\boldsymbol{\sigma}}\cdot\hat{\boldsymbol{h}}(\boldsymbol{r}) - \check{\underline{\Delta}}\circ\check{\underline{g}}_s\right]_-.} \tag{1.4.6}$$

This differential equation describes the diffusion of the Green functions, where the diffusion constant is defined as[5]

$$D \equiv \frac{\hbar^2 v_F^2\tau_{\text{imp}}}{3} = \frac{\hbar^2}{3}v_F\ell_e. \tag{1.4.7}$$

[5]In the dirty limit, we define the zero-temperature superconducting coherence length $\xi \equiv \sqrt{\hbar D/\Delta_0}$, where Δ_0 is the band gap at $T = 0$ [27]. This coherence length is the distance over

As described in appendix D.5, the Keldysh component of the 8×8 Green function can be written in terms of the probability distribution function $\underline{\hat{h}}$,

$$\underline{\hat{g}}_s^K = \underline{\hat{g}}_s^R \circ \underline{\hat{h}} - \underline{\hat{h}} \circ \underline{\hat{g}}_s^A. \tag{1.4.8}$$

This function can be found by solving the diffusion equation

$$\boxed{-D\tilde{\nabla}_{\boldsymbol{r}} \cdot \left(\tilde{\nabla}_{\boldsymbol{r}} \underline{\hat{h}} - \underline{\hat{g}}_s^R (\tilde{\nabla}_{\boldsymbol{r}} \underline{\hat{h}}) \underline{\hat{g}}_s^A\right) = i\underline{\hat{g}}_s^R \left[\underline{\hat{E}}_{\hat{h}}, \underline{\hat{h}}\right]_- - i\left[\underline{\hat{E}}_{\hat{h}}, \underline{\hat{h}}\right]_- \underline{\hat{g}}_s^A,} \tag{1.4.9}$$

where

$$\underline{\hat{E}}_{\hat{h}} = \epsilon \underline{\hat{\rho}}_3 + \underline{\hat{\boldsymbol{\sigma}}} \cdot \hat{\boldsymbol{h}}(\boldsymbol{r}) - \underline{\hat{\Delta}}. \tag{1.4.10}$$

To solve the Usadel equation numerically, it is useful to exploit the symmetries in the Green functions. This can be done by writing the expressions in the $\underline{\gamma}$, $\underline{\tilde{\gamma}}$ parametrization [39, 40] (see appendix F.3), where the differential equation for $\underline{\gamma}$ is found to be [30]

$$\begin{aligned}
\boxed{D\underline{\gamma}'' = {} & -2i\epsilon\,\underline{\gamma} - i\boldsymbol{h} \cdot (\underline{\boldsymbol{\sigma}}\underline{\gamma} - \underline{\gamma}\underline{\boldsymbol{\sigma}}^*) - \Delta(\underline{\sigma}_2 - \underline{\gamma}\underline{\sigma}_2\underline{\gamma}) \\
& + \frac{1}{\tau_{\mathrm{sf}}}\left[(2\underline{N} - 1)\underline{\gamma} - \underline{\gamma}(1 - 2\underline{\tilde{N}})\right] + D\Big\{ - 2\underline{\gamma}'\underline{\tilde{N}}\underline{\tilde{\gamma}}\underline{\gamma}' \\
& + 2i\left[(\underline{\boldsymbol{A}}_z + \underline{\gamma}\underline{\boldsymbol{A}}_z^*\underline{\tilde{\gamma}})\underline{N}\underline{\gamma}' + \underline{\gamma}'\underline{\tilde{N}}(\underline{\boldsymbol{A}}_z^* + \underline{\tilde{\gamma}}\underline{\boldsymbol{A}}_z\underline{\gamma})\right] \\
& + 2(\underline{\boldsymbol{A}}\underline{\gamma} + \underline{\gamma}\underline{\boldsymbol{A}}^*)\underline{\tilde{N}}(\underline{\boldsymbol{A}}^* + \underline{\tilde{\gamma}}\underline{\boldsymbol{A}}\underline{\gamma}) + \underline{\boldsymbol{A}}^2\underline{\gamma} - \underline{\gamma}(\underline{\boldsymbol{A}}^*)^2\Big\}.}
\end{aligned} \tag{1.4.11}$$

The corresponding equation for $\underline{\tilde{\gamma}}$ can be found by tilde conjugating the above, where $i, \varepsilon, \underline{\gamma}, \underline{N}, \boldsymbol{\mathcal{A}} \leftrightarrow -i, -\varepsilon, \underline{\tilde{\gamma}}, \underline{\tilde{N}}, \boldsymbol{\mathcal{A}}^*$, with the energy ε measured relative to the Fermi surface.

1.5 Boundary conditions to the Usadel equation

Boundary conditions for non-equilibrium and non-stationary phenomena can be derived by setting the first term of the Usadel equation to zero [41]. In this thesis, we ignore spin-flip scattering, which allows us to write the conditions in a

which superconducting properties vary [37]. For most materials the coherence length is known, which allows us to use the more convenient relation $D = \xi^2\Delta_0/\hbar$. The diffusion constant is directly related to the relevant energy scale of the system, the Thouless energy $E_{\mathrm{th}} = \hbar D/L^2$, where L is the length of the system [38].

much simpler form [20]. For non-ideal interfaces one should use the generalized boundary conditions [42], which are described in detail in Ref. 21.

Using the notation from Refs. [42–44], where $r = G_\beta/G_b$ is the ratio between the conductance of the material considered and the barrier, and τ is the transmission coefficient per channel, the boundary conditions to the Usadel equation are given by

$$r\underline{\check{G}}_\beta \nabla_{\boldsymbol{r}} \underline{\check{G}}_\beta = \frac{2\pi^2 \left[\underline{\check{G}}_\beta, \underline{\check{G}}_\alpha\right]_-}{4\pi^2 - \tau\left(\left[\underline{\check{G}}_\alpha, \underline{\check{G}}_\beta\right]_+ + 2\pi^2\right)}. \tag{1.5.1}$$

Here $G_B = G_0 n\tau$, where $G_0 = e^2/\pi\hbar$ is the conductance quantum, n the number of channels, and $n\tau$ is the transmission coefficient of the whole barrier for all channels combined, and α and β refer to the two sides of the interface. In the case of tunnel junctions τ will be much smaller than one, in which case eq. (1.5.1) simplifies considerably [20, 45]:

$$2r\underline{\check{G}}_\beta \nabla_{\boldsymbol{r}} \underline{\check{G}}_\beta = \left[\underline{\check{G}}_\alpha, \underline{\check{G}}_\beta\right]_- . \tag{1.5.2}$$

This expression is usually referred to as the Kuprianov-Lukichev boundary condition. To include spin-orbit coupling, we again replace the regular derivative by the covariant derivative [17, 30]:

$$\boxed{2r\underline{\check{G}}_\beta \tilde{\nabla}_{\boldsymbol{r}} \underline{\check{G}}_\beta = \left[\underline{\check{G}}_\alpha, \underline{\check{G}}_\beta\right]_- .} \tag{1.5.3}$$

In terms of the $\underline{\gamma}$, $\underline{\tilde{\gamma}}$ parametrization (see appendix F.2), this can be written as [30]

$$\boxed{\begin{aligned}
r_\alpha \nabla_{\boldsymbol{r}} \underline{\gamma}_\alpha &= (1 - \underline{\gamma}_\alpha \underline{\tilde{\gamma}}_\beta)(1 - \underline{\gamma}_\beta \underline{\tilde{\gamma}}_\beta)^{-1}(\underline{\gamma}_\beta - \underline{\gamma}_\alpha) + i\boldsymbol{\mathcal{A}}\underline{\gamma}_\alpha + i\underline{\gamma}_\alpha \boldsymbol{\mathcal{A}}^*, \\
r_\alpha \nabla_{\boldsymbol{r}} \underline{\tilde{\gamma}}_\alpha &= (1 - \underline{\tilde{\gamma}}_\alpha \underline{\gamma}_\beta)(1 - \underline{\tilde{\gamma}}_\beta \underline{\gamma}_\beta)^{-1}(\underline{\tilde{\gamma}}_\beta - \underline{\tilde{\gamma}}_\alpha) - i\boldsymbol{\mathcal{A}}^*\underline{\tilde{\gamma}}_\alpha - i\underline{\tilde{\gamma}}_\alpha \boldsymbol{\mathcal{A}}, \\
r_\beta \nabla_{\boldsymbol{r}} \underline{\gamma}_\beta &= (1 - \underline{\gamma}_\beta \underline{\tilde{\gamma}}_\alpha)(1 - \underline{\gamma}_\alpha \underline{\tilde{\gamma}}_\alpha)^{-1}(\underline{\gamma}_\beta - \underline{\gamma}_\alpha) + i\boldsymbol{\mathcal{A}}\underline{\gamma}_\beta + i\underline{\gamma}_\beta \boldsymbol{\mathcal{A}}^*, \\
r_\beta \nabla_{\boldsymbol{r}} \underline{\tilde{\gamma}}_\beta &= (1 - \underline{\tilde{\gamma}}_\beta \underline{\gamma}_\alpha)(1 - \underline{\tilde{\gamma}}_\alpha \underline{\gamma}_\alpha)^{-1}(\underline{\tilde{\gamma}}_\beta - \underline{\tilde{\gamma}}_\alpha) - i\boldsymbol{\mathcal{A}}^*\underline{\tilde{\gamma}}_\beta - i\underline{\tilde{\gamma}}_\beta \boldsymbol{\mathcal{A}}.
\end{aligned}} \tag{1.5.4}$$

Note that these are vectorial expressions, so for example the derivative $\partial_z \underline{\gamma}$ only contains the z-component $\mathcal{A}_z$ of the vector potential.

In this discussion we have assumed that the transmission is spin independent. Accounting for spin dependence of reflection and transmission would require the introduction of an extra term $ir_\phi \left[\hat{\tau}_0 \otimes \underline{\sigma}_3, \underline{\hat{g}}\right]_-$ on the rhs of equation (1.5.3), and a term $ir_\phi \left[\underline{\sigma}_3, \underline{\tilde{\gamma}}\right]_-$ to its parametrized form in equation (1.5.4), where the parameter r_ϕ (now assumed zero) describes the spin-dependent interfacial phase

shift [27]. When considering boundaries that are not tunnel junctions, it is no longer a good approximation to use the bulk solutions in the connecting material. The Usadel equation then needs to be solved self-consistently, where it is solved on both sides of a boundary, with the solutions on each side being used in the boundary conditions for the other.

1.6 Bulk solutions to the Usadel equation

The quasiclassical Green function (see appendix C.2) can by contour integration be shown to equal to [40, 46]

$$\begin{aligned}\hat{\underline{g}}^R(\varepsilon) = &\frac{|\varepsilon|\Theta(\varepsilon^2 - |\Delta|^2) - i\varepsilon\Theta(|\Delta|^2 - \varepsilon^2)}{\sqrt{|\varepsilon^2 - |\Delta|^2|}}\,\hat{\underline{\rho}}_3 \\ &- \frac{\mathrm{sign}(\varepsilon)\Theta(\varepsilon^2 - |\Delta|^2) - i\Theta(|\Delta|^2 - \varepsilon^2)}{\sqrt{|\varepsilon^2 - |\Delta|^2|}}\,\hat{\Delta}\end{aligned} \tag{1.6.1}$$

in bulk materials. We now parametrize the isotropic (subscript s) quasiclassical retarded Green function as [47][6]

$$\hat{\underline{g}}_s^R(\boldsymbol{r}, \varepsilon) = \begin{pmatrix} \cosh\theta & i\underline{\sigma}_2 \sinh\theta\, e^{i\chi} \\ i\underline{\sigma}_2 \sinh\theta\, e^{-i\chi} & -\cosh\theta \end{pmatrix}. \tag{1.6.2}$$

Noting the off-diagonal structure in spin space of the pair potential (see equation (D.1.9)), we find that

$$\cosh\theta = \frac{|\varepsilon|\Theta(\varepsilon^2 - |\Delta|^2) - i\varepsilon\Theta(|\Delta|^2 - \varepsilon^2)}{\sqrt{|\varepsilon^2 - |\Delta|^2|}} \tag{1.6.3}$$

and

$$\sinh\theta\, e^{i\chi} = -\frac{\mathrm{sign}(\varepsilon)\Theta(\varepsilon^2 - |\Delta|^2) - i\Theta(|\Delta|^2 - \varepsilon^2)}{\sqrt{|\varepsilon^2 - |\Delta|^2|}}\,\Delta. \tag{1.6.4}$$

Both $|\varepsilon| > |\Delta|$ and $|\varepsilon| < |\Delta|$ then lead to

$$\tanh\theta\, e^{i\chi} = \frac{\Delta}{\varepsilon}. \tag{1.6.5}$$

[6] This parametrization can be extended to include spin structure due to magnetization by introducing vector components,

$$\hat{\underline{g}}_s^R = \hat{\tau}_3(g_0\underline{\sigma}_0 + \boldsymbol{g}\boldsymbol{\sigma}) + \hat{\tau}_1(f_0\underline{\sigma}_0 + \boldsymbol{f}\boldsymbol{\sigma}),$$

where the vectors $\boldsymbol{g}$ and $\boldsymbol{f}$ are proportional to a "triplet vector" $\boldsymbol{M}$ [48].

As a superconducting reservoir has $\Delta = |\Delta| e^{i\phi_0}$, this gives us

$$\chi = \phi_0, \qquad \theta = \operatorname{atanh}\left(\frac{|\Delta|}{\varepsilon}\right). \tag{1.6.6}$$

Using the relations

$$\cosh(\operatorname{atanh}(x)) = \frac{1}{\sqrt{1-x^2}}, \quad \text{and} \quad \sinh(\operatorname{atanh}(x)) = \frac{x}{\sqrt{1-x^2}}, \tag{1.6.7}$$

we find for the bulk solutions [20, 40, 49]

$$\boxed{\hat{\underline{g}}_s^R = \begin{pmatrix} \dfrac{\varepsilon}{\sqrt{\varepsilon^2 - |\Delta|^2}} & i\underline{\sigma}_2 \dfrac{|\Delta|}{\sqrt{\varepsilon^2 - |\Delta|^2}} e^{i\phi_0} \\ i\underline{\sigma}_2 \dfrac{|\Delta|}{\sqrt{\varepsilon^2 - |\Delta|^2}} e^{-i\phi_0} & -\dfrac{\varepsilon}{\sqrt{\varepsilon^2 - |\Delta|/\varepsilon}} \end{pmatrix}}. \tag{1.6.8}$$

The advanced Green function is found through the relation [49]

$$\hat{\underline{g}}^A = -\hat{\underline{\rho}}_3 \left(\hat{\underline{g}}^R\right)^\dagger \hat{\underline{\rho}}_3. \tag{1.6.9}$$

1.6.1 Bulk normal metal

In a normal metal, where $\Delta = 0$, equation (1.6.8) gives

$$\hat{\underline{g}}_s^R = \begin{pmatrix} 1 & 0 \\ 0 & -1 \end{pmatrix}. \tag{1.6.10}$$

In terms of the gamma parametrization (see appendix F.2), this means

$$2N - 1 = 2(1 - \underline{\gamma}\tilde{\underline{\gamma}})^{-1} - 1 = 1 \qquad \Rightarrow \qquad \underline{\gamma}_{\mathrm{N}} = \tilde{\underline{\gamma}}_{\mathrm{N}} = 0. \tag{1.6.11}$$

1.6.2 Bulk superconductor

Combining the top left components of equations (F.1.1) and (F.2.1) we see that

$$\begin{aligned} \underline{N}(1 + \underline{\gamma}\tilde{\underline{\gamma}}) = \cosh\theta \quad &\Rightarrow \quad 1 + \underline{\gamma}\tilde{\underline{\gamma}} = (1 - \underline{\gamma}\tilde{\underline{\gamma}})\cosh\theta \\ &\Rightarrow \quad \underline{\gamma}\tilde{\underline{\gamma}}(1 + \cosh\theta) = \cosh\theta - 1 \\ &\Rightarrow \quad \underline{\gamma}\tilde{\underline{\gamma}} = \frac{\cosh\theta - 1}{\cosh\theta + 1}\,\underline{\sigma}_0, \end{aligned} \tag{1.6.12}$$

Using this for the top-right component of $\hat{\underline{g}}^R$:

$$2\underline{N}\underline{\gamma} = i\underline{\sigma}_2 \sinh\theta\, e^{i\chi} \quad \Rightarrow \quad \underline{\gamma} = i\underline{\sigma}_2 \frac{\sinh\theta\, e^{i\chi}}{\cosh\theta + 1}. \tag{1.6.13}$$

Similarly, the bottom-left gives

$$\underline{\tilde{\gamma}} = -\frac{1}{2}(\underline{1} - \underline{\tilde{\gamma}\gamma})i\underline{\sigma}_2 \sinh\theta\, e^{-i\chi} = -i\underline{\sigma}_2 \frac{\sinh\theta\, e^{-i\chi}}{\cosh\theta + 1}. \tag{1.6.14}$$

Plugging in the result from equation (1.6.6), this gives

$$\boxed{\begin{aligned} \underline{\gamma}_{\mathrm{BCS}} &= i\underline{\sigma}_2 \frac{\sinh[\operatorname{atanh}(|\Delta|/\varepsilon)]\, e^{i\phi_0}}{\cosh[\operatorname{atanh}(|\Delta|/\varepsilon)] + 1}, \\ \underline{\tilde{\gamma}}_{\mathrm{BCS}} &= -i\underline{\sigma}_2 \frac{\sinh[\operatorname{atanh}(|\Delta|/\varepsilon)]\, e^{-i\phi_0}}{\cosh[\operatorname{atanh}(|\Delta|/\varepsilon)] + 1}. \end{aligned}} \tag{1.6.15}$$

1.7 Observables

To compare the theoretical and numerical results to experiments, we calculate a few measurable physical quantities. Here we will discuss equilibrium observables: the densities of single-particle states, and singlet and triplet Cooper pairs. After having introduced non-equilibrium theory, we will also cover electric conductivity in section 2.6.

1.7.1 Density of states

In our quasiclassical description, we only look at behaviour close to the Fermi surface. Here, the density of states (DOS) for a bulk normal metal is practically constant, and a bulk superconductor creates a band gap by combining pairs of electrons and pairs of holes around the Fermi energy into singlets, that show up as single-particle peaks on the left and right of this gap, respectively (see figure 1.1).

Throughout the systems we are considering, we can calculate the single-particle DOS from [27, 53]

$$\boxed{N(\varepsilon)/N_0 = \mathbb{R}\left[\mathrm{Tr}(\underline{g}^R)\right]/2.} \tag{1.7.1}$$

For ferromagnetic systems, we will be interested in the DOS for the spin up and spin down particles independently, which we find by by multiplying with

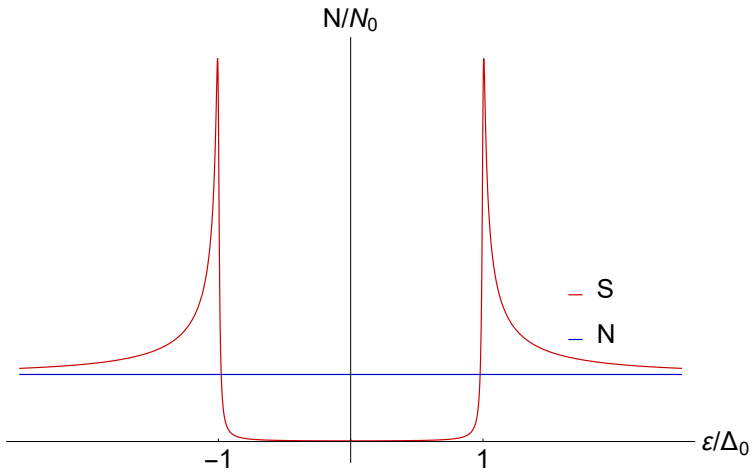

Figure 1.1: The DOS for a bulk superconductor and a normal metal. The superconducting DOS is plotted with an inelastic scattering $\eta = \Delta_0/100$. The band gap is typically on the order of 10^{-6} to 10^{-4} eV [50–52].

$(\underline{\sigma}_0 + \underline{\sigma}_3)/2$ and $(\underline{\sigma}_0 - \underline{\sigma}_3)/2$:

$$\boxed{\begin{aligned} N_\uparrow(\varepsilon)/N_0 &= \mathbb{R}\left\{\mathrm{Tr}\left[\begin{pmatrix}1 & 0\\ 0 & 0\end{pmatrix}\underline{g}^R\right]\right\}, \\ N_\downarrow(\varepsilon)/N_0 &= \mathbb{R}\left\{\mathrm{Tr}\left[\begin{pmatrix}0 & 0\\ 0 & 1\end{pmatrix}\underline{g}^R\right]\right\}. \end{aligned}} \tag{1.7.2}$$

1.7.2 Singlet and triplet parameters

By writing out the top-left component of the normalization $(\hat{\underline{g}}^R)^2 = \hat{\underline{1}}$ [54], and using the definition in equation (C.2.5), we find

$$\underline{g}^R\underline{g}^R - \underline{f}^R\underline{f}^R = \underline{1} \quad \Rightarrow \quad \underline{g} = \left(\underline{1} + \underline{f}\tilde{\underline{f}}\right)^{1/2} \approx 1 + \underline{f}\tilde{\underline{f}}/2 \tag{1.7.3}$$

The DOS in equation (1.7.1) can now be rewritten as

$$N(\varepsilon)/N_0 \approx 1 + \mathbb{R}\left[\mathrm{Tr}(\underline{f}\tilde{\underline{f}})\right]/4. \tag{1.7.4}$$

Looking more closely at the components of $\underline{f}$, we see that

$$\begin{aligned}\underline{f} &= \begin{pmatrix} f_{\uparrow\uparrow} & f_{\uparrow\downarrow} \\ f_{\downarrow\uparrow} & f_{\downarrow\downarrow} \end{pmatrix} \\ &= \begin{pmatrix} f_{\uparrow\uparrow} & (f_{\uparrow\downarrow} + f_{\downarrow\uparrow})/2 + (f_{\uparrow\downarrow} - f_{\downarrow\uparrow})/2 \\ (f_{\uparrow\downarrow} + f_{\downarrow\uparrow})/2 - (f_{\uparrow\downarrow} - f_{\downarrow\uparrow})/2 & f_{\downarrow\downarrow} \end{pmatrix} \\ &= \begin{pmatrix} f_{\uparrow\uparrow} & (f_t + f_s)/\sqrt{2} \\ (f_t - f_s)/\sqrt{2} & f_{\downarrow\downarrow} \end{pmatrix},\end{aligned} \tag{1.7.5}$$

introducing the singlet and triplet anomalous Green functions f_s and f_t. We can now write

$$\boxed{N(\varepsilon)/N_0 \approx 1 - \frac{\mathbb{R}\left(f_s \tilde{f}_s\right)}{4} + \frac{\mathbb{R}\left(f_{\uparrow\uparrow}\tilde{f}_{\uparrow\uparrow} + f_{\downarrow\downarrow}\tilde{f}_{\downarrow\downarrow} + f_t\tilde{f}_t\right)}{4}.} \tag{1.7.6}$$

We find that singlet Cooper pairs lower the local DOS, whereas triplet pairs enhance it. To quantify the presence of these pairs, we define the singlet and triplet parameters,

$$\begin{aligned} N_s &= \frac{\mathbb{R}\left(f_s \tilde{f}_s\right)}{4}, \\ N_t &= \frac{\mathbb{R}\left(f_{\uparrow\uparrow}\tilde{f}_{\uparrow\uparrow} + f_{\downarrow\downarrow}\tilde{f}_{\downarrow\downarrow} + f_t\tilde{f}_t\right)}{4}. \end{aligned} \tag{1.7.7}$$

These parameters are always positive at $\varepsilon = 0$, where $f\tilde{f} = |f|^2$, which means they both leave clear signatures on the density of states: singlets cause a zero-energy dip, whereas triplet cause a zero-energy peak. The singlet and triplet densities can be found by taking the absolute values of these parameters and integrating over energy. Note that while $f_t = (f_{\uparrow\downarrow} + f_{\downarrow\uparrow})/\sqrt{2}$ consists of pairs with opposite spin, $f_{\uparrow\uparrow}$ and $f_{\downarrow\downarrow}$ don't. This means that the former will still undergo pair breaking due to magnetic interactions, while the latter two remain unaffected. These unaffected states, able to penetrate deeper into ferromagnets, are therefore referred to as "long-range triplets".

Chapter 2

Distribution functions and currents

To describe non-equilibrium phenomena, we need to know not just the density of states, but also the occupation of these states. This is described by the distribution function, and we will show in this chapter that for systems without spin-orbit coupling, this function can be found analytically from the equilibrium solutions. For systems that do include spin-orbit coupling, a more general boundary value problem, a set of coupled differential equations for the components of the distribution function and their corresponding boundary conditions, is derived.

In systems out of equilibrium, all sorts of currents can flow through the junction, which we combine into a single tensor in section 2.1. By writing the components of the distribution function in a similar way in section 2.2, we see in sections 2.3 and that these are directly related to their corresponding currents. In section 2.3 we show that the currents can now be written in terms of the boundary conditions at either side of the nanowire. Comparing this result to the divergence of the current tensor in section 2.4, we find that we can write the currents at any point in the wire as the covariant derivative of their corresponding distribution functions. Finally, in section 2.5, we use this to find an analytical expression for the currents at any point in the wire, which we apply to the zero-temperature differential conductivity in section 2.6. The more general boundary value problems that describe the distribution functions in any system, without any of the assumptions made for the analytical solution, are presented in sections 2.7 and 2.8.

The main relevance of the analytical solution is the amount of time it saves in numerical calculations. While it would take around a day on a regular desktop machine to calculate the differential conductivity spectrum for a single set of parameters, the analytical solutions reduces this to less than a minute. This allows

researchers to gain more insight in the systems they consider, as the conductivity for a range of parameters can be investigated in the time it would otherwise take to compute it for a single configuration.

2.1 The current tensor

As shown in appendix E.1, the average velocity of particles can be written as the derivatives of the field operators,

$$\langle \boldsymbol{v} \rangle = -\frac{i\hbar}{2m} \lim_{\boldsymbol{r}\to\boldsymbol{r}'} \left\langle \left(\tilde{\nabla}_{\boldsymbol{r}} - \tilde{\nabla}_{\boldsymbol{r}'} \right) \psi^\dagger(\boldsymbol{r}')\psi(\boldsymbol{r}) \right\rangle . \tag{2.1.1}$$

By comparing this to the definition of the Keldysh Green function in equation (C.1.1), and introducing relative coordinates, the spectral current tensor is

$$\boldsymbol{j}_{ij}(\varepsilon) = -iv_F \int \frac{d^3p}{(2\pi)^3}\, \hat{\boldsymbol{p}} \operatorname{Tr}\left[\hat{\tau}_i \underline{\sigma}_j \underline{\hat{G}}^K(\varepsilon, \boldsymbol{p}) \right]. \tag{2.1.2}$$

Introducing the quasiclassical Green function, the current can now be written as

$$\boldsymbol{I}_{ij} = -\frac{N_0 v_F}{2} \int d\varepsilon \left\langle \hat{\boldsymbol{p}} \operatorname{Tr}\left[\hat{\tau}_i \underline{\sigma}_j \underline{\hat{g}}^K(\varepsilon, \boldsymbol{p}) \right] \right\rangle_{\boldsymbol{p}} . \tag{2.1.3}$$

In the dirty limit, the Green function is expanded in spherical harmonics, where appendix E.3 shows that the second term in the expansion can be constructed from the first, leaving us

$$\boxed{\boldsymbol{I}_{ij} = \frac{N_0 D}{2} \int d\varepsilon \operatorname{Tr}\left(\hat{\tau}_i \underline{\sigma}_j \left[\underline{\check{g}}_s \tilde{\nabla}_{\boldsymbol{r}} \underline{\check{g}}_s \right]^K \right).} \tag{2.1.4}$$

2.2 Pauli-decomposed distribution functions

Choosing the distribution function $\underline{\hat{\hbar}}$ to be diagonal in Nambu (particle-hole) space, the distribution function can be split up in longitudinal and transverse distribution functions [55, 56], which can each be further decomposed into a scalar and a vector component:

$$\boxed{\begin{aligned} \underline{\hat{\hbar}} &= \hat{\tau}_0 \otimes \underline{\hbar}_L + \hat{\tau}_3 \otimes \underline{\hbar}_T \\ &= \hat{\tau}_0 \otimes \left(\hbar_{L0}\, \underline{\sigma}_0 + \boldsymbol{\hbar}_{\boldsymbol{L}} \cdot \underline{\boldsymbol{\sigma}} \right) + \hat{\tau}_3 \otimes \left(\hbar_{T0}\, \underline{\sigma}_0 + \boldsymbol{\hbar}_{\boldsymbol{T}} \cdot \underline{\boldsymbol{\sigma}} \right) \\ &= \sum_{\substack{i=0,3 \\ j=0,1,2,3}} \hat{\tau}_i \underline{\sigma}_j \hbar_{ij}, \end{aligned}} \tag{2.2.1}$$

renaming $\underline{\hbar}_L = \underline{\hbar}_0$ and $\underline{\hbar}_T = \underline{\hbar}_3$. Each of these distribution functions has its own physical interpretation. For example, the function $\hbar_{00}$ describes the particle current and the magnitude of the order parameter, while $\hbar_{30}$ describes the phase of the order parameter and the electric current [49, 57–59]. The functions $\hbar_{0i}$ and $\hbar_{3i}$, $i = 1, 2, 3$ describe the spin-heat and spin-electric currents. In the absence of any spin structure, only $\hbar_{00}$ and $\hbar_{30}$ are nonzero. In this case, a bulk material with a voltage V applied to it has the distribution function [20, 49]

$$\hat{\underline{\hbar}} = \hat{\underline{\rho}}_0 \hat{\underline{\hbar}}_{00} + \hat{\underline{\rho}}_3 \hat{\underline{\hbar}}_{30} = \begin{pmatrix} \tanh\left(\beta \dfrac{\varepsilon + eV}{2}\right) & 0 \\ 0 & \tanh\left(\beta \dfrac{\varepsilon - eV}{2}\right) \end{pmatrix}, \tag{2.2.2}$$

where $\beta = 1/k_{\mathrm{B}}T$, e is the electron charge and V is the voltage. If the voltage is zero as well, only $\hbar_{00}$ remains, and we can write [43]

$$\hat{\underline{g}}^K = \hat{\underline{g}}^R \hat{\underline{\hbar}} - \hat{\underline{\hbar}} \hat{\underline{g}}^A = (\hat{\underline{g}}^R - \hat{\underline{g}}^A) \tanh(\beta\varepsilon/2). \tag{2.2.3}$$

2.3 Currents across a boundary

The Kuprianov-Lukichev boundary conditions [45], generalized to include the magnetic vector potential to first order [30], are given by

$$\boxed{2r \check{\underline{g}}_{\alpha,\beta} \tilde{\nabla}_{\boldsymbol{r}} \check{\underline{g}}_{\alpha,\beta} = \left[\check{\underline{g}}_\alpha, \check{\underline{g}}_\beta\right]_-}. \tag{2.3.1}$$

Substituting these into equation (2.1.4), the current can be written in terms of the Green functions on both sides of either boundary:

$$I_{ij}(\varepsilon, x = 0, L) = \frac{N_0 D}{4r} \int d\varepsilon \, \mathrm{Tr}\left(\hat{\tau}_i \underline{\sigma}_j \left[\check{\underline{g}}_\alpha, \check{\underline{g}}_\beta\right]_-^K\right)\Big|_{x=0,L}. \tag{2.3.2}$$

Expanding the distribution functions in their Pauli components using the definition in equation (2.2.1), we find, after computing the trace, the simpler expression

$$\left[\frac{1}{2r} \mathrm{Tr}\left(\hat{\tau}_i \underline{\sigma}_j \left[\check{\underline{g}}_\alpha, \check{\underline{g}}_\beta\right]_-^K\right)\right]_{z=0,L} = \sum_{\substack{\iota=\alpha,\beta \\ k=0,3 \\ l=0,1,2,3}} \left[\frac{1}{2r} C_{ijkl\iota} \hbar_{kl\iota}\right]_{z=0,L}, \tag{2.3.3}$$

where, writing κ for the side opposite to ι,

$$C_{ijkl\iota} = \mathrm{Tr}\left(\hat{\tau}_i \underline{\sigma}_j \left[(\hat{\underline{g}}_\iota^R \hat{\tau}_k \underline{\sigma}_l - \hat{\tau}_k \underline{\sigma}_l \hat{\underline{g}}_\iota^A) \hat{\underline{g}}_\kappa^A - \hat{\underline{g}}_\kappa^R (\hat{\underline{g}}_\iota^R \hat{\tau}_k \underline{\sigma}_l - \hat{\tau}_k \underline{\sigma}_l \hat{\underline{g}}_\iota^A)\right]\right). \tag{2.3.4}$$

As will be shown in section 2.5, this can be written as an 8×8 matrix $C^{8\times8}_{ijkl\iota}$ operating on the vectors $\hbar^{8\times1}_{kl\alpha}$ and $\hbar^{8\times1}_{kl\beta}$.[1] The current in equation (2.3.2) can now be written in terms of the constants $C_{ijkl\iota}$ and the distribution function components $\hbar_{kl\iota}$:

$$\boxed{I_{ij}(\varepsilon, x=0, L) = \frac{N_0 D}{4r} \int d\varepsilon \sum_{\substack{\iota=\alpha,\beta \\ k=0,3 \\ l=0,1,2,3}} \left[C_{ijkl\iota}\hbar_{kl\iota}\right]_{z=0,L}.} \tag{2.3.5}$$

The current through the boundary at $x = 0$ is not necessarily equal to the current through the boundary at $x = L$, as not all currents are conserved [55, 60].

2.4 Current tensor for conserved currents

For those currents that are conserved, such as the particle current $\boldsymbol{I}_{00}$ and the electric current $q\boldsymbol{I}_{30}$, we can write for the divergence of the spectral current defined in equation (2.1.4) ($\boldsymbol{I} = \int d\varepsilon\, \boldsymbol{j}$)

$$\nabla_{\boldsymbol{r}} \cdot \boldsymbol{j}_{ij} = \frac{N_0 D}{2} \nabla_{\boldsymbol{r}} \cdot \mathrm{Tr}\left(\hat{\tau}_i \underline{\sigma}_j \left[\underline{\check{g}}_s \tilde{\nabla}_{\boldsymbol{r}} \underline{\check{g}}_s\right]^K\right) = 0. \tag{2.4.1}$$

Defining the diffusion coefficients M_{ijkl},

$$M_{ijkl} = \mathrm{Tr}\left(\hat{\tau}_i \underline{\sigma}_j \hat{\tau}_k \underline{\sigma}_l - \hat{\tau}_i \underline{\sigma}_j \underline{\hat{g}}^R_s \hat{\tau}_k \underline{\sigma}_l \underline{\hat{g}}^A_s\right), \tag{2.4.2}$$

and the spectral supercurrent coefficients Q_{ij},[2]

$$Q_{ij} = \mathrm{Tr}\left[\hat{\tau}_i \underline{\sigma}_j \left(\underline{\hat{g}}^R \tilde{\nabla}_{\boldsymbol{r}} \underline{\hat{g}}^R - \underline{\hat{g}}^A \tilde{\nabla}_{\boldsymbol{r}} \underline{\hat{g}}^A\right)\right], \tag{2.4.3}$$

equation (2.4.1) is more concisely written as

$$\nabla_{\boldsymbol{r}} \cdot \sum_{k,l} Q_{kl} \hbar_{kl} + M_{ijkl} \tilde{\nabla}_{\boldsymbol{r}} \hbar_{kl} = 0, \tag{2.4.4}$$

[1] For more details on different notations, parametrizations and the mapping between them, see section F.5.

[2] These coefficients are similar to M_{ij} and Q defined in Ref. 49, but with Pauli matrices in spin space added. Note that $Q_{00} = 0$ since

$$\mathrm{Tr}\left(\underline{\hat{g}}^R \underline{\hat{g}}^{R\prime}\right) = \frac{1}{2}\mathrm{Tr}\left(\underline{\hat{g}}^R \underline{\hat{g}}^{R\prime} + \underline{\hat{g}}^{R\prime} \underline{\hat{g}}^R\right) = \frac{1}{2}\mathrm{Tr}\left(\nabla\left[\underline{\hat{g}}^R\right]^2\right) = 0 = \mathrm{Tr}\left(\underline{\hat{g}}^A \underline{\hat{g}}^{A\prime}\right).$$

which implies

$$\sum_{k,l} Q_{kl} h_{kl} + M_{ijkl} \tilde{\nabla}_{\boldsymbol{r}} h_{kl} = C_{ij}, \tag{2.4.5}$$

where C_{ij} are constants. Looking at the boundary conditions in equation (2.3.1), we find the top-right (Keldysh) component to contain

$$\hat{\underline{g}}^R(\tilde{\nabla}_{\boldsymbol{r}}\hat{\underline{g}}^R)\hat{\underline{h}} + (\tilde{\nabla}_{\boldsymbol{r}}\hat{\underline{h}}) - \hat{\underline{g}}^R(\tilde{\nabla}_{\boldsymbol{r}}\hat{\underline{h}})\hat{\underline{g}}^A - \hat{\underline{h}}\hat{\underline{g}}^A(\tilde{\nabla}_{\boldsymbol{r}}\hat{\underline{g}}^A) = \frac{1}{2r}\left[\check{\underline{g}}_\alpha, \check{\underline{g}}_\beta\right]_-^K. \tag{2.4.6}$$

Multiplying both sides by $\hat{\tau}_i\underline{\sigma}_j$ and taking the trace, we find an expression similar to equation (2.4.5):

$$\sum_{k,l} Q_{kl} h_{kl} + M_{ijkl} \tilde{\nabla}_{\boldsymbol{r}} h_{kl}\Big|_{\alpha,\beta} = \frac{1}{2r}\,\mathrm{Tr}\left(\hat{\tau}_i\underline{\sigma}_j\left[\check{\underline{g}}_\alpha, \check{\underline{g}}_\beta\right]_-^K\right). \tag{2.4.7}$$

As the distribution functions are continuous all the way up to the boundary, the right-hand sides of eqs. (2.4.5, 2.4.7) must be equal. We end up with the eight equations

$$\boxed{C_{ij} = \sum_{k,l} Q_{kl} h_{kl} + M_{ijkl} \tilde{\nabla}_{\boldsymbol{r}} h_{kl} = \sum_{\substack{\iota=\alpha,\beta \\ k=0,3 \\ l=0,1,2,3}} \left[\frac{1}{2r} C_{ijkl\iota} h_{kl\iota}\right]_{z=0,L},} \tag{2.4.8}$$

where $i = 0, 3$ and $j = 0, 1, 2, 3$. The conserved currents can now be expressed in terms of the distribution functions at any position $\boldsymbol{r}$ in the wire by

$$\boldsymbol{I}_{ij}(\varepsilon) = \frac{N_0 D}{2}\int d\varepsilon \sum_{k,l} Q_{kl} h_{kl} + M_{ijkl}\tilde{\nabla}_{\boldsymbol{r}} h_{kl}. \tag{2.4.9}$$

2.5 Currents in systems with zero boundary resistance on one side

The current in equation (2.3.5) can be calculated if we know the distribution functions on both sides of one of the boundaries. Suppose we have a wire between $z = 0$ and $z = L$, with some bulk materials to the left and right of it. In this section we will calculate the currents assuming that one of the ends of the wire has zero boundary resistance, and that there are no supercurrents that flow through the boundary[3]. In this special case, we do not need to actually find the

[3] This assumption means we exclude Josephson junctions.

distribution functions within the wire, their bulk values will be enough to describe all non-equilibrium behaviour.

By moving the constants M_{ijkl} to the other side of equation (2.4.8), we find an expression for the derivatives of the distribution functions. To avoid having to take the inverse of a rank four tensor, we combine the longitudinal and transverse distribution functions in a single vector:

$$\hat{\underline{\hbar}}^{4\times4} = \begin{pmatrix} \underline{\hbar}_L + \underline{\hbar}_T & 0 \\ 0 & \underline{\hbar}_L - \underline{\hbar}_T \end{pmatrix} \longmapsto \begin{pmatrix} \hbar_{L,0} \\ \vdots \\ \hbar_{L,3} \\ \hbar_{T,0} \\ \vdots \\ \hbar_{T,3} \end{pmatrix} = \begin{pmatrix} \hbar_{00} \\ \vdots \\ \hbar_{03} \\ \hbar_{30} \\ \vdots \\ \hbar_{33} \end{pmatrix} = \hbar_{kl}^{8\times1}, \tag{2.5.1}$$

and accordingly,

$$M_{ijkl}^{2\times4\times2\times4} \longmapsto \begin{pmatrix} M_{0000} & \dots & M_{0003} & M_{0030} & \dots & M_{0033} \\ \vdots & \ddots & & & & \vdots \\ M_{0300} & & \ddots & & & \vdots \\ M_{3000} & & & \ddots & & \vdots \\ \vdots & & & & \ddots & \vdots \\ M_{3300} & \dots & \dots & \dots & \dots & M_{3333} \end{pmatrix} = M_{ijkl}^{8\times8}. \tag{2.5.2}$$

The two matrices $C_{ijkl\alpha}$ and $C_{ijkl\beta}$ have the same structure as M_{ijkl}. Embracing Einstein notation from now on, where summation is implied for repeated indices,

$$\tilde{\nabla}_{\boldsymbol{r}} \hbar_{kl}(\boldsymbol{r}) = M_{ijkl}^{-1}(\boldsymbol{r}) \left[\frac{1}{2r} C_{ijkl\iota} \hbar_{kl\iota} \right]_{z=0,L}. \tag{2.5.3}$$

As shown in section B.2, the covariant derivative can be replaced by

$$\tilde{\nabla}_{\boldsymbol{r}} \hat{\underline{\hbar}} = \nabla_{\boldsymbol{r}} \hat{\underline{\hbar}} - i \left[\hat{\underline{\boldsymbol{\mathcal{A}}}}, \hat{\underline{\hbar}} \right]_-, \tag{2.5.4}$$

where the commutator equals

$$\hat{\underline{\boldsymbol{\mathcal{A}}}} = \begin{pmatrix} \underline{\boldsymbol{\mathcal{A}}} & 0 \\ 0 & -\underline{\boldsymbol{\mathcal{A}}}^* \end{pmatrix} \quad \Rightarrow \quad \left[\hat{\underline{\boldsymbol{\mathcal{A}}}}, \hat{\underline{\hbar}} \right]_- = \begin{pmatrix} [\underline{\boldsymbol{\mathcal{A}}}, \underline{x}]_- & 0 \\ 0 & [\underline{\tilde{x}}, \underline{\boldsymbol{\mathcal{A}}}^*]_- \end{pmatrix}. \tag{2.5.5}$$

As long as the spin-orbit coupling is along the magnetization direction, this commutator equals zero. This is not generally true, which means that the method

derived here is mainly useful for solving systems with just a magnetic structure.[4] In the absence of spin-orbit coupling, or in the case the coupling aligns with the magnetic field, we now find an expression for the gradient of the distribution functions:

$$\boxed{\nabla_{\boldsymbol{r}} \mathcal{h}_{kl}(\boldsymbol{r}) = M^{-1}_{ijkl}(\boldsymbol{r}) \left[\frac{1}{2r} C_{ijkl\iota} \mathcal{h}_{kl\iota} \right]_{z=0,L}}. \tag{2.5.6}$$

This can be used to find the distribution functions at any position in the wire, given that we know their values at some other point.

In what follows we will assume that the ratio between the resistance of the left boundary and the wire is $r_L = 0$, whereas on the right $r_R \neq 0$. To find the current, we need to know the distribution functions $\underline{\hat{\mathcal{h}}}(L_-)$ and $\underline{\hat{\mathcal{h}}}(L_+)$. The latter is simply the bulk value on the right, and $\underline{\hat{\mathcal{h}}}(L_-)$ can be expressed in terms of $\underline{\hat{\mathcal{h}}}(x_+)$ by integrating eq. (2.5.6) [61]:

$$\mathcal{h}_{kl}(L_-) - \mathcal{h}_{kl}(0_+) = \frac{1}{2r_R} C_{ijkl\iota} \mathcal{h}_{kl\iota} \int_{0_+}^{L_-} M^{-1}_{ijkl}(x)\, dx. \tag{2.5.7}$$

Assuming the left boundary to have zero interface resistance

$$r_L = 0 \;\Rightarrow\; \mathcal{h}_{kl}(0_+) = \mathcal{h}_{kl}(0_-), \tag{2.5.8}$$

we can express the unknown $\mathcal{h}_{kl}(L_-)$ in terms of just bulk distribution functions and the known retarded and advanced Green functions:

$$\begin{aligned} \mathcal{h}_{kl}(L_-) = &\left(1 - \frac{C_{ijkl}(L_-)}{2r_R} \int_{0_+}^{L_-} \frac{dx}{M_{ijkl}(x)} \right)^{-1} \\ &\times \left(\frac{C_{ijkl}(L_+)}{2r_R} \int_{0_+}^{L_-} \frac{dx}{M_{ijkl}(x)}\, \mathcal{h}_{kl}(L_+) + \mathcal{h}_{kl}(0_-) \right). \end{aligned} \tag{2.5.9}$$

Defining the constants

$$\boxed{\begin{aligned} A_{ijkl} &= \left(2r_R\, C^{-1}_{ijkl}(L_-) - \int_{0_+}^{L_-} \frac{dx}{M_{ijkl}(x)} \right)^{-1}, \\ B_{ijkl} &= \frac{C_{ijkl}(L_+)}{2r_R} + A\, \frac{C_{ijkl}(L_+)}{2r_R} \int_{0_+}^{L_-} \frac{dx}{M_{ijkl}(x)}, \end{aligned}} \tag{2.5.10}$$

[4] Usually magnetization itself induces currents in the plane orthogonal to the magnetization, where the vector potential would point along these currents. In nanowires, however, there is simply no room for such currents as momentum is really only possible along the wire.

we can now easily express the current tensor as

$$\boxed{I_{ij}(\varepsilon) = \frac{N_0 D}{4r_R} \int d\varepsilon \left[A_{ijkl} \hbar_{kl}(0_-) + B_{ijkl} \hbar_{kl}(L_+) \right].} \tag{2.5.11}$$

2.6 Electric conductivity

Without other phenomena accounted for, the flow of particles is proportional to the number of states that are available. The current, or energy-integrated spectral current, is therefore proportional to the difference between the numbers of states available for particles moving in opposite directions. As the differential conductance is the voltage-derivative of the current, we expect the voltage dependence of the conductance to resemble the energy dependence of the density of states. To account for the dependence of the density of states on the position in the wire, we could make the comparison with macroscopic resistors in series, and guess that

$$\frac{1}{\sigma_{\text{junction}}(eV)} \approx \sum_i \frac{1}{\sigma_i(eV)} \propto \int \frac{dz}{N(\varepsilon = eV, z)}, \tag{2.6.1}$$

which in practice means that the conductivity will look like the density of states in the "bottleneck" of the system.

2.6.1 Zero-temperature conductivity in the absence of SOC

By taking the voltage derivative of the I_{30} component of the current tensor in eq. (2.5.11), we find an expression for the electric conductivity:

$$\boxed{\sigma(eV) = \frac{qN_0 D}{4r_R} \, \partial_{eV} \int_{-\infty}^{\infty} \left[A_{30kl}(\varepsilon) \hbar_{kl}(0_-) + B_{30kl}(\varepsilon) \hbar_{kl}(L_+) \right] \, d\varepsilon.} \tag{2.6.2}$$

At zero temperature[5], assuming there is no magnetization in the bulk materials and that the voltage V is applied on the left, equation (2.2.2) becomes for either

[5] At finite temperature, the distribution functions need to be calculated for the voltage range where their derivatives are nonzero, after which the derivative is taken. There is no need to calculate the retarded and advanced Green functions multiple times (as they do not depend on the voltage), so also finite-temperature conductances can be found quickly with this method.

side

$$\begin{aligned}
\begin{pmatrix} \hbar_{00} \\ \hbar_{01,02,03} \\ \hbar_{30} \\ \hbar_{31,32,33} \end{pmatrix}_{0_-} &= \begin{pmatrix} [\Theta(\varepsilon + eV) + \Theta(\varepsilon - eV)]/2 \\ 0 \\ [\Theta(\varepsilon + eV) - \Theta(\varepsilon - eV)]/2 \\ 0 \end{pmatrix}, \\
\begin{pmatrix} \hbar_{00} \\ \hbar_{01,02,03} \\ \hbar_{30} \\ \hbar_{31,32,33} \end{pmatrix}_{L_+} &= \begin{pmatrix} \Theta(\varepsilon) \\ 0 \\ 0 \\ 0 \end{pmatrix}.
\end{aligned} \tag{2.6.3}$$

Their voltage derivatives are, assuming $\underline{\hat{\hbar}}_{0_-} = \underline{\hat{\hbar}}_{0_+}$,

$$\begin{aligned}
\partial_{eV} \begin{pmatrix} \hbar_{00} \\ \hbar_{01,02,03} \\ \hbar_{30} \\ \hbar_{31,32,33} \end{pmatrix}_{0_-} &= \begin{pmatrix} [\delta(\varepsilon + eV) - \delta(\varepsilon - eV)]/2 \\ 0 \\ [\delta(\varepsilon + eV) + \delta(\varepsilon - eV)]/2 \\ 0 \end{pmatrix}, \\
\partial_{eV} \begin{pmatrix} \hbar_{00} \\ \hbar_{01,02,03} \\ \hbar_{30} \\ \hbar_{31,32,33} \end{pmatrix}_{L_+} &= \begin{pmatrix} 0 \\ 0 \\ 0 \\ 0 \end{pmatrix},
\end{aligned} \tag{2.6.4}$$

leaving us the conductivity

$$\sigma(eV) = \frac{qN_0D}{8r_R} \left[A_{3000}(-eV) + A_{3030}(-eV) - A_{3000}(eV) + A_{3030}(eV) \right]. \tag{2.6.5}$$

In the absence of magnetic fields, there is perfect spin symmetry and all entries in the matrix A are even in energy [62]:

$$\sigma(eV) = \frac{qN_0D}{4r_R} A_{3030}(eV). \tag{2.6.6}$$

With the method described in this section, the zero-temperature conductivity of a junction can be found just by solving the boundary value problem in equations (1.4.11) and (1.5.4). Doing so for 200 energies typically takes around a minute on a desktop machine. [6] This method can only be used in some limiting cases:

[6] The bottleneck for such calculations is the processor, the times cited here are for an Intel®Core™i7-6700HQ at 2.60GHz, where the program has been parallelized to use all four cores.

- The current is conserved (so that equation (2.4.1) holds). This holds for particle and charge currents, but not for spin currents in the presence of spin-orbit coupling [60][7].

- The vector potential commutes with the distribution function within the wire (so we can replace (2.5.3) $\mapsto$ (2.5.6)). This is always true for the magnetic vector potential (which is real-valued), but not for the generalized vector potential that includes spin-orbit coupling [30, 36].

- One of the boundaries needs to be transparent (so equation (2.5.8) applies).

In the general case, the boundary value problem derived in section 2.8 needs to be solved. Here we cannot make the same convenient assumption as we did in equation (2.6.3), where the distribution functions became step functions around $\varepsilon - eV$. This means that in order to find the electric conductivity, we need to solve the problem for both multiple energies and multiple voltages. For a typical accuracy of integrating the spectral current over 200 energies, and drawing a plot for 100 voltages, one needs about a day of computation time.

2.7 Boundary value problem for the distribution functions without magnetic fields

In a system without a magnetic field, only $\hbar_{00}$ and $\hbar_{30}$ need to be considered [20]. In this case, the divergence of eq. (2.4.8) gives the two coupled differential equations

$$\begin{cases} \nabla_{\boldsymbol{r}} \cdot \sum\limits_{k=0,3} Q_{k0} \hbar_{k0} + M_{00k0} \tilde{\nabla}_{\boldsymbol{r}} \hbar_{k0} = 0, \\ \\ \nabla_{\boldsymbol{r}} \cdot \sum\limits_{k=0,3} Q_{k0} \hbar_{k0} + M_{30k0} \tilde{\nabla}_{\boldsymbol{r}} \hbar_{k0} = 0. \end{cases} \tag{2.7.1}$$

The second of these equations describes the conservation of the electric current. From this we can also find a very simple expression for the electric current in the absence of magnetic fields. Without particle-hole imbalance, M_{0030} is zero [49], so in the absence of supercurrents we would be left with only one term [55]:

$$\boldsymbol{j}_e(\varepsilon) = \frac{qN_0D}{2} M_{3030} \tilde{\nabla}_{\boldsymbol{r}} \hbar_{T,d}. \tag{2.7.2}$$

[7] The cited article suggests an alternative way of defining the spin current in systems with spin-orbit coupling, where the $j_{\boldsymbol{\sigma}} \propto \langle \boldsymbol{\sigma} \partial_t \boldsymbol{r} \rangle$ used in this thesis is replaced by $j_{\boldsymbol{\sigma}} \propto \langle \partial_t (\boldsymbol{\sigma} \boldsymbol{r}) \rangle$, adding a torque term $\boldsymbol{\tau} = \langle \boldsymbol{r} \partial_t \boldsymbol{\sigma} \rangle$. This current is conserved, but is not trivial to measure.

From equation (2.4.7) we find the two boundary conditions

$$\begin{aligned}\sum_{k=0,3} Q_{k0}\mathfrak{h}_{k0} + M_{00k0}\tilde{\nabla}_{\boldsymbol{r}}\mathfrak{h}_{k0} &= \frac{1}{2r}\,\mathrm{Tr}\left(\hat{\tau}_0\underline{\sigma}_0\left[\underline{\check{g}}_\alpha, \underline{\check{g}}_\beta\right]_-^K\right),\\ \sum_{k=0,3} Q_{k0}\mathfrak{h}_{k0} + M_{30k0}\tilde{\nabla}_{\boldsymbol{r}}\mathfrak{h}_{k0} &= \frac{1}{2r}\,\mathrm{Tr}\left(\hat{\tau}_3\underline{\sigma}_0\left[\underline{\check{g}}_\alpha, \underline{\check{g}}_\beta\right]_-^K\right).\end{aligned} \tag{2.7.3}$$

In section 2.7 we found the general equations of motion for the distribution functions. The system can be solved quite easily in this most simplified case, where we find after uncoupling equations (2.7.1) for $\mathfrak{h}''_{00}$ and $\mathfrak{h}''_{30}$,

$$\begin{aligned}\mathfrak{h}''_{L,d} &= \frac{\left(M'_{0000}M_{3030} - M_{3000}M'_{0030}\right)\mathfrak{h}'_{L,d} + \left(M'_{3000}M_{3030} - M_{3000}M'_{3030}\right)\mathfrak{h}'_{T,d}}{M_{3000}M_{0030} - M_{0000}M_{3030}},\\ \mathfrak{h}''_{T,d} &= \frac{\left(M'_{0000}M_{0030} - M_{0000}M'_{0030}\right)\mathfrak{h}'_{L,d} + \left(M'_{3000}M_{0030} - M_{0000}M'_{3030}\right)\mathfrak{h}'_{T,d}}{M_{0000}M_{3030} - M_{3000}M_{0030}}.\end{aligned} \tag{2.7.4}$$

Combining the two, the system can be described as a first-order ordinary differential equation of the four-element vector y:

$$\boxed{y = \begin{pmatrix}\mathfrak{h}_{L,d}\\ \mathfrak{h}_{T,d}\\ \mathfrak{h}'_{L,d}\\ \mathfrak{h}'_{T,d}\end{pmatrix} = \begin{pmatrix}y_1\\ y_2\\ y_3\\ y_4\end{pmatrix}, \qquad y' = \begin{pmatrix}0 & 0 & 1 & 0\\ 0 & 0 & 0 & 1\\ 0 & 0 & A & B\\ 0 & 0 & C & D\end{pmatrix} y,} \tag{2.7.5}$$

where

$$\begin{aligned}A &= \frac{M'_{0000}M_{3030} - M_{3000}M'_{0030}}{M_{3000}M_{0030} - M_{0000}M_{3030}}, \quad B = \frac{M'_{3000}M_{3030} - M_{3000}M'_{3030}}{M_{3000}M_{0030} - M_{0000}M_{3030}},\\ C &= \frac{M'_{0000}M_{0030} - M_{0000}M'_{0030}}{M_{0000}M_{3030} - M_{3000}M_{0030}}, \quad D = \frac{M'_{3000}M_{0030} - M_{0000}M'_{3030}}{M_{0000}M_{3030} - M_{3000}M_{0030}}.\end{aligned} \tag{2.7.6}$$

The boundary conditions in this case become

$$\begin{aligned}\left(Q_{30}\mathfrak{h}_{T,d} + M_{0000}\mathfrak{h}'_{L,d} + M_{3000}\mathfrak{h}'_{T,d}\right)_{\alpha,\beta} &= \frac{1}{2r}\,\mathrm{Tr}\left(\left[\underline{\check{g}}_\alpha, \underline{\check{g}}_\beta\right]_-^K\right),\\ \left(Q_{30}\mathfrak{h}_{L,d} + M_{0030}\mathfrak{h}'_{L,d} + M_{3030}\mathfrak{h}'_{T,d}\right)_{\alpha,\beta} &= \frac{1}{2r}\,\mathrm{Tr}\left(\hat{\rho}_3\left[\underline{\check{g}}_\alpha, \underline{\check{g}}_\beta\right]_-^K\right).\end{aligned} \tag{2.7.7}$$

After solving for the two components of the distribution function, equation (2.3.5) can be used to calculate the components of the current tensor.

2.8 General boundary value problem for the distribution functions

2.8.1 Differential equations

To calculate the distribution function, we need a differential equation that can be solved numerically. We do this by rewriting equation (D.5.3) in such a way that all dependence on $\hat{\underline{h}}''$ is on the left, and all terms including $\hat{\underline{h}}'$ and $\hat{\underline{h}}$ are on the right. Isolating first all terms containing $\tilde{\nabla}^2_{\boldsymbol{r}}\hat{\underline{h}}$:

$$\begin{aligned}\hat{\underline{g}}^R_s(\tilde{\nabla}^2_{\boldsymbol{r}}\hat{\underline{h}}) - (\tilde{\nabla}^2_{\boldsymbol{r}}\hat{\underline{h}})\hat{\underline{g}}^A_s = \frac{i}{D}\,\hat{\underline{g}}^R_s\left[\hat{\underline{E}}_{\hbar}\,,\hat{\underline{h}}\right]_- \hat{\underline{g}}^A_s - \frac{i}{D}\left[\hat{\underline{E}}_{\hbar}\,,\hat{\underline{h}}\right]_- \\ -(\tilde{\nabla}_{\boldsymbol{r}}\hat{\underline{g}}^R_s)(\tilde{\nabla}_{\boldsymbol{r}}\hat{\underline{h}}) - \hat{\underline{g}}^R_s(\tilde{\nabla}_{\boldsymbol{r}}\hat{\underline{h}})(\tilde{\nabla}_{\boldsymbol{r}}\hat{\underline{g}}^A_s)\hat{\underline{g}}^A_s\end{aligned} \tag{2.8.1}$$

Expanding the covariant Laplacian $\tilde{\nabla}^2_{\boldsymbol{r}}$ using equation (1.3.4), we find

$$\tilde{\nabla}^2_{\boldsymbol{r}}\hat{\underline{h}} = \nabla^2_{\boldsymbol{r}}\hat{\underline{h}} - 2i\left[\underline{\hat{\boldsymbol{\mathcal{A}}}},\nabla_{\boldsymbol{r}}\hat{\underline{h}}\right]_- - i\left[\nabla_{\boldsymbol{r}}\underline{\hat{\boldsymbol{\mathcal{A}}}},\hat{\underline{h}}\right]_- - \left[\underline{\hat{\boldsymbol{\mathcal{A}}}},\left[\underline{\hat{\boldsymbol{\mathcal{A}}}},\hat{\underline{h}}\right]_-\right]_-, \tag{2.8.2}$$

with which we can now isolate the second spatial derivative of the distribution function:

$$\begin{aligned}\hat{\underline{g}}^R_s\hat{\underline{h}}'' - \hat{\underline{h}}''\hat{\underline{g}}^A_s = \frac{i}{D}\,\hat{\underline{g}}^R_s\left[\hat{\underline{E}}_{\hbar}\,,\hat{\underline{h}}\right]_-\hat{\underline{g}}^A_s - \frac{i}{D}\left[\hat{\underline{E}}_{\hbar}\,,\hat{\underline{h}}\right]_- - (\tilde{\nabla}_{\boldsymbol{r}}\hat{\underline{g}}^R_s)(\tilde{\nabla}_{\boldsymbol{r}}\hat{\underline{h}}) \\ -\hat{\underline{g}}^R_s(\tilde{\nabla}_{\boldsymbol{r}}\hat{\underline{h}})(\tilde{\nabla}_{\boldsymbol{r}}\hat{\underline{g}}^A_s)\hat{\underline{g}}^A_s + \hat{\underline{g}}^R_s\Big(2i\left[\underline{\hat{\boldsymbol{\mathcal{A}}}},\nabla_{\boldsymbol{r}}\hat{\underline{h}}\right]_- \\ +i\left[\nabla_{\boldsymbol{r}}\underline{\hat{\boldsymbol{\mathcal{A}}}},\hat{\underline{h}}\right]_- + \left[\underline{\hat{\boldsymbol{\mathcal{A}}}},\left[\underline{\hat{\boldsymbol{\mathcal{A}}}},\hat{\underline{h}}\right]_-\right]_-\Big) - \Big(2i\left[\underline{\hat{\boldsymbol{\mathcal{A}}}},\nabla_{\boldsymbol{r}}\hat{\underline{h}}\right]_- \\ +i\left[\nabla_{\boldsymbol{r}}\underline{\hat{\boldsymbol{\mathcal{A}}}},\hat{\underline{h}}\right]_- + \left[\underline{\hat{\boldsymbol{\mathcal{A}}}},\left[\underline{\hat{\boldsymbol{\mathcal{A}}}},\hat{\underline{h}}\right]_-\right]_-\Big)\hat{\underline{g}}^A_s \\ = \hat{\underline{\mathcal{E}}}^{4\times4}_{\mathrm{ODE}}.\end{aligned} \tag{2.8.3}$$

Using the methods derived in appendix F.5, we can write this as

$$\left[\mathcal{F}_{\hat{\underline{h}}}(\hat{\underline{g}}^R_s,\hat{\underline{1}}) - \mathcal{F}_{\hat{\underline{h}}}(\hat{\underline{1}},\hat{\underline{g}}^A_s)\right]\nabla^2_{\boldsymbol{r}}f\hat{\underline{h}} = f\hat{\underline{\mathcal{E}}}^{4\times4}_{\mathrm{ODE}} = \hat{\underline{\mathcal{E}}}^{16\times1}_{\mathrm{ODE}}, \tag{2.8.4}$$

where we have written the matrices $\hat{\underline{h}}$ and $\hat{\underline{\mathcal{E}}}^{4\times4}_{\mathrm{ODE}}$ out in their components using the flat-mapping f. Moving the matrix $\mathcal{F}_{\hat{\underline{h}}}(\hat{\underline{g}}^R_s,\hat{\underline{1}}) - \mathcal{F}_{\hat{\underline{h}}}(\hat{\underline{1}},\hat{\underline{g}}^A_s)$ to the right by left

division[8], we find an expression for $\nabla^2_{\boldsymbol{r}} f \hat{\underline{\hbar}}$:

$$\boxed{\nabla^2_{\boldsymbol{r}} \vec{x} = \left[\mathcal{F}_{\hat{\underline{\hbar}}}(\hat{\underline{g}}^R_s, \hat{\underline{1}}) - \mathcal{F}_{\hat{\underline{\hbar}}}(\hat{\underline{1}}, \hat{\underline{g}}^A_s)\right] \backslash \hat{\underline{\mathcal{E}}}^{16\times 1}_{\mathrm{ODE}}.} \tag{2.8.5}$$

Here the notation $\vec{x}$ is introduced for the 8×1 vector with the nonzero components of $\hat{\underline{\hbar}}$, which we parametrize as [40, 63]

$$\boxed{\hat{\underline{\hbar}} = \begin{pmatrix} \underline{x} & 0 \\ 0 & -\underline{\tilde{x}} \end{pmatrix}.} \tag{2.8.6}$$

2.8.2 Boundary conditions

We start off from the Lukichev-Kuprianov boundary condition in equation (1.5.3),

$$2r\underline{\check{G}}_{\alpha,\beta}\tilde{\nabla}_{\boldsymbol{r}}\underline{\check{G}}_{\alpha,\beta} = \left[\underline{\check{G}}_{\alpha}, \underline{\check{G}}_{\beta}\right]_{-}. \tag{2.8.7}$$

Expanding the 8×8 Green functions into their components, we find the top-right component of this expression to contain

$$\begin{aligned} 2r(&\hat{\underline{g}}^R_{\alpha,\beta}(\tilde{\nabla}_{\boldsymbol{r}}\hat{\underline{g}}^R_{\alpha,\beta})\hat{\underline{\hbar}}_{\alpha,\beta} + \tilde{\nabla}_{\boldsymbol{r}}\hat{\underline{\hbar}}_{\alpha,\beta} - \hat{\underline{g}}^R_{\alpha,\beta}(\tilde{\nabla}_{\boldsymbol{r}}\hat{\underline{\hbar}}_{\alpha,\beta})\hat{\underline{g}}^A_{\alpha,\beta} - \hat{\underline{\hbar}}_{\alpha,\beta}\hat{\underline{g}}^A_{\alpha,\beta}\tilde{\nabla}_{\boldsymbol{r}}\hat{\underline{g}}^A_{\alpha,\beta}) = \\ &\hat{\underline{g}}^R_{\alpha}\hat{\underline{g}}^R_{\beta}\hat{\underline{\hbar}}_{\beta} - \hat{\underline{g}}^R_{\alpha}\hat{\underline{\hbar}}_{\beta}\hat{\underline{g}}^A_{\beta} + \hat{\underline{g}}^R_{\alpha}\hat{\underline{\hbar}}_{\alpha}\hat{\underline{g}}^A_{\beta} - h_{\alpha}\hat{\underline{g}}^A_{\alpha}\hat{\underline{g}}^A_{\beta} - \hat{\underline{g}}^R_{\beta}\hat{\underline{g}}^R_{\alpha}\hat{\underline{\hbar}}_{\alpha} + \hat{\underline{g}}^R_{\beta}\hat{\underline{\hbar}}_{\alpha}\hat{\underline{g}}^A_{\alpha} \\ &-\hat{\underline{g}}^R_{\beta}\hat{\underline{\hbar}}_{\beta}\hat{\underline{g}}^A_{\alpha} + \hat{\underline{\hbar}}_{\beta}\hat{\underline{g}}^A_{\beta}\hat{\underline{g}}^A_{\alpha}. \end{aligned} \tag{2.8.8}$$

[8] The left division $A\backslash B$ can intuitively be understood as the inverse of the left multiplication of B by A. This is not necessarily equal to the left multiplication of B by the inverse of A though, as A in this case does not have a uniquely defined inverse.

Similarly to how we did in the previous section, we isolate the terms with $\nabla\hat{\underline{h}}$ terms on one side by expanding the covariant derivative:

$$\begin{aligned}
\hat{\underline{g}}^R_{\alpha,\beta}\hat{\underline{h}}'_{\alpha,\beta} - \hat{\underline{h}}'_{\alpha,\beta}\hat{\underline{g}}^A_{\alpha,\beta} = {}& \hat{\underline{g}}^R_{\alpha,\beta}\hat{\underline{h}}_{\alpha,\beta}\hat{\underline{g}}^A_{\alpha,\beta}\tilde{\nabla}_{\boldsymbol{r}}\hat{\underline{g}}^A_{\alpha,\beta} - (\tilde{\nabla}_{\boldsymbol{r}}\hat{\underline{g}}^R_{\alpha,\beta})\hat{\underline{h}}_{\alpha,\beta} \\
& + \frac{1}{2r}\Big(\hat{\underline{g}}^R_{\alpha,\beta}\hat{\underline{g}}^R_{\alpha}\hat{\underline{g}}^R_{\beta}\hat{\underline{h}}_{\beta} - \hat{\underline{g}}^R_{\alpha,\beta}\hat{\underline{g}}^R_{\alpha}\hat{\underline{h}}_{\beta}\hat{\underline{g}}^A_{\beta} \\
& + \hat{\underline{g}}^R_{\alpha,\beta}\hat{\underline{g}}^R_{\alpha}\hat{\underline{h}}_{\alpha}\hat{\underline{g}}^A_{\beta} - \hat{\underline{g}}^R_{\alpha,\beta}\hat{\underline{h}}_{\alpha}\hat{\underline{g}}^A_{\alpha}\hat{\underline{g}}^A_{\beta} - \hat{\underline{g}}^R_{\alpha,\beta}\hat{\underline{g}}^R_{\beta}\hat{\underline{g}}^R_{\alpha}\hat{\underline{h}}_{\alpha} \\
& + \hat{\underline{g}}^R_{\alpha,\beta}\hat{\underline{g}}^R_{\beta}\hat{\underline{h}}_{\alpha}\hat{\underline{g}}^A_{\alpha} - \hat{\underline{g}}^R_{\alpha,\beta}\hat{\underline{g}}^R_{\beta}\hat{\underline{h}}_{\beta}\hat{\underline{g}}^A_{\alpha} + \hat{\underline{g}}^R_{\alpha,\beta}\hat{\underline{h}}_{\beta}\hat{\underline{g}}^A_{\beta}\hat{\underline{g}}^A_{\alpha}\Big) \\
& + i\left(\hat{\underline{g}}^R_{\alpha,\beta}\left[\boldsymbol{\mathcal{A}},\hat{\underline{h}}_{\alpha,\beta}\right]_- - \left[\boldsymbol{\mathcal{A}},\hat{\underline{h}}_{\alpha,\beta}\right]_-\hat{\underline{g}}^A_{\alpha,\beta}\right) \\
& = \hat{\underline{\mathcal{E}}}_{\mathrm{BC}}.
\end{aligned} \tag{2.8.9}$$

Similarly to equation (2.8.5), we now find

$$\boxed{\nabla_{\boldsymbol{r}}\vec{x}\Big|_{x=0,L} = \left[\mathcal{F}_{\hat{\underline{h}}}(\hat{\underline{g}}^R_{\alpha,\beta},\hat{\underline{1}}) - \mathcal{F}_{\hat{\underline{h}}}(\hat{\underline{1}},\hat{\underline{g}}^A_{\alpha,\beta})\right]\setminus\hat{\underline{\mathcal{E}}}^{16\times 1}_{\mathrm{BC}}.} \tag{2.8.10}$$

To solve this boundary value problem for $\hat{\underline{h}}$, the equilibrium equations presented in sections 1.4 and 1.5 need to be solved first. Generally one would like to solve the non-equilibrium equations for multiple values of the voltage bias, it should be noted that the equilibrium problem is independent of the voltage and thus only needs to be solved once.

Chapter 3

Systems

In this chapter we solve the Usadel equation introduced in chapter 1 for a nanowires that connect normal metal and superconducting bulk materials. Both equilibrium and non-equilibrium properties are described using the methods provided in chapters 1 and 2. We consider different types of wire: normal metals (N), ferromagnets (F) and ferromagnets with spin-orbit coupling (F+SOC) (see figure 3.1).

In section 3.1 we desribe a normal-metal nanowire, where we see the appearance of a zero-bias conductance peak (ZBCP) that cannot be explained by the density of states alone. When adding a magnetic field in section 3.2, we see that the ZBCP is Zeeman splitted[1]. In section 3.3 we find that rotating the magnetic field throughout the wire causes some of the singlet pairs induced from the superconducting reservoir to convert to long-range triplets, which are sought-after as they allow for superconducting properties to penetrate deeper into adjoined magnetic materials [18, 22]. In section 3.4, we see that by applying a magnetic field along or orthogonal to the wire, we can switch between a zero-energy density dip and a zero-energy density peak in the density of states. Interestingly, we find that the Zeeman splitting of the zero-bias conduction peak by the magnetic field is weakened by the spin-mixing of spin-orbit coupling orthogonal to the magnetic field.

[1] For an accessible derivation and insightful discussion of the Zeeman effect, see pp. 277-82 in Ref. 64.

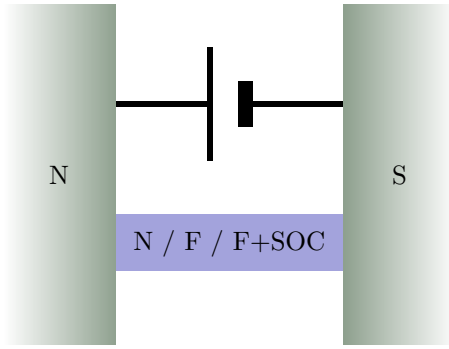

Figure 3.1: We will consider different types of nanowire junctions, in which a normal or ferromagnetic wire connects a bulk normal metal to a bulk superconductor.

3.1 Electric current in NNS junctions

As described in section 2.6, we expect the voltage-dependence of the conductivity to look like the energy-dependence of the density of states. Comparing the graphs in figure 3.2, we see that when the interface with the superconductor is transparent ($r_R = 0$), the conductance resembles the density of states in a normal metal, which means that the bottleneck to the particle flow is wire itself. For more opaque interfaces, the conductivity looks like the density of states on the superconducting side; the bottleneck becomes the availability of states in the material the carriers are tunneling to or from. This does not fully explain what we see in the conductance graph though, there is another feature: a zero-bias conductance peak (ZBCP) [61].

Without the suppression by a voltage bias or finite temperature, Andreev reflected [65] holes have wave functions with a phase equal to the transmitted electrons, allowing for constructive interference [66, 67]. These interferences enhance the proximity effect in normal metal-superconductor junctions, resulting in a higher carrier density and thus conductivity [61, 66]. This increased conductivity around zero voltage is expressed in a ZBCP. For junctions with high transparency, the enhanced proximity effect reduces the conductance, resulting in a zero-bias conductance dip (ZBCD) instead [62]. In figure 3.2 we see the ZBCP on the right for higher boundary resistances, and the ZBCD on the left for $r_R \ll 1$.

The relevance of the Thouless energy as an energy scale is shown in figure 3.3, where the conductivity is shown as a function of both the potential bias and the length of the system. The Thouless energy is related to this length through $E_{\text{th}} = \Delta_0(\xi/L)^2$, where ξ is the superconducting coherence length, the distance

over which the BCS wavefunction decays. We see that for very small systems the interferences described above occur even when a voltage is applied, whereas they become more improbable even at $eV = 0$ as the wire length is increased. The results of this section are in agreement with the numerical studies in Refs. [40, 62].

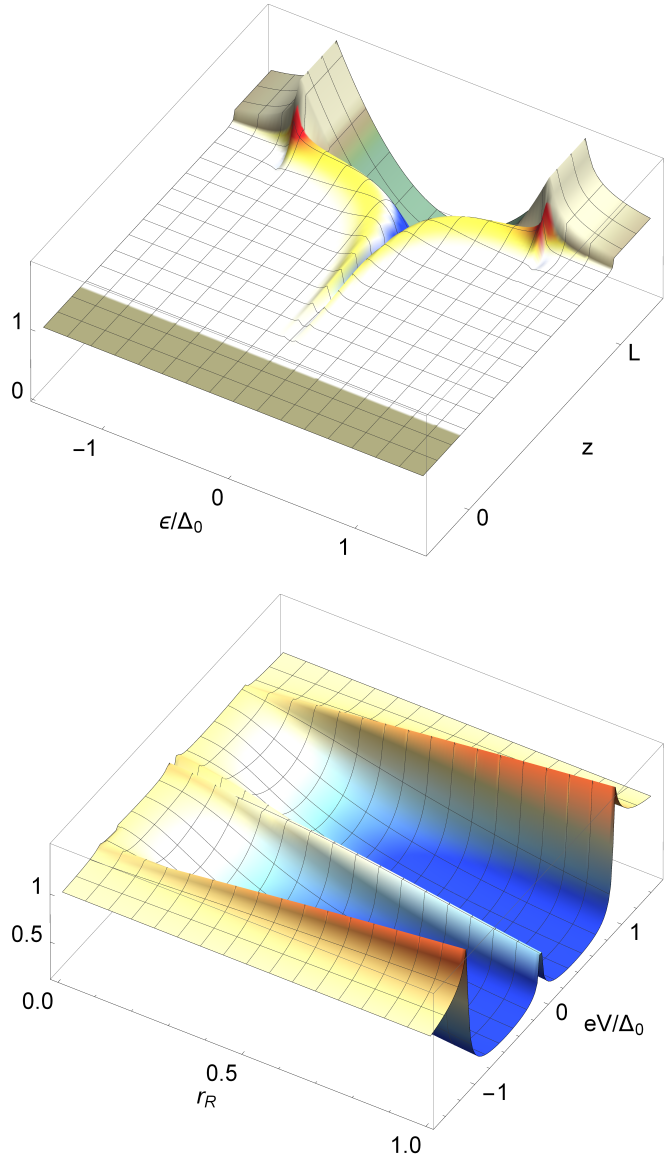

Figure 3.2: The DOS and conductivity of an NNS junction. The first is a function of energy and position in the wire, normalized to the DOS in the bulk normal metal, with the parameters $r_L = r_R = 0.1$ and $L = 10\xi$ (temperature map in the wire, army colours in the bulk materials). The second is a function of voltage bias and resistance on the N/S boundary, normalized to $\sigma(eV \gg \Delta_0)$. The parameters are $r_L = 0$ and $L = 10\xi$.

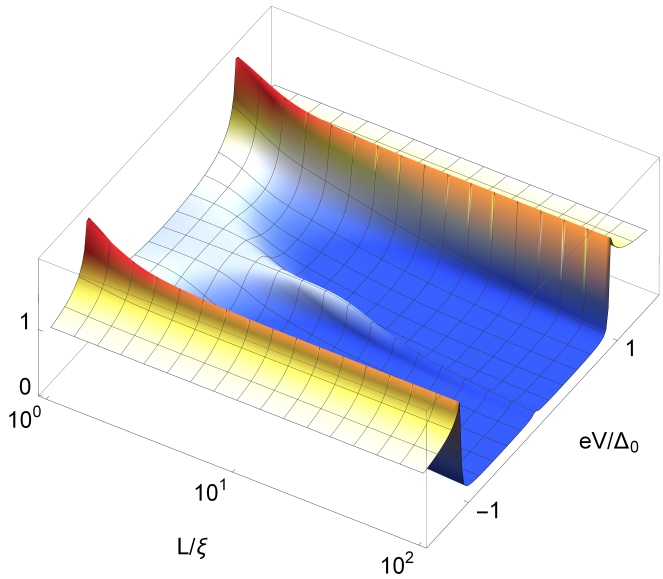

Figure 3.3: The conductivity of an NNS junction as a function of the nanowire length, on a logarithmic scale. The parameters are $r_L = 0$, $r_R = 1$.

3.2 Electric current in NFS junctions

In ferromagnetic materials a magnetic field acts on the electrons flowing through the material. By coupling to the spin of the electrons, this field either increases or decreases their energy, splitting the energy bands into spin sub-bands. When looking at the densities of states of up and down spins independently, we find that while they still align with the DOS in the superconductor close to the boundary, deeper into the wire they shift by the amount of energy added by the field (see figure 3.4) [68]. This shift is independent of the orientation of the field, as we only consider the coupling between the magnetic field and the spin. We will see in section 3.4 however, that the orientation of the magnetic field becomes important when spin-orbit coupling is included, as it should for very thin wires.

A similar effect can be seen in the conductivity of the junction as a function of voltage bias and magnetization, the zero-bias conduction peak we observed in NNS junctions is Zeeman splitted similarly, as shown in figure 3.5. Note that the peaks at $eV = \pm\Delta_0$ and the size of the gap between them remain unchanged under an increase of the magnetic field, as these features are related to the number of available states in the superconducting reservoir, which we here consider to remain unchanged under magnetization of the wire. The results presented here can be compared to the data in Refs. [19–21].

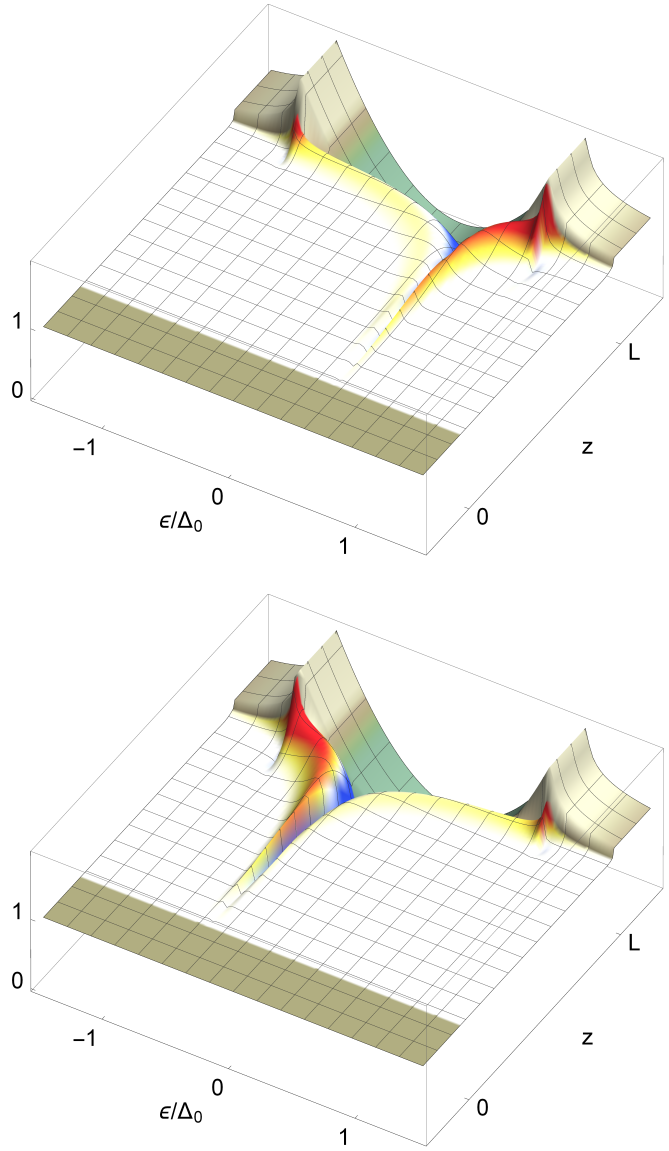

Figure 3.4: The densities of states of an NFS junction for spin-up and spin-down particles, as functions of both energy and position in the wire, normalized to the DOS in the bulk normal metal. The parameters are $r_L = r_R = 0.1$, $\boldsymbol{h} = 50E_{\text{th}}$ and $L = 10\xi$.

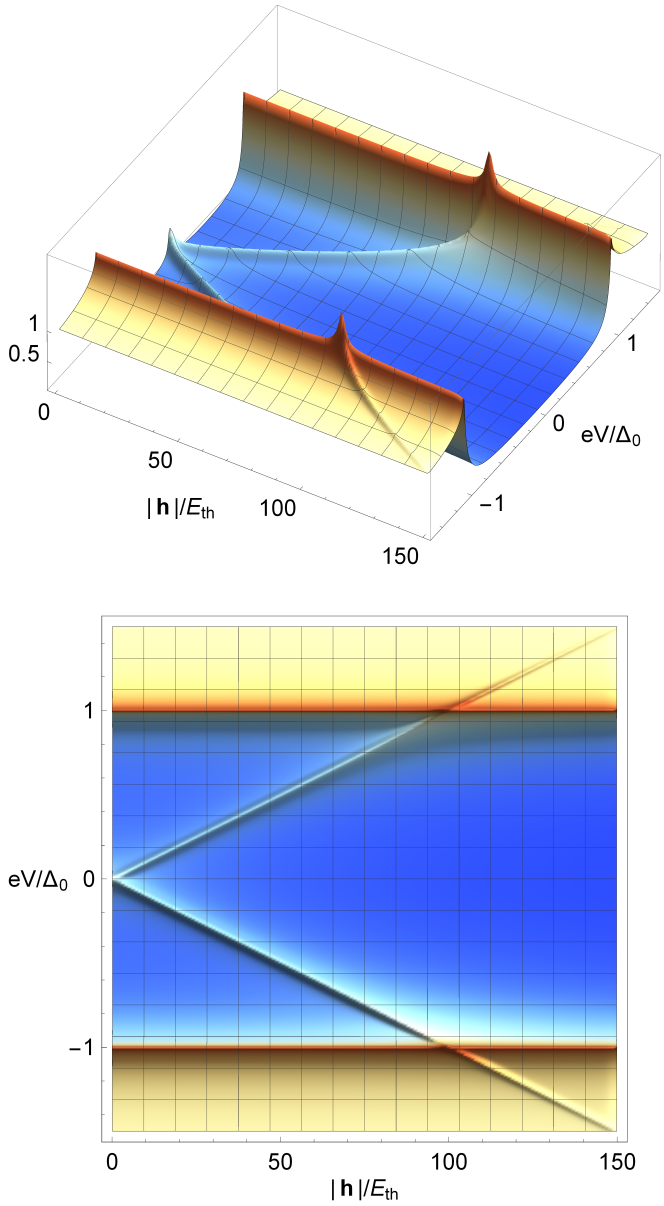

Figure 3.5: The conductivity of an NFS junction as a function of both voltage bias and magnetization, normalized to $\sigma(eV \gg \Delta_0)$. The results are independent of the direction of $\boldsymbol{h}$. The parameters are $r_L = 0$, $r_R = 1$, and $L = 10\xi$.

3.3 Junctions with Néel and Bloch walls

In this section we will consider two very specific types of inhomogeneous ferromagnets: those with continuous rotations of the magnetization throughout the material, either around the wire (a Bloch wall) or in the plane along and orthogonal to it (a Néel wall). Both are shown in figure 3.6.

Whereas a homogeneous magnetic field only creates short-ranged triplet pairs f_t (described in section 1.7.2), inhomogeneity of the field allows for the different electrons in a Cooper pair to on average rotate in opposite directions as they move through the wire in different directions. We will see in this section that the relative densities of the short and long-range triplets are periodic in the number of complete rotations the magnetization makes.

For stronger magnetic fields, the triplet formation happens faster both as a function of position in the wire, and as a function of the rotation of the field. For very strong fields the electron spins align with the field and rotate along as they pass through the wire, and share of short and long-range triplets becomes periodic with the number of total rotations the field makes. For a single complete flip of the field through the wire, two electrons moving in opposite directions flip both spins, ending up in the short-range state $f_t = (f_{\uparrow\downarrow} + f_{\downarrow\uparrow})/\sqrt{2}$. For a rotation of the field by $\pi/2$, the spins in a singlet pair align, and the long-range triplets $f_{\uparrow\uparrow}$ and $f_{\downarrow\downarrow}$ are formed. This periodicity is shown in figure 3.8.

The conductivity of the junction depends heavily on the total rotation of the magnetization, as shown in figure 3.7, where the mixing of different spin components of the Green functions due to the disordering effect of the inhomogeneity reduces the Zeeman splitting of the ZBCP and broadens the peaks. For highly inhomogeneous ferromagnets (such as for $\Delta\theta(\boldsymbol{h}, \hat{\boldsymbol{e}}_z) = 40\pi$ in the graph), the magnetization changes over much shorter distances than the Green functions decay. The magnetization then averages out to zero, and we end up with a single zero-bias conductance peak, as we saw in the NNS case in section 3.1. Note that this peak is not a sign of triplets, but rather a feature of Andreev reflection.

It is worth noting that in the absence of spin-orbit coupling, Bloch and Néel walls leave identical expressions in the equilibrium properties of the junction. This is because without this coupling the magnetic interactions are completely independent of the orientation of the wire, whether it point along or perpendicular to the direction around which the magnetization rotates. Note that long-range triplets in the x and y directions will not show up as diagonal components in the anomalous Green function $\underline{f}$, as their corresponding Pauli matrices are off-diagonal.

The study of Bloch and Néel walls can be extended by accounting for spin-dependent interfacial phase shifts, as discussed in section 1.5. Such phase shifts themselves also have a triplet-creating effect [69]. For a study of similar systems

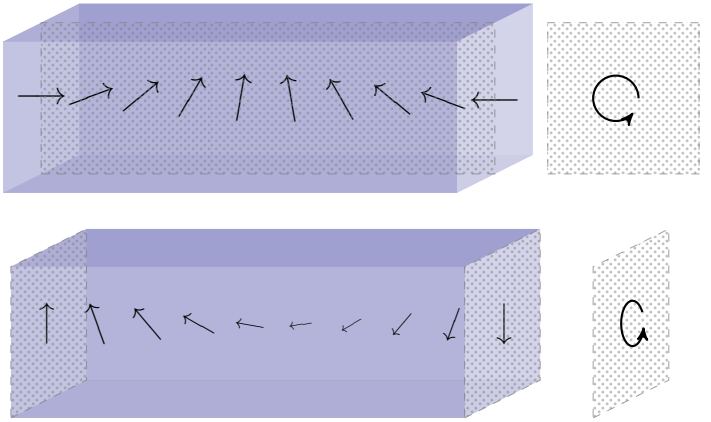

Figure 3.6: There are two types of inhomogeneous ferromagnets we will consider: Néel walls (above) and Bloch walls (below). The former has a magnetization that rotates around a direction perpendicular to the wire, the latter rotates around the orientation of the wire.

for much weaker magnetic fields ($|\boldsymbol{h}| \ll \hat{\Delta}_0$), see reference 48.

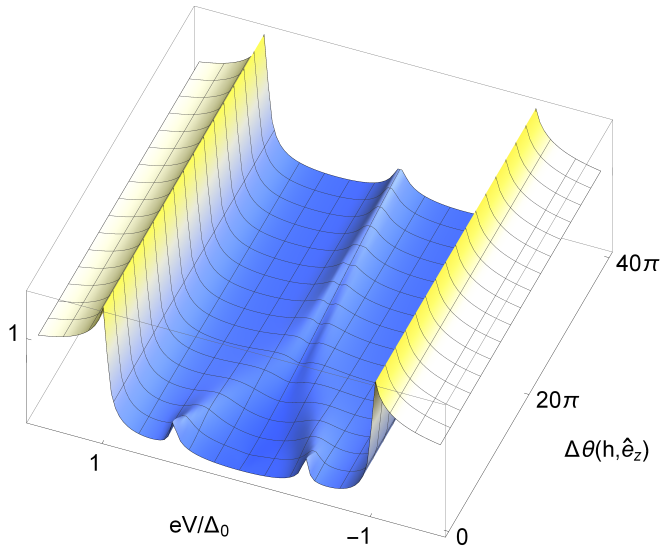

Figure 3.7: The conductivity of a Néel wall with $|\boldsymbol{h}| = 50E_{\mathrm{th}}$ as a function of the total rotation of the magnetization throughout the wire. The parameters are $r_L = r_R = 0.1$, $L = 10\xi$.

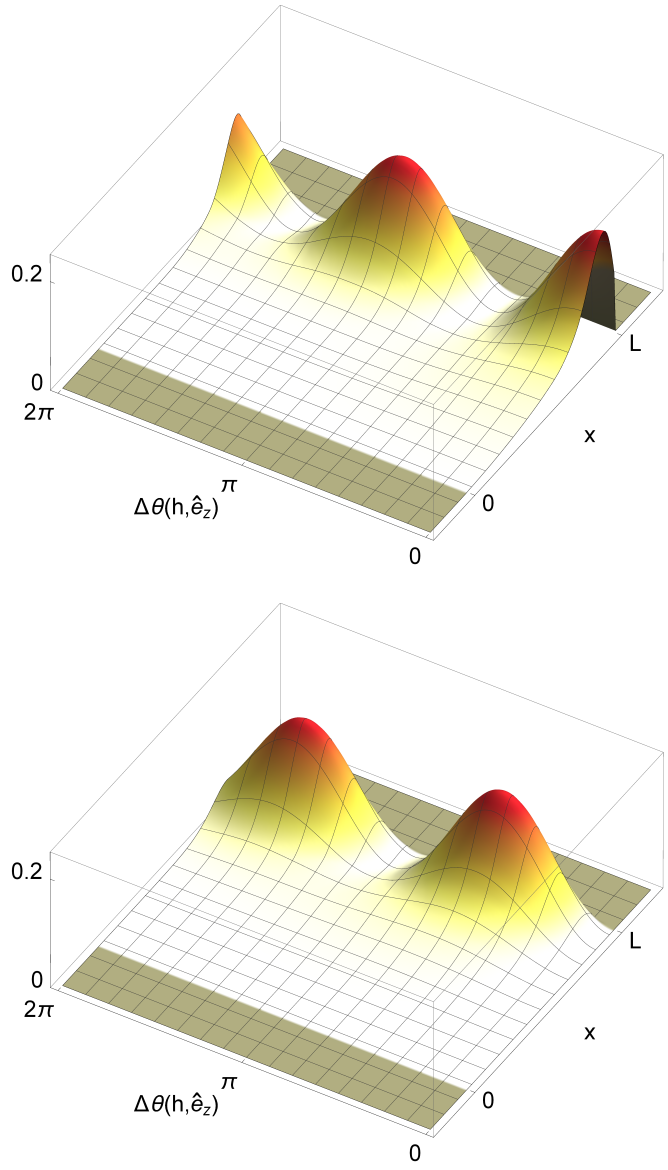

Figure 3.8: The formation of short-ranged (above) and long-ranged (below) triplets in a Néel wall, as a function of the total difference in angle between the magnetic field orientation on the superconducting side and the normal-metal side. The parameters are $r_L = r_R = 0.1$, $L = 10\xi$, and $|\boldsymbol{h}| = 50E_{\text{th}}$.

3.4 NFS junctions with spin-orbit coupling

When the spin is coupled to the momentum, particles with the same momentum but opposing spins will receive an opposite energy contribution from the coupling. Hence, similarly to what we saw in homogeneous ferromagnets in section 3.2, the energy bands will split up into spin sub-bands [34]. Whereas in inhomogeneous ferromagnets, as discussed in section 3.3, the triplet density depends on the misalignment of the magnetization between different points in the wire, in homogeneous ferromagnets with Rashba and Dresselhaus coupling it determined by the misalignment of the magnetization and the spin-orbit coupling. Comparable to the results for Bloch and Néel walls, we see in figure 3.9 that the triplet density is lowest for complete alignment of the magnetic field and the spin-orbit coupling, and highest for complete anti-alignment. The relative variation of singlet, short-range and long-range triplets as a function of the magnetization direction allows for a switch between a zero-energy dip (singlet-dominated) and a zero-energy peak (triplet-dominated), as shown in figure 3.10. Note that even though the Dresselhaus coupling points along the wire, while the Rashba couplings point outwards, they both have the same effect on the density of states when looking only at the orientation of the field relative to the coupling. For a wire with only one Rashba coupling direction (which would necessarily need to be non-symmetric in the x and y-directions), the upper graph would be identical to the lower one, shifted by $\pi/2$. Note that neither the Dresselhaus nor the Rashba coupling have any effect on the density of states in the absence of magnetic fields.

When looking at the differential conductivity of ferromagnetic nanowire junctions with Rasha coupling along the two directions orthogonal to the wire in figure 3.11, we see that the Zeeman splitting of the zero-bias conduction peak (black curve) by a magnetic field (red curve) is reduced by the spin-mixing of spin-orbit coupling orthogonal to the magnetic field (blue curve for one, and green curve for two orthogonal coupling directions). This effect is very similar to that observed in the conductivity of inhomogeneous ferromagnets, as was shown in section 3.3. We conclude that by applying and rotating a magnetic field, the electric behaviour of the junction can be varied considerably.

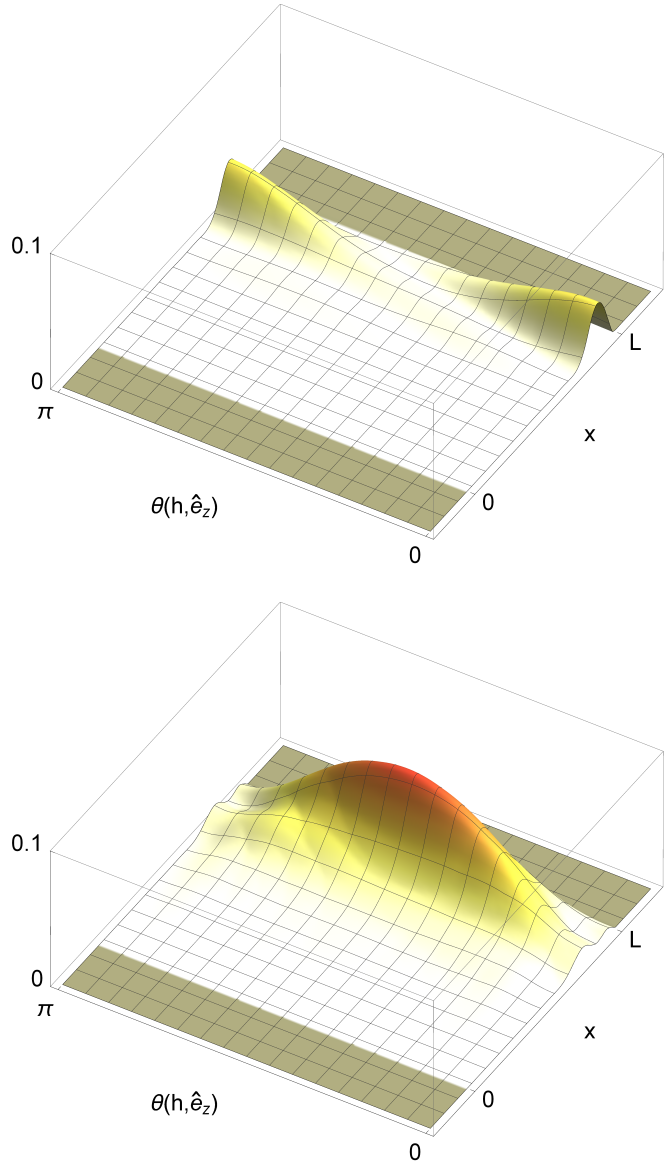

Figure 3.9: The formation of short-ranged (above) and long-ranged (below) triplets in a ferromagnets with spin-orbit coupling, as a function of the angle between the magnetization and the z-direction (along the wire). The parameters are $\alpha_x = \alpha_y = 5$, $\beta = 0$, $r_L = r_R = 0.1$, $L = 10\xi$, and $|\boldsymbol{h}| = 50E_{\text{th}}$.

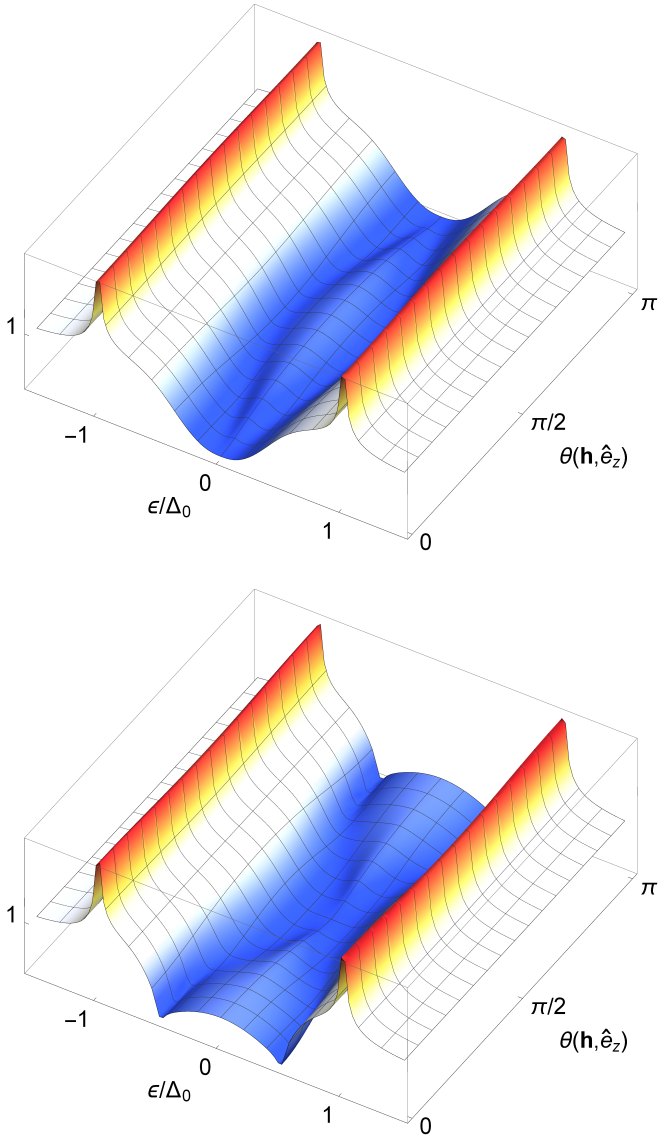

Figure 3.10: The DOS at $x = L$ of an NFS junction as a function of the angle $\theta(\boldsymbol{h}, \hat{\boldsymbol{e}}_z)$ between the magnetic field and the wire orientation, for $|\boldsymbol{h}| = 50E_{\mathrm{th}}$, $r_L = 0$, $r_R = 0.1$, and $L = 10\xi$. The top graph shows pure Rashba coupling with $\alpha_x = \alpha_y = 5$, $\beta = 0$, the bottom graph pure Dresselhaus coupling with $\alpha_x = \alpha_y = 0$, $\beta = 5$.

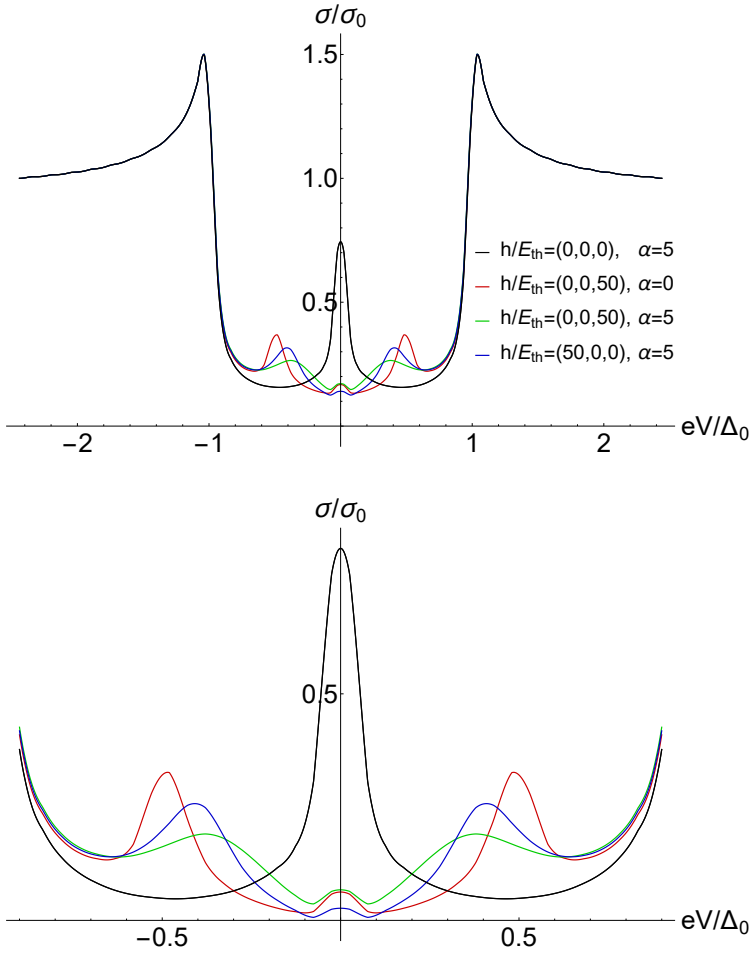

Figure 3.11: The conductivity of a ferromagnetic nanowire for different values of the magnetization and Rashba coupling, with $\beta = 0$, $T = 0.02T_c$, $r_L = 0$, $r_R = 1$, and $L = 10\xi$. (Close up in the plot below.)

Conclusion and outlook

In this thesis different methods to calculate non-equilibrium properties of ferromagnetic superconducting junctions have been presented. An analytical method is derived for and applied to systems without spin-orbit coupling, and a numerical method is presented for systems that do include this. It is found that the density of both short and long-range triplets can be tuned by varying either the inhomogeneity of the magnetization or the orientation of homogeneous magnetic fields with respect to the intrinsic spin-orbit coupling. It is found that for very thin wires, with a diameter below 10 nm, the Rashba coupling due to the confining potential of the wire has a strong diminishing effect on the Zeeman splitting of the differential conductivity spectrum.

The analytical method presented in this thesis allows for the investigation of non-equilibrium effects in inhomogeneous ferromagnetic structures other than Bloch and Néel walls, and should be extended to describe junctions other than nanowires. This method can also be used for research on spin currents, a relevant topic within spintronics.

Appendices

Appendix A

Fourier transformations

Both the main text and the appendices on the derivations of the Usadel equation and the non-equilibrium expressions make heavy use of transformations between spacetime and momentum-energy space. For a complete overview, we cover here the definitions of four-vectors (section A.1), Fourier transformations (sections A.2 and A.3), and different products (sections A.4 through A.7).

A.1 Four-vectors and the metric tensor

Combining the time and position coordinates t and $\boldsymbol{r} = x\hat{\boldsymbol{e}}_x + y\hat{\boldsymbol{e}}_y + z\hat{\boldsymbol{e}}_y$ into one four-dimensional vector, the contravariant four-vector is denoted as

$$x^\mu = \begin{pmatrix} ct \\ x \\ y \\ z \end{pmatrix}.$$

Using the spacelike or Pauli convention, the covariant four-vector is defined as

$$x_\mu = g_{\mu\nu}x^\nu = \left[\begin{pmatrix} -1 & 0 & 0 & 0 \\ 0 & 1 & 0 & 0 \\ 0 & 0 & 1 & 0 \\ 0 & 0 & 0 & 1 \end{pmatrix} \begin{pmatrix} ct \\ x \\ y \\ z \end{pmatrix} \right]^T = \begin{pmatrix} -ct & x & y & z \end{pmatrix}.$$

In a similar fashion we can define the momentum four-vectors:

$$p^\mu = \begin{pmatrix} E/c \\ p_x \\ p_y \\ p_z \end{pmatrix}, \qquad p_\mu = \begin{pmatrix} -E/c & p_x & p_y & p_z \end{pmatrix}.$$

A.2 General Fourier transformations

We define the Fourier transformations between the generic coordinates q and p as follows:

$$\mathscr{F}(f(q)) = \int dq\, e^{-iqp}\, f(q), \qquad \mathscr{F}^{-1}(f(p)) = \frac{1}{2\pi}\int dp\, e^{iqp}\, f(p).$$

A.3 Fourier transformations in spacetime

Using the definitions in section A.1, a Fourier transformation from spacetime to energy-momentum space can be written as

$$\begin{aligned}
\mathscr{F}\left(f(x^\mu)\right) &= \int d^4x\, e^{-ix_\mu p^\mu}\, f(x^\mu) = \int d^4x\, e^{-ix_\mu g^{\mu\nu} p_\nu}\, f(x^\mu) \\
&= \int dt \int d\boldsymbol{r}\, e^{-i(ct,\boldsymbol{r})\cdot(-E/c,\boldsymbol{p})}\, f(ct,\boldsymbol{r}) \\
&= \int dt\, e^{itE} \int d\boldsymbol{r}\, e^{-i\boldsymbol{r}\cdot\boldsymbol{p}}\, f(ct,\boldsymbol{r}) \\
&= f(E/c,\boldsymbol{p}).
\end{aligned}$$

It is now possible to extract the Fourier transformations between time and energy, and between position space and momentum space. Writing them separately, we find

$$\mathscr{F}_{E\leftarrow t} = \int dt\, e^{itE}, \qquad \mathscr{F}^{-1}_{t\leftarrow E} = \frac{1}{2\pi}\int dE\, e^{-itE},$$

$$\mathscr{F}_{\boldsymbol{p}\leftarrow\boldsymbol{r}} = \int d\boldsymbol{r}\, e^{-i\boldsymbol{r}\cdot\boldsymbol{p}}, \qquad \mathscr{F}^{-1}_{\boldsymbol{r}\leftarrow\boldsymbol{p}} = \frac{1}{2\pi}\int d\boldsymbol{p}\, e^{i\boldsymbol{r}\cdot\boldsymbol{p}}.$$

Note the sign difference between the position-momentum and time-energy transformations.

A.4 Convolutions

The convolution $*$ of two functions $f(x)$ and $g(x)$ is given by

$$f(x) * g(x) \equiv \int dx'\, f(x')g(x-x').$$

Using this, we can calculate $\mathscr{F}\big(f(q)\big) * \mathscr{F}\big(g(q)\big)$:

$$\begin{aligned}
\mathscr{F}\big(f(q)\big) * \mathscr{F}\big(g(q)\big) &= \int dp' \left(\int dq_1\, e^{-iq_1p'}\, f(q_1) \right) \left(\int dq_2\, e^{-iq_2(p-p')} g(q_2) \right) \\
&= \int dq_2\, e^{-iq_2p}\, g(q_2) \left(\int dp'\, e^{iq_2p'} \int dq_1\, e^{-iq_1p'}\, f(q_1) \right) \\
&= \int dq_2\, e^{-iq_2p}\, g(q_2)\, \mathscr{F}^{-1}_{q_2 \leftarrow p'} \left(\mathscr{F}_{p' \leftarrow q_1}\big(f(q_1)\big) \right) \\
&= \mathscr{F}\big(f(q) \cdot g(q)\big).
\end{aligned} \tag{A.4.1}$$

Similarly, we can also calculate $\mathscr{F}\big(f(q) * g(q)\big)$:

$$\begin{aligned}
\mathscr{F}\big(f(q) * g(q)\big) &= \int dq_1\, e^{-iq_1p} \int dq_2\, f(q_2) g(q_1 - q_2) \\
&= \int dq_1\, e^{-i(q_1-q_2)p}\, g(q_1 - q_2) \int dq_2\, e^{-iq_2p}\, f(q_2) \\
&= \int dq_1'\, e^{-i(q_1')p}\, g(q_1') \int dq_2\, e^{-iq_2p}\, f(q_2) \\
&= \mathscr{F}\big(f(q)\big) \cdot \mathscr{F}\big(g(q)\big).
\end{aligned} \tag{A.4.2}$$

A.5 The star product

The star product is defined as follows:

$$A(q_1, q_2) \odot B(q_1, q_2) \equiv \mathscr{F}_{p \leftarrow q_\delta} \left(\int dq\, A(q_1, q) B(q, q_2) \right).$$

This can be written as[1]

$$\begin{aligned}
A(q_1, q_2) \odot B(q_1, q_2) = e^{i(\partial^A_{q_\mu} \partial^B_p - \partial^A_p \partial^B_{q_\mu})/2}\, \mathscr{F}_{p \leftarrow q_\delta}\big(A(q_1, q_2)\big) \\
\cdot \mathscr{F}_{p \leftarrow q_\delta}\big(B(q_1, q_2)\big),
\end{aligned}$$

[1] Here we use the notation ∂^A_x for the differential operator ∂_x operating on A. For example, $\partial^A_x(AB) = (\partial_x A)B$ and $\partial^B_x(AB) = A(\partial_x B)$. The exponential function of the operator is defined by its power series $\exp(\partial^A_x) = \sum_{n=0}^{\infty} (\partial^A_x)^n / n!$.

which can be shown as follows.

$$
\begin{aligned}
&A(q_1,q_2)\ \odot B(q_1,q_2)\\
&\qquad = \mathscr{F}_{p\leftarrow q_\delta}\left(\int dq\, A(q_1,q)B(q,q_2)\right)\\
&\qquad = \mathscr{F}_{p\leftarrow q_\delta}\left(\int dq\, A(q_\mu+\tfrac{1}{2}q_\delta,q)B(q,q_\mu-\tfrac{1}{2}q_\delta)\right)\\
&\qquad = \mathscr{F}_{p\leftarrow q_\delta}\left(\int dq\, A(q_\mu+\tfrac{1}{2}q_\delta,q_\mu+q)B(q_\mu+q,q_\mu-\tfrac{1}{2}q_\delta)\right)\\
&\qquad = \int dq_\delta\, e^{-iq_\delta p}\int dq\, A(q_\mu+\tfrac{1}{2}q_\delta,q_\mu+q)B(q_\mu+q,q_\mu-\tfrac{1}{2}q_\delta).
\end{aligned}
$$

Introducing the coupled variables u and v:

$$
\left\{\begin{array}{l} u=q+\frac{1}{2}q_\delta \\ \\ v=q-\frac{1}{2}q_\delta \end{array}\right. , \quad \left\{\begin{array}{l} q=\dfrac{u-v}{2} \\ \\ q_\delta=u+v \end{array}\right. \quad \Rightarrow \quad \mathscr{J}=\left\|\begin{array}{cc} \dfrac{\partial q}{\partial u} & \dfrac{\partial q}{\partial v} \\ \\ \dfrac{\partial q_\delta}{\partial u} & \dfrac{\partial q_\delta}{\partial v} \end{array}\right\|=1,
$$

the integral becomes

$$
\begin{aligned}
A\odot B = \int du\int dv\, e^{-i(u+v)p}\, A\left(q_\mu+\frac{u+v}{2},q_\mu+\frac{u-v}{2}\right)\\
\times B\left(q_\mu+\frac{u-v}{2},q_\mu-\frac{u+v}{2}\right).
\end{aligned}
$$

The two arguments of both functions are similar, apart from a shift by u or v, which allows us to simplify the equations by defining

$$
\tilde{A}(q,y)=A\left(q+\frac{y}{2},q-\frac{y}{2}\right),
$$

$$
\tilde{A}\left(q_\mu+\frac{u}{2},v\right)=A\left(q_\mu+\frac{u+v}{2},q_\mu+\frac{u-v}{2}\right),
$$

$$
\tilde{B}(q,y)=B\left(q+\frac{y}{2},q-\frac{y}{2}\right),
$$

$$
\tilde{B}\left(q_\mu-\frac{v}{2},u\right)=B\left(q_\mu+\frac{u-v}{2},q_\mu-\frac{u+v}{2}\right),
$$

leading to

$$A \odot B = \int du \int dv \, e^{-i(u+v)p} \, \tilde{A}\left(q_\mu + \frac{u}{2}, v\right) \tilde{B}\left(q_\mu - \frac{v}{2}, u\right). \tag{A.5.1}$$

In order to extract the Fourier transforms, we need to create two independent integrals. This can be done by Taylor expanding the functions $\tilde{A}$ and $\tilde{B}$, absorbing the u dependence of $\tilde{A}$ and the v dependence of $\tilde{B}$ in infinite sums that can be taken out of the integral. As the Taylor expansion of $\tilde{A}$ around $u = 0$,

$$\tilde{A}\left(q_\mu + \frac{u}{2}, v\right) = \sum_{n=0}^{\infty} \left[\partial_u^n \tilde{A}\left(q_\mu + \frac{u}{2}, v\right)\right]_{u=0} \frac{u^n}{n!},$$

can be written in terms of derivations to q_μ instead of u using

$$\frac{df(a + \frac{1}{2}b)}{db} = \frac{1}{2} \frac{df(a + \frac{1}{2})}{da},$$

we can write

$$\tilde{A}\left(q_\mu + \frac{u}{2}, v\right) = \sum_{n=0}^{\infty} \frac{(u/2)^n}{n!} \, \partial_{q_\mu}^n \tilde{A}\left(q_\mu, v\right).$$

Similarly,

$$\tilde{B}\left(q_\mu - \frac{v}{2}, u\right) = \sum_{n=0}^{\infty} \frac{(-v/2)^n}{n!} \, \partial_{q_\mu}^n \tilde{B}\left(q_\mu, u\right).$$

Substituting this back into equation (A.5.1), we find

$$\begin{aligned} A \odot B = & \sum_{n,m=0}^{\infty} \frac{1}{n!} \frac{1}{m!} \int dv \, \left(\frac{-v}{2}\right)^m e^{-ivp} \, \partial_{q_\mu}^n \tilde{A}\left(q_\mu, v\right) \\ & \times \int du \, \left(\frac{u}{2}\right)^n e^{-iup} \, \partial_{q_\mu}^m \tilde{B}\left(q_\mu, u\right) \\ = & \sum_{n,m=0}^{\infty} \frac{(\partial_{q_\mu}^A)^n}{n!} \frac{(\partial_{q_\mu}^B)^m}{m!} \int dv \left(\frac{-i\partial_p}{2}\right)^m e^{-ivp} \, \tilde{A}\left(q_\mu, v\right) \\ & \times \int du \left(\frac{i\partial_p}{2}\right)^n e^{-iup} \, \tilde{B}\left(q_\mu, u\right). \end{aligned} \tag{A.5.2}$$

As the functions $\tilde{A}(q_\mu, v)$ and $\tilde{B}(q_\mu, u)$ do not depend on p, we can simply put the operators ∂_p in front of the integrals:

$$\begin{aligned} A \odot B &= \sum_{n,m=0}^{\infty} \frac{(\partial_{q_\mu}^A)^n}{n!} \frac{(\partial_{q_\mu}^B)^m}{m!} \left(\frac{-i\partial_p}{2}\right)^m A(q_\mu, p) \left(\frac{i\partial_p}{2}\right)^n B(q_\mu, p) \\ &= \sum_{n,m=0}^{\infty} \frac{(i\partial_{q_\mu}^A \partial_p^B)^n/2}{n!} \frac{(-i\partial_p^A \partial_{q_\mu}^B)^m/2}{m!} A(q_\mu, p) B(q_\mu, p) \\ &= e^{i(\partial_{q_\mu}^A \partial_p^B - \partial_p^A \partial_{q_\mu}^B)/2} A(q_\mu, p) B(q_\mu, p). \end{aligned} \tag{A.5.3}$$

A.5.1 The star product in case one of the arguments depends on only a single coordinate

Whereas the normal star product was defined as

$$A(q_1, q_2) \odot B(q_1, q_2) \equiv \mathscr{F}_{p \leftarrow q_\delta} \left(\int dq\, A(q_1, q) B(q, q_2) \right),$$

the star product of two functions where one depends only on a single variable is defined simply as

$$A(q_1) \odot B(q_1, q_2) \equiv \mathscr{F}_{p \leftarrow q_\delta} \big(A(q_1) B(q_1, q_2) \big).$$

Writing this down in the mixed representation as

$$A(q_1) \odot B(q_1, q_2) = \int dq_\delta\, e^{-iq_\delta p}\, A(q_\mu + \tfrac{1}{2} q_\delta) B(q_\mu + \tfrac{1}{2} q_\delta, q_\mu - \tfrac{1}{2} q_\delta),$$

we can without further ado Taylor expand A:

$$A(q_\mu + \tfrac{1}{2} q_\delta) = \sum_{n=0}^{\infty} \frac{(q_\delta/2)^n}{n!}\, \partial_{q_\mu}^n A(q_\mu).$$

Bringing the terms that do not depend on q_δ outside the integral, this gives

$$\begin{aligned} A(q_1) \odot B(q_1, q_2) &= \sum_{n=0}^{\infty} \frac{(\partial^A_{q_\mu})^n}{n!} A(q_\mu) \\ &\quad \times \int dq_\delta \left(\frac{q_\delta}{2}\right)^n e^{-iq_\delta p}\, B(q_\mu + \tfrac{1}{2}q_\delta, q_\mu - \tfrac{1}{2}q_\delta) \\ &= \sum_{n=0}^{\infty} \frac{(i\partial^A_{q_\mu}\partial^B_p/2)^n}{n!} A(q_\mu) \\ &\quad \times \int dq_\delta\, e^{-iq_\delta p}\, B(q_\mu + \tfrac{1}{2}q_\delta, q_\mu - \tfrac{1}{2}q_\delta) \\ &= e^{i(\partial^A_{q_\mu}\partial^B_p)/2}\, A(q_\mu)B(q_\mu, p). \end{aligned} \tag{A.5.4}$$

A.6 The bullet product

The bullet product is a special case of the star product in which both the spatial and time coordinates are convoluted:

$$A(x_1, x_2) \bullet B(x_1, x_2) = \mathscr{F}\left(\int d\boldsymbol{r} \int dt\, A(x_1, x)B(x, x_2)\right),$$

where x, x_1 and x_2 are four-vectors. This is similar to equation (A.5.3), with the difference that here we replace the scalar coordinates with four-vectors:

$$A(x_1, x_2) \bullet B(x_1, x_2) = e^{i(\partial^A_x\partial^B_p - \partial^A_p\partial^B_x)/2} A(x, p)B(x, p).$$

Here the subscript μ on the four-vectors is left out to avoid confusion. The double derivatives $\partial^A_x\partial^B_p$ and $\partial^A_p\partial^B_x$ are invariant inner products between two operators with four components:

$$\partial^A_x\partial^B_p = \left(\partial^A_x\right)_\mu \left(\partial^B_p\right)^\mu = \begin{pmatrix} \partial^A_{-ct} & \nabla^A_{\boldsymbol{r}} \end{pmatrix} \begin{pmatrix} \partial^B_{E/c} \\ \nabla^B_{\boldsymbol{p}} \end{pmatrix} = -\partial^A_t\partial^B_E + \nabla^A_{\boldsymbol{r}}\nabla^B_{\boldsymbol{p}}. \tag{A.6.1}$$

An other way to trace the origin of the minus sign in front of the first term is to look at the first and second line of equations (A.5.2, A.5.4), where the exponential function would have the opposite sign, as derived in section A.3.

With this we can write the bullet product explicitly in terms of time and position coordinates:

$$\begin{aligned} &A(\boldsymbol{r}_1,t_1;\boldsymbol{r}_2,t_2)\bullet B(\boldsymbol{r}_1,t_1;\boldsymbol{r}_2,t_2)\\ &\qquad=\mathscr{F}_{\boldsymbol{p}\leftarrow\boldsymbol{r}_\delta,\,\varepsilon\leftarrow t_\delta}\left(\int d\boldsymbol{r}\int dt\,A(\boldsymbol{r}_1,t_1;\boldsymbol{r},t)B(\boldsymbol{r},t;\boldsymbol{r}_2,t_2)\right) \qquad \text{(A.6.2)}\\ &\qquad=e^{\frac{i}{2}\left(-\partial_t^A\partial_\varepsilon^B+\partial_\varepsilon^A\partial_t^B+\nabla_{\boldsymbol{r}}^A\nabla_{\boldsymbol{p}}^B-\nabla_{\boldsymbol{p}}^A\nabla_{\boldsymbol{r}}^B\right)}A(\boldsymbol{r},t,\boldsymbol{p},\varepsilon)B(\boldsymbol{r},t,\boldsymbol{p},\varepsilon), \end{aligned}$$

where the spatial and time coordinates on the right hand side are the average coordinates in the mixed representation.

A.6.1 The bullet product in case one of the arguments depends on only a single set of coordinates

If one of the functions depends on only one set of coordinates, the bullet product simplifies to

$$A(x_1)\bullet B(x_1,x_2)=\mathscr{F}\left(A(x_1)B(x_1,x_2)\right).$$

In correspondence with equation (A.5.4), this can be written as

$$A(x_1)\bullet B(x_1,x_2)=e^{i\left(\partial_x^A\partial_p^B\right)/2}A(x)B(x,p).$$

Making use of equation (A.6.1) again, this brings us to

$$\begin{aligned} A(\boldsymbol{r}_1,t_1)\bullet B(\boldsymbol{r}_1,t_1;\boldsymbol{r}_2,t_2)&=\mathscr{F}_{\boldsymbol{p}\leftarrow\boldsymbol{r}_\delta,\,\varepsilon\leftarrow t_\delta}\left(A(\boldsymbol{r}_1,t_1)B(\boldsymbol{r}_1,t_1;\boldsymbol{r}_2,t_2)\right)\\ &=e^{i\left(-\partial_t^A\partial_\varepsilon^B+\nabla_{\boldsymbol{r}}^A\nabla_{\boldsymbol{p}}^B\right)/2}A(\boldsymbol{r},t)B(\boldsymbol{r},t,\boldsymbol{p},\varepsilon). \end{aligned}$$

Similarly, the bullet product in case the second set of coordinates is shared is given by

$$B(\boldsymbol{r}_1,t_1;\boldsymbol{r}_2,t_2)\bullet A(\boldsymbol{r}_2,t_2)=e^{i\left(\partial_t^A\partial_\varepsilon^B-\nabla_{\boldsymbol{r}}^A\nabla_{\boldsymbol{p}}^B\right)/2}B(\boldsymbol{r},t,\boldsymbol{p},\varepsilon)A(\boldsymbol{r},t).$$

These two equations can be used to define commutators. Using the shorthand notation

$$A=A(\boldsymbol{r}_1,t_1),\qquad B=B(\boldsymbol{r}_1,t_1;\boldsymbol{r}_2,t_2),$$

the bullet commutator and anticommutator can be defined as

$$[A\overset{\bullet}{,}B]_\pm=e^{i\left(-\partial_t^A\partial_\varepsilon^B+\nabla_{\boldsymbol{r}}^A\nabla_{\boldsymbol{p}}^B\right)/2}AB\pm e^{i\left(\partial_t^A\partial_\varepsilon^B-\nabla_{\boldsymbol{r}}^A\nabla_{\boldsymbol{p}}^B\right)/2}BA.$$

A.7 The ring product

The ring product is a special case of the bullet product in which only the time and energy derivatives remain. In the case where both functions depend on two sets of coordinates, this means that

$$A(\boldsymbol{r}_1, t_1; \boldsymbol{r}_2, t_2) \circ B(\boldsymbol{r}_1, t_1; \boldsymbol{r}_2, t_2) = e^{\frac{i}{2}\left(-\partial_t^A \partial_\varepsilon^B + \partial_\varepsilon^A \partial_t^B\right)} A(\boldsymbol{r}, t, \boldsymbol{p}, \varepsilon) B(\boldsymbol{r}, t, \boldsymbol{p}, \varepsilon).$$

Similarly, in the case where one of the functions depends on only a single set of coordinates, we get

$$A(\boldsymbol{r}_1, t_1) \circ B(\boldsymbol{r}_1, t_1; \boldsymbol{r}_2, t_2) = e^{i\left(-\partial_t^A \partial_\varepsilon^B\right)/2} A(\boldsymbol{r}, t) B(\boldsymbol{r}, t, \boldsymbol{p}, \varepsilon)$$

or

$$B(\boldsymbol{r}_1, t_1; \boldsymbol{r}_2, t_2) \circ A(\boldsymbol{r}_2, t_2) = e^{i\left(\partial_t^A \partial_\varepsilon^B\right)/2} B(\boldsymbol{r}, t, \boldsymbol{p}, \varepsilon) A(\boldsymbol{r}, t).$$

Appendix B

Electromagnetic properties

To account for electromagnetic interactions, the regular derivative is often replaced by the covariant derivative in the main text. This appendix covers both its derivation and some often-invoked properties.

B.1 The covariant derivative

An electromagnetic gauge transformation represented by the unitary operator U with $U^{-1} = U^\dagger$ is given by [70]

$$\boldsymbol{A} \longmapsto \boldsymbol{A} - \frac{1}{e}\nabla\lambda, \qquad U(\boldsymbol{r}) = e^{i\lambda(\boldsymbol{r})}, \qquad U^\dagger(\boldsymbol{r}) = e^{-i\lambda(\boldsymbol{r})}.$$

This transforms the annihilation operator as

$$\psi_\sigma \longmapsto \psi_\sigma{}' = U\psi_\sigma.$$

Gauge invariance of the number operator helps us derive the transformation of the creation operator:

$$\psi_\sigma^\dagger\psi_\sigma \longmapsto (\psi_\sigma^\dagger)'U\psi_\sigma = \psi_\sigma^\dagger\psi_\sigma \qquad \Rightarrow \qquad \psi_\sigma^\dagger \longmapsto (\psi_\sigma^\dagger)' = \psi_\sigma^\dagger U^\dagger.$$

The normal spatial derivatives of ψ_σ and $\psi_\sigma^\dagger$ would under such a transformation behave as

$$\nabla\psi_\sigma \longmapsto \nabla(U\psi_\sigma) \;= U(\nabla + i\nabla\lambda)\psi_\sigma,$$

$$\nabla\psi_\sigma^\dagger \longmapsto \nabla(\psi_\sigma^\dagger U^\dagger) = U(\nabla - i\nabla\lambda)\psi_\sigma^\dagger.$$

Defining the covariant derivative $\tilde{\nabla}$ such that it commutes with the gauge transformation, this must satisfy

$$\tilde{\nabla}(U\psi_\sigma) = U\tilde{\nabla}\psi_\sigma, \quad \tilde{\nabla}(\psi_\sigma^\dagger U^\dagger) = (\tilde{\nabla}\psi_\sigma^\dagger)U^\dagger.$$

Writing $\tilde{\nabla}$ as the normal derivative with a correction term,

$$\tilde{\nabla} = \nabla + X,$$

this means that

$$\tilde{\nabla}\psi_\sigma \longmapsto U(\nabla + i\nabla\lambda + X')\psi_\sigma \quad \Rightarrow \quad X\psi_\sigma \longmapsto UX'\psi_\sigma = U(X - i\nabla\lambda)\psi_\sigma,$$

$$\tilde{\nabla}\psi_\sigma^\dagger \longmapsto U(\nabla - i\nabla\lambda + X')\psi_\sigma^\dagger \quad \Rightarrow \quad X\psi_\sigma^\dagger \longmapsto UX'\psi_\sigma^\dagger = U(X + i\nabla\lambda)\psi_\sigma^\dagger.$$

We find that X behaves as $\pm ie\boldsymbol{A}$, and hence

$$\tilde{\nabla} = \nabla \pm ie\boldsymbol{A}, \tag{B.1.1}$$

where the upper sign is for the annihilation operator and the lower sign for the creation operator.

B.2 The covariant derivative acting on pairs of operators

Taking into account the matrix structure of the vector potential in this thesis, the 4×4 and 8×8 dimensional structures of $\boldsymbol{A}$ are given by [30]

$$\hat{\underline{\boldsymbol{A}}} = \begin{pmatrix} \underline{\boldsymbol{A}} & 0 \\ 0 & -\underline{\boldsymbol{A}}^\star \end{pmatrix}, \qquad \check{\underline{\boldsymbol{A}}} = \check{\mathbb{1}} \otimes \begin{pmatrix} \underline{\boldsymbol{A}} & 0 \\ 0 & -\underline{\boldsymbol{A}}^\star \end{pmatrix}. \tag{B.2.1}$$

The covariant derivatives then operate on ψ and $\psi^\dagger$ as follows:

$$\tilde{\nabla}\psi = \nabla\psi + ie\hat{\underline{\boldsymbol{A}}}\psi,$$

$$\tilde{\nabla}\psi^\dagger = \nabla\psi^\dagger - ie\psi^\dagger\hat{\underline{\boldsymbol{A}}}.$$

The covariant derivatives of the two products $\psi\psi^\dagger$ and $\psi^\dagger\psi$ are therefore:

$$\begin{aligned}
\tilde{\nabla}\left(\psi\psi^\dagger\right) &= \left(\tilde{\nabla}\psi\right)\psi^\dagger + \psi\left(\tilde{\nabla}\psi^\dagger\right) \\
&= \left(\nabla\psi + ie\underline{\hat{\boldsymbol{A}}}\psi\right)\psi^\dagger + \psi\left(\nabla\psi^\dagger - ie\psi^\dagger\underline{\hat{\boldsymbol{A}}}\right) \\
&= \nabla\left(\psi\psi^\dagger\right) + ie\left[\underline{\hat{\boldsymbol{A}}}, \psi\psi^\dagger\right]_- , \\
\tilde{\nabla}\left(\psi^\dagger\psi\right) &= \left(\tilde{\nabla}\psi^\dagger\right)\psi + \psi^\dagger\left(\tilde{\nabla}\psi\right) \\
&= \left(\nabla\psi^\dagger - ie\psi^\dagger\underline{\hat{\boldsymbol{A}}}\right)\psi + \psi^\dagger\left(\nabla\psi + ie\underline{\hat{\boldsymbol{A}}}\psi\right) \\
&= \nabla\left(\psi^\dagger\psi\right).
\end{aligned} \tag{B.2.2}$$

Appendix C

Green's functions

This thesis is written in the language of quasiclassical theory, where the dynamics of te system are described by the Green functions, which describe correlations between the field operators. The formalism is introduced with definitions of the most important objects, with references to relevant literature where needed.

C.1 The Keldysh formalism

Using the Keldysh formalism, we write the Green functions as [46, 47, 71, 72]

$$\begin{aligned} G^R_{\sigma\sigma'}(\boldsymbol{r},t;\boldsymbol{r}',t') &\equiv -i\left\langle \left[\psi_\sigma(\boldsymbol{r},t),\psi^\dagger_{\sigma'}(\boldsymbol{r}',t')\right]_\pm \right\rangle \Theta(t-t'), \\ G^A_{\sigma\sigma'}(\boldsymbol{r},t;\boldsymbol{r}',t') &\equiv +i\left\langle \left[\psi_\sigma(\boldsymbol{r},t),\psi^\dagger_{\sigma'}(\boldsymbol{r}',t')\right]_\pm \right\rangle \Theta(t'-t), \\ G^K_{\sigma\sigma'}(\boldsymbol{r},t;\boldsymbol{r}',t') &\equiv -i\left\langle \left[\psi_\sigma(\boldsymbol{r},t),\psi^\dagger_{\sigma'}(\boldsymbol{r}',t')\right]_\mp \right\rangle, \end{aligned} \tag{C.1.1}$$

where the order of the times t and t' in the Heaviside step function determines whether the annihilation happens before or after the creation. The sign $\pm$ and $\mp$ denote the difference between bosons and fermions, with the upper sign for fermions and the lower sign for bosons. In the retarded Green function the creation happens before the annihilation, whereas annihilation comes first in the advanced Green function. These functions provide information about the transport of particles: the retarded Green function gives the probability amplitude for a particle to be at $\boldsymbol{r}$ at time t given that it was at $\boldsymbol{r}'$ at time t [25], the advanced Green function describes the same for holes. The Keldysh function is the only function defined

as a commutator instead of an anticommutator (or anticommutator instead of a commutator in case of bosons), providing non-equilibrium information [47, 63].

The anomalous Green functions give correlations between two annihilation operators (as their conjugates do for two creation operators):

$$F^R_{\sigma\sigma'}(\boldsymbol{r},t;\boldsymbol{r}',t') \equiv -i\left\langle \left[\psi_\sigma(\boldsymbol{r},t),\psi_{\sigma'}(\boldsymbol{r}',t')\right]_\pm \right\rangle \Theta(t-t'),$$

$$F^A_{\sigma\sigma'}(\boldsymbol{r},t;\boldsymbol{r}',t') \equiv +i\left\langle \left[\psi_\sigma(\boldsymbol{r},t),\psi_{\sigma'}(\boldsymbol{r}',t')\right]_\pm \right\rangle \Theta(t'-t),$$

$$F^K_{\sigma\sigma'}(\boldsymbol{r},t;\boldsymbol{r}',t') \equiv -i\left\langle \left[\psi_\sigma(\boldsymbol{r},t),\psi_{\sigma'}(\boldsymbol{r}',t')\right]_\mp \right\rangle .$$

In non-superconducting systems we would not expect any correlation between two particles at different locations and times, and the anomalous Green functions should be zero. In the case of superconductivity, however, we see a time-delayed interaction between electrons of opposite spin, and these functions will yield nonzero values. The singlet and triplet densities can be calculated from the different spin-space components of these functions, as described in section 1.7.2.

We now focus on fermions, assuming spin-1/2 particles. The one-dimensional Green functions have two spin indices, allowing four different spin combinations. We can combine these four correlations in one function, forming 2×2 matrices:

$$\underline{G}^{R,A,K} \equiv \begin{pmatrix} G^{R,A,K}_{\uparrow\uparrow} & G^{R,A,K}_{\uparrow\downarrow} \\ G^{R,A,K}_{\downarrow\uparrow} & G^{R,A,K}_{\downarrow\downarrow} \end{pmatrix}, \qquad \underline{F}^{R,A,K} \equiv \begin{pmatrix} F^{R,A,K}_{\uparrow\uparrow} & F^{R,A,K}_{\uparrow\downarrow} \\ F^{R,A,K}_{\downarrow\uparrow} & F^{R,A,K}_{\downarrow\downarrow} \end{pmatrix}.$$

The elements of the matrices describe different scenarios, the top-right element of $\underline{G}^R$ for example gives the probability of a spin-up particle at spacetime coordinate $\boldsymbol{r},t$ to induce a spin-down particle at $\boldsymbol{r}',t'$. Going one step further, we can define the 4×4 Green functions:

$$\hat{\underline{G}}^R = \begin{pmatrix} \underline{G}^R & \underline{F}^R \\ -\tilde{\underline{F}}^R & -\tilde{\underline{G}}^R \end{pmatrix}, \quad \hat{\underline{G}}^A = \begin{pmatrix} \underline{G}^A & \underline{F}^A \\ -\tilde{\underline{F}}^A & -\tilde{\underline{G}}^A \end{pmatrix}, \quad \hat{\underline{G}}^K = \begin{pmatrix} \underline{G}^K & \underline{F}^K \\ -\tilde{\underline{F}}^K & -\tilde{\underline{G}}^K \end{pmatrix}. \tag{C.1.2}$$

These matrices can be rewritten in terms of the Nambu 4-vector from eq. (1.1.3) such that

$$\begin{aligned} \hat{\underline{G}}^R &= -i\hat{\underline{\rho}}_3 \left\langle \left[\psi(\boldsymbol{r},t),\psi^\dagger(\boldsymbol{r}',t')\right]_+ \right\rangle \Theta(t-t'), \\ \hat{\underline{G}}^A &= +i\hat{\underline{\rho}}_3 \left\langle \left[\psi(\boldsymbol{r},t),\psi^\dagger(\boldsymbol{r}',t')\right]_+ \right\rangle \Theta(t'-t), \\ \hat{\underline{G}}^K &= -i\hat{\underline{\rho}}_3 \left\langle \left[\psi(\boldsymbol{r},t),\psi^\dagger(\boldsymbol{r}',t')\right]_- \right\rangle . \end{aligned} \tag{C.1.3}$$

Here the commutators are interpreted component-wise, meaning that

$$\left\langle \left[\psi(\boldsymbol{r},t),\psi^\dagger(\boldsymbol{r}',t')\right]_\pm \right\rangle_{ij} = \left\langle \left[\psi_i(\boldsymbol{r},t),\psi_j^\dagger(\boldsymbol{r}',t')\right]_\pm \right\rangle. \tag{C.1.4}$$

Combining the above 4×4 functions into one 8×8 matrix, we write[1]

$$\check{\underline{G}} = \begin{pmatrix} \hat{\underline{G}}^R & \hat{\underline{G}}^K \\ 0 & \hat{\underline{G}}^A \end{pmatrix}. \tag{C.1.5}$$

C.2 The quasiclassical approximation

In the quasiclassical approximation we assume that the net transport happens at the Fermi surface [24]. In this case the small-scale oscillations of the Green function are well defined. As we are generally interested in the behaviour of the Green function over distances much larger than the Fermi wavelength, we can compensate for these oscillations and focus on the outline that envelops them.

Taking into the assumption that the momentum is confined to the Fermi surface, the envelope of the Green function can be described by [46, 47, 73]

$$\boxed{\check{\underline{g}}^R(\boldsymbol{r},\boldsymbol{p},\epsilon,t) = \frac{i}{\pi}\int \delta(|\boldsymbol{p}|-|\boldsymbol{p}_F|)\,\mathscr{F}[\check{\underline{G}}^R(\boldsymbol{r},t;\boldsymbol{r}',t')]d\xi_{\boldsymbol{p}},} \tag{C.2.1}$$

where we integrate over kinetic energy,

$$\xi_{\boldsymbol{p}} = \frac{\boldsymbol{p}^2}{2m}. \tag{C.2.2}$$

By writing a factor i/π in front of the integral here, we assure that the function $\check{\underline{g}}$ is normalized such that [54]

$$\check{\underline{g}} \bullet \check{\underline{g}} = \check{\underline{1}}. \tag{C.2.3}$$

We have now defined the quasiclassical Green function

$$\check{\underline{g}} = \begin{pmatrix} \hat{\underline{g}}^R & \hat{\underline{g}}^K \\ 0 & \hat{\underline{g}}^A \end{pmatrix}, \tag{C.2.4}$$

with components

$$\hat{\underline{g}}^R = \begin{pmatrix} \underline{g}^R & \underline{f}^R \\ -\tilde{\underline{f}}^R & -\tilde{\underline{g}}^R \end{pmatrix}, \quad \hat{\underline{g}}^A = \begin{pmatrix} \underline{g}^A & \underline{f}^A \\ -\tilde{\underline{f}}^A & -\tilde{\underline{g}}^A \end{pmatrix}, \quad \hat{\underline{g}}^K = \begin{pmatrix} \underline{g}^K & \underline{f}^K \\ -\tilde{\underline{f}}^K & -\tilde{\underline{g}}^K \end{pmatrix}. \tag{C.2.5}$$

It follows from our normalization condition that

$$\hat{\underline{g}}^R \bullet \hat{\underline{g}}^R = \hat{\underline{g}}^A \bullet \hat{\underline{g}}^A = 1, \qquad \hat{\underline{g}}^R \bullet \hat{\underline{g}}^K + \hat{\underline{g}}^K \bullet \hat{\underline{g}}^A = 0. \tag{C.2.6}$$

[1] The choice of arranging the components like this has been motivated in Ref. 46.

Appendix D

Full derivation of the Usadel equation

The systems in chapter 3 are studied by solving the equilibrium and non-equilibrium diffusion equations. These equations are components of the Usadel equation, which is derived in this appendix.

D.1 Equations of motion for the field operators

As described in sections 1.2.1 to 1.2.3, the Hamiltonian in equation (1.2.1) contains sets of two and four field operators. As these are fermion fields, which satisfy the anticommutation relations in equation (1.1.2), it will be useful to express the right-hand side of the Heisenberg relations in equation (1.2.1) in terms of anticommutators.

Looking more closely at the Hamiltonian, we find that there the terms can be grouped by their type of summation. There is one term involving only a spatial integral ($\mathcal{H}_{\mathrm{BCS}}$), two terms involving a spatial integral and a single spin sum ($\mathcal{H}_0$ and $\mathcal{H}_{\mathrm{imp}}$), and one term involving a spatial integral and a double spin sum ($\mathcal{H}_{\mathrm{sf}}$).

Starting with $\mathcal{H}_{\mathrm{BCS}}$, we encounter the following expression:

$$\begin{aligned}\Big[\psi_\sigma(\boldsymbol{r},t), \int d\boldsymbol{r}' \Big(\Delta^\star(\boldsymbol{r}',t)\psi_\downarrow(\boldsymbol{r}',t)\psi_\uparrow(\boldsymbol{r}',t) + \Delta(\boldsymbol{r}',t)\psi_\uparrow^\dagger(\boldsymbol{r}',t)\psi_\downarrow^\dagger(\boldsymbol{r}',t)\Big)\Big]_- \\ = \int d\boldsymbol{r}' \Big(\Big[\psi_\sigma(\boldsymbol{r},t), \Delta^\star(\boldsymbol{r}',t)\psi_\downarrow(\boldsymbol{r}',t)\psi_\uparrow(\boldsymbol{r}',t)\Big]_- \\ + \Big[\psi_\sigma(\boldsymbol{r},t), \Delta(\boldsymbol{r}',t)\psi_\uparrow^\dagger(\boldsymbol{r}',t)\psi_\downarrow^\dagger(\boldsymbol{r}',t)\Big]_- \Big).\end{aligned} \tag{D.1.1}$$

As the gap function Δ is a mere scalar, it can be pulled out of the integral, leaving us with the commutators

$$\Big[\psi_\sigma(\boldsymbol{r},t),\psi_\downarrow(\boldsymbol{r}',t)\psi_\uparrow(\boldsymbol{r}',t)\Big]_- \qquad \text{and} \qquad \Big[\psi_\sigma(\boldsymbol{r},t),\psi^\dagger_\uparrow(\boldsymbol{r}',t)\psi^\dagger_\downarrow(\boldsymbol{r}',t)\Big]_- .$$

Using now that

$$[A,BC]_- = [A,B]_+ C - B\,[A,C]_+ , \tag{D.1.2}$$

we find the anticommutators we were looking for:

$$\begin{aligned}
\Big[\psi_\sigma(\boldsymbol{r},t),\psi_\downarrow(\boldsymbol{r}',t)\psi_\uparrow(\boldsymbol{r}',t)\Big]_- &= \underbrace{\Big[\psi_\sigma(\boldsymbol{r},t),\psi_\downarrow(\boldsymbol{r}',t)\Big]_+}_{0}\psi_\uparrow(\boldsymbol{r}',t) \\
&\quad -\psi_\downarrow(\boldsymbol{r}',t)\underbrace{\Big[\psi_\sigma(\boldsymbol{r},t),\psi_\uparrow(\boldsymbol{r}',t)\Big]_+}_{0}, \\
\Big[\psi_\sigma(\boldsymbol{r},t),\psi^\dagger_\uparrow(\boldsymbol{r}',t)\psi^\dagger_\downarrow(\boldsymbol{r}',t)\Big]_- &= \underbrace{\Big[\psi_\sigma(\boldsymbol{r},t),\psi^\dagger_\uparrow(\boldsymbol{r}',t)\Big]_+}_{\delta(\boldsymbol{r}-\boldsymbol{r}')\delta_{\sigma,\uparrow}}\psi^\dagger_\downarrow(\boldsymbol{r}',t) \\
&\quad -\psi^\dagger_\uparrow(\boldsymbol{r}',t)\underbrace{\Big[\psi_\sigma(\boldsymbol{r},t),\psi^\dagger_\downarrow(\boldsymbol{r}',t)\Big]_+}_{\delta(\boldsymbol{r}-\boldsymbol{r}')\delta_{\sigma,\downarrow}}.
\end{aligned}$$

Substituting these results back in equation (D.1.1), we find

$$\begin{aligned}
\big[\psi_\sigma(\boldsymbol{r},t),\mathcal{H}_{\text{BCS}}\big]_- &= \int d\boldsymbol{r}'\Delta(\boldsymbol{r}',t)\Big(\delta(\boldsymbol{r}-\boldsymbol{r}')\delta_{\sigma,\uparrow}\psi^\dagger_\downarrow(\boldsymbol{r}',t) \\
&\quad -\psi^\dagger_\uparrow(\boldsymbol{r}',t)\delta(\boldsymbol{r}-\boldsymbol{r}')\delta_{\sigma,\sigma'}\Big) \\
&= \Delta(\boldsymbol{r},t)\left(\delta_{\sigma,\uparrow}\psi^\dagger_\downarrow(\boldsymbol{r},t)-\delta_{\sigma,\downarrow}\psi^\dagger_\uparrow(\boldsymbol{r},t)\right).
\end{aligned}$$

Similarly, the commutator between $\psi^\dagger_\sigma$ and $\mathcal{H}_{\text{BCS}}$ is found to be

$$\big[\psi^\dagger_\sigma(\boldsymbol{r},t),\mathcal{H}_{\text{BCS}}\big]_- = \Delta^\star(\boldsymbol{r},t)\left(\delta_{\sigma,\downarrow}\psi_\uparrow(\boldsymbol{r},t)-\delta_{\sigma,\uparrow}\psi_\downarrow(\boldsymbol{r},t)\right),$$

which can be checked with

$$\big[\psi^\dagger_\sigma,\mathcal{H}\big]_- = i\partial_t\psi^\dagger_\sigma = -\left(i\partial_t\psi_\sigma\right)^\dagger = -\Big(\big[\psi_\sigma,\mathcal{H}\big]_-\Big)^\dagger . \tag{D.1.3}$$

Moving on to the next part of the Hamiltonian, by writing

$$H_{0+\mathrm{imp}} = -\frac{\hbar^2}{2m}\tilde{\nabla}^2 + q\varphi - \mu + V_{\mathrm{imp}}(\boldsymbol{r}),$$

the commutator becomes, employing again equation (D.1.2),

$$\begin{aligned}\left[\psi_\sigma(\boldsymbol{r},t), \mathcal{H}_0 + \mathcal{H}_{\mathrm{imp}}\right]_- &= \sum_{\sigma'}\int d\boldsymbol{r}' \left[\psi_\sigma(\boldsymbol{r},t), \psi^\dagger_{\sigma'}(\boldsymbol{r}',t) H_{0+\mathrm{imp}}\psi_{\sigma'}(\boldsymbol{r}',t)\right]_- \\ &= \sum_{\sigma'}\int d\boldsymbol{r}' \underbrace{\left[\psi_\sigma(\boldsymbol{r},t), \psi^\dagger_{\sigma'}(\boldsymbol{r}',t)\right]_+}_{\delta(\boldsymbol{r}-\boldsymbol{r}')\delta_{\sigma,\sigma'}} H_{0+\mathrm{imp}}\psi_{\sigma'}(\boldsymbol{r}',t) \\ &\quad -\psi^\dagger_{\sigma'}(\boldsymbol{r}',t)\underbrace{\left[\psi_\sigma(\boldsymbol{r},t), H_{0+\mathrm{imp}}\psi_{\sigma'}(\boldsymbol{r}',t)\right]_+}_{0}.\end{aligned}$$

Performing the sum and integration, we are left with

$$\left[\psi_\sigma(\boldsymbol{r},t), \mathcal{H}_0 + \mathcal{H}_{\mathrm{imp}}\right]_- = H_{0+\mathrm{imp}}\psi_\sigma(\boldsymbol{r},t). \tag{D.1.4}$$

Comparably, using equation (D.1.3), we find

$$\left[\psi^\dagger_\sigma(\boldsymbol{r},t), \mathcal{H}_0 + \mathcal{H}_{\mathrm{imp}}\right]_- = -\psi^\dagger_\sigma(\boldsymbol{r},t) H^\dagger_{0+\mathrm{imp}}, \tag{D.1.5}$$

where $H^\dagger_{0+\mathrm{imp}}$ works to the left. The last remaining terms are the commutator between ψ_σ and $\mathcal{H}_{\mathrm{sf}}$ and $\mathcal{H}_{\mathbf{h}}$. Looking at $\mathcal{H}_{\mathrm{sf}}$ first:

$$\begin{aligned}&\left[\psi_\sigma(\boldsymbol{r},t), \mathcal{H}_{\mathrm{sf}}\right]_- \\ &\quad= \sum_{\sigma',\sigma''}\int d\boldsymbol{r}' \left[\psi_\sigma(\boldsymbol{r},t), \psi^\dagger_{\sigma''}(\boldsymbol{r},t)\left[\underline{\boldsymbol{\sigma}}\cdot\boldsymbol{S}(\boldsymbol{r}')\right]_{\sigma''\sigma'} V_{\mathrm{sf}}(\boldsymbol{r}')\psi_{\sigma'}(\boldsymbol{r}',t)\right]_- \\ &\quad= \sum_{\sigma',\sigma''}\int d\boldsymbol{r}' \underbrace{\left[\psi_\sigma(\boldsymbol{r},t), \psi^\dagger_{\sigma''}(\boldsymbol{r},t)\right]_+}_{\delta(\boldsymbol{r}-\boldsymbol{r}')\delta_{\sigma,\sigma''}} \left[\underline{\boldsymbol{\sigma}}\cdot\boldsymbol{S}(\boldsymbol{r}')\right]_{\sigma''\sigma'} V_{\mathrm{sf}}(\boldsymbol{r}')\psi_{\sigma'}(\boldsymbol{r}',t) \\ &\qquad -\psi^\dagger_{\sigma''}(\boldsymbol{r},t)\underbrace{\left[\psi_\sigma(\boldsymbol{r},t), \left[\underline{\boldsymbol{\sigma}}\cdot\boldsymbol{S}(\boldsymbol{r}')\right]_{\sigma''\sigma'} V_{\mathrm{sf}}(\boldsymbol{r}')\psi_{\sigma'}(\boldsymbol{r}',t)\right]_+}_{0} \\ &\quad= \sum_{\sigma'}\left[\underline{\boldsymbol{\sigma}}\cdot\boldsymbol{S}(\boldsymbol{r})\right]_{\sigma\sigma'} V_{\mathrm{sf}}(\boldsymbol{r})\psi_{\sigma'}(\boldsymbol{r},t),\end{aligned}$$

and thus

$$\left[\psi^\dagger_\sigma(\boldsymbol{r},t),\mathcal{H}_{\rm sf}\right]_- = -\sum_{\sigma'}\psi^\dagger_{\sigma'}(\boldsymbol{r},t)V_{\rm sf}(\boldsymbol{r})\left[\underline{\boldsymbol{\sigma}}\cdot\boldsymbol{S}(\boldsymbol{r})\right]^\dagger_{\sigma'\sigma},$$

and

$$\left[\psi^\dagger_\sigma(\boldsymbol{r},t),\mathcal{H}_{\mathbf{h}}\right]_- = \sum_{\sigma'}\psi^\dagger_{\sigma'}(\boldsymbol{r},t)\left[\underline{\boldsymbol{\sigma}}\cdot\boldsymbol{h}(\boldsymbol{r})\right]^\dagger_{\sigma'\sigma}, \tag{D.1.6}$$

where the indices on the spin interaction are switched as the dagger conjugation includes both complex conjugation and transposition. Collecting terms,

$$\begin{aligned}
i\partial_t\psi_\sigma(\boldsymbol{r},t) &= H_{0+\rm imp}\psi_\sigma(\boldsymbol{r},t)+\Delta(\boldsymbol{r},t)\left(\delta_{\sigma,\uparrow}\psi^\dagger_\downarrow(\boldsymbol{r},t)-\delta_{\sigma,\downarrow}\psi^\dagger_\uparrow(\boldsymbol{r},t)\right)\\
&\quad+\sum_{\sigma'}\left[\underline{\boldsymbol{\sigma}}\cdot\boldsymbol{S}(\boldsymbol{r})\right]_{\sigma\sigma'}V_{\rm sf}(\boldsymbol{r})\psi_{\sigma'}(\boldsymbol{r},t)-\sum_{\sigma'}\left[\underline{\boldsymbol{\sigma}}\cdot\boldsymbol{h}(\boldsymbol{r})\right]_{\sigma\sigma'}\psi_{\sigma'}(\boldsymbol{r},t),\\
i\partial_t\psi^\dagger_\sigma(\boldsymbol{r},t) &= -\psi^\dagger_\sigma(\boldsymbol{r},t)H^\dagger_{0+\rm imp}+\Delta^\star(\boldsymbol{r},t)\left(\delta_{\sigma,\downarrow}\psi_\uparrow(\boldsymbol{r},t)-\delta_{\sigma,\uparrow}\psi_\downarrow(\boldsymbol{r},t)\right)\\
&\quad-\sum_{\sigma'}\psi^\dagger_{\sigma'}(\boldsymbol{r},t)V_{\rm sf}(\boldsymbol{r})\left[\underline{\boldsymbol{\sigma}}\cdot\boldsymbol{S}(\boldsymbol{r})\right]^\dagger_{\sigma'\sigma}+\sum_{\sigma'}\psi^\dagger_{\sigma'}(\boldsymbol{r},t)\left[\underline{\boldsymbol{\sigma}}\cdot\boldsymbol{h}(\boldsymbol{r})\right]^\dagger_{\sigma'\sigma}.
\end{aligned}$$

Writing

$$\underline{V}=V_{\rm sf}\left[\underline{\boldsymbol{\sigma}}\cdot\boldsymbol{S}\right]-\underline{\boldsymbol{\sigma}}\cdot\boldsymbol{h},$$

we can rewrite the last two terms here as a matrix multiplication:

$$\sum_{\sigma'}\psi^\dagger_{\sigma'}V^\dagger_{\sigma'\sigma}=\sum_{\sigma'}V^\dagger_{\sigma'\sigma}\psi^\dagger_{\sigma'}=\sum_{\sigma'}V^\star_{\sigma\sigma'}\psi^\dagger_{\sigma'}=\underline{V}^\star_\sigma\psi^\dagger,$$

where $\underline{V}_\sigma$ is the σth row of $\underline{V}$, so that we end up with

$$\begin{aligned}
i\partial_t\psi_\sigma &= H_{0+\rm imp}\psi_\sigma+\Delta\left(\delta_{\sigma,\uparrow}\psi^\dagger_\downarrow-\delta_{\sigma,\downarrow}\psi^\dagger_\uparrow\right)+\underline{V}_\sigma\psi_{\sigma'},\\
i\partial_t\psi^\dagger_\sigma &= -\psi^\dagger_\sigma H^\dagger_{0+\rm imp}+\Delta^\star\left(\delta_{\sigma,\downarrow}\psi_\uparrow-\delta_{\sigma,\uparrow}\psi_\downarrow\right)-\underline{V}^\star_\sigma\psi^\dagger_{\sigma'}.
\end{aligned}$$

Using the definitions in equation (1.1.3), these two equations can be combined:

$$i\partial_t\begin{pmatrix}\psi_\uparrow\\ \psi_\downarrow\\ \psi^\dagger_\uparrow\\ \psi^\dagger_\downarrow\end{pmatrix}=\begin{pmatrix}H'+V_{\uparrow\uparrow} & V_{\uparrow\downarrow} & 0 & \Delta\\ V_{\downarrow\uparrow} & H'+V_{\downarrow\downarrow} & -\Delta & 0\\ 0 & -\Delta^\star & -H'^\star-\boldsymbol{V}^\star_{\uparrow\uparrow} & -\boldsymbol{V}^\star_{\uparrow\downarrow}\\ \Delta^\star & 0 & -\boldsymbol{V}^\star_{\downarrow\uparrow} & -H'^\star-\boldsymbol{V}^\star_{\downarrow\downarrow}\end{pmatrix}\begin{pmatrix}\psi_\uparrow\\ \psi_\downarrow\\ \psi^\dagger_\uparrow\\ \psi^\dagger_\downarrow\end{pmatrix},$$

where $H' = H_{0+\mathrm{imp}}$. We recognize the symmetry of equation (D.1.3) clearly; the bottom half of the matrix is simply minus the conjugate of the line above. To express this, we move this minus sign to the lhs of the equation in the form of $\underline{\hat{\rho}}_3$. Applying also equation (D.1.3), we find

$$\boxed{i\underline{\hat{\rho}}_3\partial_t\psi = \underline{\hat{\boldsymbol{H}}}\psi, \quad \text{and} \quad -i\partial_t\psi^\dagger\underline{\hat{\rho}}_3 = \psi^\dagger\underline{\hat{\boldsymbol{H}}}^\dagger.} \tag{D.1.7}$$

where

$$\begin{aligned}\underline{\hat{\boldsymbol{H}}} &= \begin{pmatrix} H'+V_{\uparrow\uparrow} & V_{\uparrow\downarrow} & 0 & \Delta \\ V_{\downarrow\uparrow} & H'+V_{\downarrow\downarrow} & -\Delta & 0 \\ 0 & \Delta^\star & H'^\star+V^\star_{\uparrow\uparrow} & V^\star_{\downarrow\uparrow} \\ -\Delta^\star & 0 & V^\star_{\uparrow\downarrow} & H'^\star+V^\star_{\downarrow\downarrow} \end{pmatrix} \\ &= \begin{pmatrix} \underline{H'}+\underline{V} & \underline{\Delta} \\ \underline{\Delta}^\dagger & \underline{H'}^\dagger+\underline{V}^\dagger \end{pmatrix},\end{aligned} \tag{D.1.8}$$

and the anti-Hermitian matrix $\underline{\Delta} = -\underline{\Delta}^\dagger$ is defined as

$$\underline{\Delta} \equiv \begin{pmatrix} 0 & \Delta \\ -\Delta & 0 \end{pmatrix}. \tag{D.1.9}$$

D.2 Equations of motion for Green's functions

The time derivative of the retarded Green function, as defined in equation (C.1.3), is given by

$$\begin{aligned}\partial_t\underline{\hat{G}}^R &= -i\underline{\hat{\rho}}_3\left\langle\left[\partial_t\psi(\boldsymbol{r},t),\psi^\dagger(\boldsymbol{r}',t')\right]_+\right\rangle\Theta(t-t') \\ &\quad -i\underline{\hat{\rho}}_3\left\langle\left[\psi(\boldsymbol{r},t),\psi^\dagger(\boldsymbol{r}',t')\right]_+\right\rangle\partial_t\Theta(t-t') \\ &= -i\left\langle\left[\underline{\hat{\rho}}_3\partial_t\psi(\boldsymbol{r},t),\psi^\dagger(\boldsymbol{r}',t')\right]_+\right\rangle\Theta(t-t') \\ &\quad -i\underline{\hat{\rho}}_3\delta(\boldsymbol{r}-\boldsymbol{r}')\delta(t-t').\end{aligned}$$

Here the matrix $\underline{\hat{\rho}}_3$ is moved into the anticommutator and to the first argument in the first term. Because $\underline{\hat{\rho}}_3$ is Hermitian, we can do this for bosons as well. This

allows us to insert equation (D.1.7):

$$\partial_t \hat{\underline{G}}^R = -i \left\langle \left[-i\hat{\underline{\boldsymbol{H}}}(\boldsymbol{r},t)\psi(\boldsymbol{r},t), \psi^\dagger(\boldsymbol{r}',t') \right]_+ \right\rangle \Theta(t-t')$$

$$-i\hat{\underline{\rho}}_3 \delta(\boldsymbol{r}-\boldsymbol{r}')\delta(t-t').$$

Since $\hat{\underline{\boldsymbol{H}}}(\boldsymbol{r},t)$ acts on neither $\boldsymbol{r}'$ nor t, we can move it outside the commutator. Multiplying also by $i\hat{\underline{\rho}}_3^{-1} = i\hat{\underline{\rho}}_3$ from the left, we get

$$i\hat{\underline{\rho}}_3 \partial_t \hat{\underline{G}}^R = -i\hat{\underline{\boldsymbol{H}}}(\boldsymbol{r},t)\hat{\underline{\rho}}_3 \left\langle \left[\psi(\boldsymbol{r},t), \psi^\dagger(\boldsymbol{r}',t') \right]_+ \right\rangle \Theta(t-t')$$

$$+\delta(\boldsymbol{r}-\boldsymbol{r}')\delta(t-t').$$

Here we recognize the definition of the Green function again, which gives us

$$\left(i\hat{\underline{\rho}}_3 \partial_t - \hat{\underline{\boldsymbol{H}}}(\boldsymbol{r},t) \right) \hat{\underline{G}}^R = \delta(\boldsymbol{r}-\boldsymbol{r}')\delta(t-t').$$

Similarly, taking the derivative of the Green function with respect to t' instead of t, we use the second equation in (D.1.7), leading to

$$\hat{\underline{G}}^R \left(i\hat{\underline{\rho}}_3 \partial_{t'} - \hat{\underline{\boldsymbol{H}}}(\boldsymbol{r}',t') \right)^\dagger = \delta(\boldsymbol{r}-\boldsymbol{r}')\delta(t-t').$$

Introducing the 8×8 Hamiltonian

$$\boxed{\check{\boldsymbol{H}} = \mathbb{1}^{2\times 2} \otimes \hat{\underline{\boldsymbol{H}}} = \begin{pmatrix} H' + \boldsymbol{V} & \boldsymbol{\Delta} & 0 & 0 \\ \boldsymbol{\Delta}^\dagger & H'^\dagger + \boldsymbol{V}^\dagger & 0 & 0 \\ 0 & 0 & H' + \boldsymbol{V} & \boldsymbol{\Delta} \\ 0 & 0 & \boldsymbol{\Delta}^\dagger & H'^\dagger + \boldsymbol{V}^\dagger \end{pmatrix},} \tag{D.2.1}$$

and the 8×8 Pauli matrix

$$\check{\underline{\rho}}_3 = \mathbb{1}^{2\times 2} \otimes \hat{\underline{\rho}}_3 = \begin{pmatrix} \underline{1} & 0 & 0 & 0 \\ 0 & -\underline{1} & 0 & 0 \\ 0 & 0 & \underline{1} & 0 \\ 0 & 0 & 0 & -\underline{1} \end{pmatrix},$$

we can now use the other definitions in equation (C.1.3) to find similar equations for the advanced and Keldysh components and combine the results in the notation of equation (C.1.5) [46, 74]:

$$\boxed{\begin{aligned} \left(i\check{\underline{\rho}}_3 \partial_t - \check{\boldsymbol{H}}(\boldsymbol{r},t) \right) \check{\underline{G}} &= \delta(\boldsymbol{r}-\boldsymbol{r}')\delta(t-t'), \\ \check{\underline{G}} \left(i\check{\underline{\rho}}_3 \partial_{t'} - \check{\boldsymbol{H}}(\boldsymbol{r}',t') \right)^\dagger &= \delta(\boldsymbol{r}-\boldsymbol{r}')\delta(t-t'). \end{aligned}} \tag{D.2.2}$$

D.3 The Eilenberger equation

Equations (D.2.2) have identical terms on the right-hand sides, which implies that the left-hand sides must be equal:

$$\left(i\check{\underline{\rho}}_3\partial_t - \check{\boldsymbol{H}}(\boldsymbol{r},t)\right)\check{\underline{G}} = \check{\underline{G}}\left(i\check{\underline{\rho}}_3\partial_{t'} - \check{\boldsymbol{H}}(\boldsymbol{r}',t')\right)^\dagger,$$

or

$$i\check{\underline{\rho}}_3\,\partial_t\check{\underline{G}} + i\partial_{t'}\check{\underline{G}}\,\check{\underline{\rho}}_3 = \check{\boldsymbol{H}}(\boldsymbol{r},t)\check{\underline{G}} - \check{\underline{G}}\check{\boldsymbol{H}}^\dagger(\boldsymbol{r}',t').$$

This equation contains two different time derivatives, which can be united by defining a relative and an average time coordinate:

$$t_\mu = \frac{t+t'}{2},\quad t_\delta = t - t' \qquad \Rightarrow \qquad \partial_t = \frac{1}{2}\partial_{t_\mu} + \partial_{t_\delta},\quad \partial_{t'} = \frac{1}{2}\partial_{t_\mu} - \partial_{t_\delta},$$

which turns the left-hand side into

$$(\text{lhs}) = i\check{\underline{\rho}}_3\left(\frac{1}{2}\partial_{t_\mu} + \partial_{t_\delta}\right)\check{\underline{G}} + i\left(\frac{1}{2}\partial_{t_\mu} - \partial_{t_\delta}\right)\check{\underline{G}}\,\check{\underline{\rho}}_3.$$

A change of coordinates in which we exchange t_δ for its Fourier transform ϵ (the energy of the system described by $\check{\underline{G}}$), allows us to discard one of the derivatives:

$$\mathscr{F}_{\epsilon\leftarrow t_\delta}\left[\partial_{t_\delta}\check{\underline{G}}\right] = \int dt_\delta\, e^{it_\delta\epsilon}\,\partial_{t_\delta}\check{\underline{G}} = e^{it_\delta\epsilon}\,\check{\underline{G}}\Big|_{-\infty}^{\infty} - \int dt_\delta\, i\epsilon\, e^{it_\delta\epsilon}\,\check{\underline{G}} = -i\epsilon\check{\underline{G}}, \tag{D.3.1}$$

which means that

$$\mathscr{F}_{\epsilon\leftarrow t_\delta}(\text{lhs}) = i\check{\underline{\rho}}_3\left(\frac{1}{2}\partial_{t_\mu} - i\epsilon\right)\check{\underline{G}} + i\left(\frac{1}{2}\partial_{t_\mu} + i\epsilon\right)\check{\underline{G}}\,\check{\underline{\rho}}_3.$$

Collecting these terms, the left-hand side can be written as

$$(\text{lhs}) = \frac{i}{2}\left[\check{\underline{\rho}}_3, \partial_{t_\mu}\check{\underline{G}}\right]_+ + \left[\epsilon\check{\underline{\rho}}_3, \check{\underline{G}}\right]_-.$$

As there are no spatial operators on this side, we can go on and implicitly Fourier transform to momentum space:

$$\frac{i}{2}\left[\check{\underline{\rho}}_3, \partial_{t_\mu}\check{\underline{G}}\right]_+ + \left[\epsilon\check{\underline{\rho}}_3, \check{\underline{G}}\right]_- = \mathscr{F}_{\epsilon\leftarrow t_\delta,\,\boldsymbol{p}\leftarrow\boldsymbol{r}_\delta}\left(\check{\boldsymbol{H}}(\boldsymbol{r},t)\check{\underline{G}} - \check{\underline{G}}\check{\boldsymbol{H}}^\dagger(\boldsymbol{r}',t')\right). \tag{D.3.2}$$

Until now, we have only specified that we consider fermions, apart from that the above equality holds true for any Hamiltonian $\check{\boldsymbol{H}}$. To gain more information, we

now have to specify the Hamiltonian. Looking at equation (D.2.1), we identify three different terms

$$\begin{aligned}
H'(\boldsymbol{r},t) &= -\frac{\hbar^2}{2m}\tilde{\nabla}^2_{\boldsymbol{r}} + q\varphi - \mu + V_{\mathrm{imp}}(\boldsymbol{r}),\\
\underline{V}(\boldsymbol{r},t) &= V_{\mathrm{sf}}(\boldsymbol{r}) \begin{pmatrix} [\underline{\boldsymbol{\sigma}}\cdot\boldsymbol{S}(\boldsymbol{r})]_{\uparrow\uparrow} & [\underline{\boldsymbol{\sigma}}\cdot\boldsymbol{S}(\boldsymbol{r})]_{\uparrow\downarrow} \\ [\underline{\boldsymbol{\sigma}}\cdot\boldsymbol{S}(\boldsymbol{r})]_{\downarrow\uparrow} & [\underline{\boldsymbol{\sigma}}\cdot\boldsymbol{S}(\boldsymbol{r})]_{\downarrow\downarrow} \end{pmatrix} - \begin{pmatrix} [\underline{\boldsymbol{\sigma}}\cdot\boldsymbol{h}(\boldsymbol{r})]_{\uparrow\uparrow} & [\underline{\boldsymbol{\sigma}}\cdot\boldsymbol{h}(\boldsymbol{r})]_{\uparrow\downarrow} \\ [\underline{\boldsymbol{\sigma}}\cdot\boldsymbol{h}(\boldsymbol{r})]_{\downarrow\uparrow} & [\underline{\boldsymbol{\sigma}}\cdot\boldsymbol{h}(\boldsymbol{r})]_{\downarrow\downarrow} \end{pmatrix}\\
&= V_{\mathrm{sf}}(\boldsymbol{r})\underline{\boldsymbol{\sigma}}\cdot\boldsymbol{S}(\boldsymbol{r}) - \underline{\boldsymbol{\sigma}}\cdot\boldsymbol{h}(\boldsymbol{r}),\\
\boldsymbol{\Delta}(\boldsymbol{r},t) &= \begin{pmatrix} 0 & \Delta(\boldsymbol{r},t) \\ -\Delta(\boldsymbol{r},t) & 0 \end{pmatrix} = i\Delta(\boldsymbol{r},t)\underline{\sigma}_2.
\end{aligned} \tag{D.3.3}$$

Using equation (B.1.1):

$$\tilde{\nabla} \equiv \nabla + ie\boldsymbol{A} \quad \Rightarrow \quad \tilde{\nabla}^2 = \nabla^2 + ie(\nabla\cdot\boldsymbol{A} + \boldsymbol{A}\cdot\nabla) - e^2\boldsymbol{A}^2,$$

and introducing the average and relative spatial coordinates $\boldsymbol{r}_\mu$ and $\boldsymbol{r}_\delta$:

$$\boldsymbol{r}_\mu = \frac{\boldsymbol{r}+\boldsymbol{r}'}{2}, \quad \boldsymbol{r}_\delta = \boldsymbol{r}-\boldsymbol{r}' \quad \Rightarrow \quad \nabla_{\boldsymbol{r}} = \frac{1}{2}\nabla_{\boldsymbol{r}_\mu} + \nabla_{\boldsymbol{r}_\delta}, \quad \nabla_{\boldsymbol{r}'} = \frac{1}{2}\nabla_{\boldsymbol{r}_\mu} - \nabla_{\boldsymbol{r}_\delta},$$

we can rewrite $\tilde{\nabla}^2_{\boldsymbol{r}}$ and $\tilde{\nabla}^2_{\boldsymbol{r}'}$. This leads to

$$\begin{aligned}
\tilde{\nabla}^2_{\boldsymbol{r}} &= \frac{1}{4}\nabla^2_{\boldsymbol{r}_\mu} + \nabla^2_{\boldsymbol{r}_\delta} + \nabla_{\boldsymbol{r}_\mu}\cdot\nabla_{\boldsymbol{r}_\delta}\\
&\quad + ie\left[\left(\frac{1}{2}\nabla_{\boldsymbol{r}_\mu} + \nabla_{\boldsymbol{r}_\delta}\right)\cdot\boldsymbol{A} + \boldsymbol{A}\cdot\left(\frac{1}{2}\nabla_{\boldsymbol{r}_\mu} + \nabla_{\boldsymbol{r}_\delta}\right)\right] - e^2\boldsymbol{A}^2,\\
\tilde{\nabla}^2_{\boldsymbol{r}'} &= \frac{1}{4}\nabla^2_{\boldsymbol{r}_\mu} + \nabla^2_{\boldsymbol{r}_\delta} - \nabla_{\boldsymbol{r}_\mu}\cdot\nabla_{\boldsymbol{r}_\delta}\\
&\quad + ie\left[\left(\frac{1}{2}\nabla_{\boldsymbol{r}_\mu} - \nabla_{\boldsymbol{r}_\delta}\right)\cdot\boldsymbol{A} + \boldsymbol{A}\cdot\left(\frac{1}{2}\nabla_{\boldsymbol{r}_\mu} - \nabla_{\boldsymbol{r}_\delta}\right)\right] - e^2\boldsymbol{A}^2.
\end{aligned} \tag{D.3.4}$$

When calculating the term $\tilde{\nabla}^2_{\boldsymbol{r}}\underline{\check{G}} - \underline{\check{G}}\left(\tilde{\nabla}^2_{\boldsymbol{r}'}\right)^\dagger$, we can discard the first two terms in $\tilde{\nabla}^2_{\boldsymbol{r}}$ and $\tilde{\nabla}^2_{\boldsymbol{r}'}$. As the latter acts to the left, they leave

$$\left(\frac{1}{4}\nabla^2_{\boldsymbol{r}_\mu} + \nabla^2_{\boldsymbol{r}_\delta}\right)\underline{\check{G}} - \underline{\check{G}}\left(\frac{1}{4}\nabla^2_{\boldsymbol{r}_\mu} + \nabla^2_{\boldsymbol{r}_\delta}\right)^\dagger = 0.$$

Fourier transforming the pair of derivatives $\nabla_{\boldsymbol{r}_\mu} \cdot \nabla_{\boldsymbol{r}_\delta}$ acting on $\underline{\check{G}}$ gives

$$\begin{aligned}
\mathscr{F}\left(\nabla_{\boldsymbol{r}_\mu} \cdot \nabla_{\boldsymbol{r}_\delta} \underline{\check{G}}\right) &= \mathscr{F}_{\epsilon \leftarrow t_\delta}\left(\int d\boldsymbol{r}_\delta \, e^{-i\boldsymbol{r}_\delta \cdot \boldsymbol{p}} \nabla_{\boldsymbol{r}_\mu} \cdot \nabla_{\boldsymbol{r}_\delta} \underline{\check{G}}\right) \\
&= \mathscr{F}_{\epsilon \leftarrow t_\delta}\left(e^{-i\boldsymbol{r}_\delta \cdot \boldsymbol{p}} \nabla_{\boldsymbol{r}_\mu} \underline{\check{G}}\Big|_{\boldsymbol{r}_\delta = -\infty}^{\boldsymbol{r}_\delta = +\infty}\right. \\
&\quad \left. - \int d\boldsymbol{r}_\delta \, \left[\nabla_{\boldsymbol{r}_\delta} e^{-i\boldsymbol{r}_\delta \cdot \boldsymbol{p}}\right] \cdot \nabla_{\boldsymbol{r}_\mu} \underline{\check{G}}\right) \\
&= \mathscr{F}_{\epsilon \leftarrow t_\delta}\left(i\boldsymbol{p} \cdot \int d\boldsymbol{r}_\delta \, e^{-i\boldsymbol{r}_\delta \cdot \boldsymbol{p}} \nabla_{\boldsymbol{r}_\mu} \underline{\check{G}}\right) \\
&= i\boldsymbol{p} \cdot \mathscr{F}_{\epsilon \leftarrow t_\delta,\, \boldsymbol{p} \leftarrow \boldsymbol{r}_\delta}\left(\nabla_{\boldsymbol{r}_\mu} \underline{\check{G}}\right).
\end{aligned}$$

With this we can calculate the contribution of the last terms in the expressions for $\tilde{\nabla}^2_{\boldsymbol{r}}$ and $\tilde{\nabla}^2_{\boldsymbol{r}'}$ in equation (D.3.4):

$$\mathscr{F}\left(\nabla_{\boldsymbol{r}_\mu} \cdot \nabla_{\boldsymbol{r}_\delta} \underline{\check{G}} + \underline{\check{G}} \left[\nabla_{\boldsymbol{r}_\mu} \cdot \nabla_{\boldsymbol{r}_\delta}\right]^\dagger\right) = 2i\boldsymbol{p} \cdot \nabla_{\boldsymbol{r}} \underline{\check{G}}.$$

Transforming $\nabla_{\boldsymbol{r}_\delta}$ to $i\boldsymbol{p}$ in a similar fashion, the remaining terms become (we write $\underline{\boldsymbol{\check{A}}}$ to express its 8×8 structure as described in appendix B.2)

$$ie\left(\frac{1}{2}\left[\nabla_{\boldsymbol{r}} \cdot \underline{\boldsymbol{\check{A}}} + \underline{\boldsymbol{\check{A}}} \cdot \nabla_{\boldsymbol{r}} \,\bullet\, ; \underline{\check{G}}\right]_+ + 2i\boldsymbol{p} \cdot \left[\underline{\boldsymbol{\check{A}}} \,\bullet\, ; \underline{\check{G}}\right]_-\right) - e^2 \left[\underline{\boldsymbol{\check{A}}}^2 \,\bullet\, ; \underline{\check{G}}\right]_-.$$

Collecting terms, we find

$$\begin{aligned}
\mathscr{F}\left(\tilde{\nabla}^2_{\boldsymbol{r}} \underline{\check{G}} - \underline{\check{G}}\left(\tilde{\nabla}^2_{\boldsymbol{r}'}\right)^\dagger\right) =& 2i\boldsymbol{p} \cdot \left(\nabla_{\boldsymbol{r}} \underline{\check{G}} + ie\left[\underline{\boldsymbol{\check{A}}} \,\bullet\, ; \underline{\check{G}}\right]_-\right) - e^2 \left[\underline{\boldsymbol{\check{A}}}^2 \,\bullet\, ; \underline{\check{G}}\right]_- \\
&+ \frac{ie}{2}\left[\nabla_{\boldsymbol{r}} \cdot \underline{\boldsymbol{\check{A}}} + \underline{\boldsymbol{\check{A}}} \cdot \nabla_{\boldsymbol{r}} \,\bullet\, ; \underline{\check{G}}\right]_+.
\end{aligned} \tag{D.3.5}$$

Fourier transforming a term $V(\boldsymbol{r})\underline{\check{G}} - \underline{\check{G}} V(\boldsymbol{r}')$ for a generic position-dependent function $V(\boldsymbol{r})$ with the help of section A.6.1 gives

$$\mathscr{F}\left[V\left(\boldsymbol{r}_\mu + \frac{1}{2}\boldsymbol{r}_\delta\right)\underline{\check{G}} - \underline{\check{G}} V\left(\boldsymbol{r}_\mu - \frac{1}{2}\boldsymbol{r}_\delta\right)\right] = \left[V(\boldsymbol{r}) \,\bullet\, ; \underline{\check{G}}\right]_-.$$

We define the diagonal matrices

$$\begin{aligned}
\check{\underline{\varphi}} &= \mathbb{1}^{2\times2} \otimes \begin{pmatrix} \varphi & 0 \\ 0 & \varphi^\dagger \end{pmatrix} \otimes \mathbb{1}^{2\times2}, \\
\check{\underline{\mu}} &= \mathbb{1}^{2\times2} \otimes \begin{pmatrix} \mu & 0 \\ 0 & \mu^\dagger \end{pmatrix} \otimes \mathbb{1}^{2\times2} = \mu\, \mathbb{1}^{8\times8}, \\
\check{\underline{V}}_{\text{imp}} &= \mathbb{1}^{2\times2} \otimes \begin{pmatrix} V_{\text{imp}}(\boldsymbol{r}) & 0 \\ 0 & V_{\text{imp}}(\boldsymbol{r})^\dagger \end{pmatrix} \otimes \mathbb{1}^{2\times2},
\end{aligned} \tag{D.3.6}$$

and the non-diagonal (not necessarily off-diagonal) matrices

$$\begin{aligned}
\check{\underline{V}}_{\text{sf}} &= \mathbb{1}^{2\times2} \otimes \begin{pmatrix} V_{\text{sf}}(\boldsymbol{r})\, \underline{\boldsymbol{\sigma}} \cdot \boldsymbol{S}(\boldsymbol{r}) & 0 \\ 0 & [V_{\text{sf}}(\boldsymbol{r})\, \underline{\boldsymbol{\sigma}} \cdot \boldsymbol{S}(\boldsymbol{r})]^\star \end{pmatrix} = \mathbb{1}^{2\times2} \otimes V_{\text{sf}}(\boldsymbol{r}) \hat{\underline{\boldsymbol{\sigma}}} \cdot \hat{\boldsymbol{S}}(\boldsymbol{r}), \\
\check{\underline{V}}_{\mathbf{h}} &= \mathbb{1}^{2\times2} \otimes \begin{pmatrix} \underline{\boldsymbol{\sigma}} \cdot \boldsymbol{h}(\boldsymbol{r}) & 0 \\ 0 & [\underline{\boldsymbol{\sigma}} \cdot \boldsymbol{h}(\boldsymbol{r})]^\star \end{pmatrix} = \mathbb{1}^{2\times2} \otimes \hat{\underline{\boldsymbol{\sigma}}} \cdot \hat{\boldsymbol{h}}(\boldsymbol{r}), \\
\check{\underline{\Delta}} &= \mathbb{1}^{2\times2} \otimes \begin{pmatrix} 0 & i\underline{\sigma}_2 \Delta(\boldsymbol{r}, t) \\ [i\underline{\sigma}_2 \Delta(\boldsymbol{r}, t)]^\star & 0 \end{pmatrix} = \mathbb{1}^{2\times2} \otimes \hat{\underline{\Delta}}(\boldsymbol{r}, t).
\end{aligned} \tag{D.3.7}$$

Combining the above components, as well as those in equation (D.3.5), the right-hand side of equation (D.3.2) becomes

$$\begin{aligned}
-\frac{i\hbar^2 \boldsymbol{p}}{m} \cdot \left(\nabla_{\boldsymbol{r}} \check{\underline{G}} + ie \left[\check{\underline{\boldsymbol{A}}} \bullet ; \check{\underline{G}} \right]_- \right) + \left[q\check{\underline{\varphi}} + \check{\underline{V}}_{\text{imp}} + \check{\underline{V}}_{\text{sf}} + \check{\underline{V}}_{\mathbf{h}} + \check{\underline{\Delta}} \bullet ; \check{\underline{G}} \right]_- \\
+ \frac{\hbar^2 e^2}{2m} \left[\check{\underline{\boldsymbol{A}}}^2 \bullet ; \check{\underline{G}} \right]_- - \frac{i\hbar^2 e}{4m} \left[\nabla_{\boldsymbol{r}} \cdot \check{\underline{\boldsymbol{A}}} + \check{\underline{\boldsymbol{A}}} \cdot \nabla_{\boldsymbol{r}} \bullet ; \check{\underline{G}} \right]_+ ,
\end{aligned} \tag{D.3.8}$$

where $\check{\underline{\mu}}$ is left out because it is a scalar that does not depend on any coordinate and therefore bullet commutes with $\check{\underline{G}}$. Writing the left-hand side of equation (D.3.2)

in a similar way, we note that[1]

$$\begin{aligned}\left[\epsilon\check{\underline{\rho}}_3 \bullet \check{\underline{G}}\right]_- &= e^{i(\partial_\epsilon^{\epsilon\check{\underline{\rho}}_3}\partial_t^{\check{\underline{G}}})/2}\,\epsilon\check{\underline{\rho}}_3\check{\underline{G}} - e^{i(-\partial_\epsilon^{\epsilon\check{\underline{\rho}}_3}\partial_t^{\check{\underline{G}}})/2}\,\check{\underline{G}}\epsilon\check{\underline{\rho}}_3 \\ &= \left(1+\frac{i}{2}\partial_\epsilon^{\epsilon\check{\underline{\rho}}_3}\partial_t^{\check{\underline{G}}}\right)\epsilon\check{\underline{\rho}}_3\check{\underline{G}} - \left(1-\frac{i}{2}\partial_\epsilon^{\epsilon\check{\underline{\rho}}_3}\partial_t^{\check{\underline{G}}}\right)\check{\underline{G}}\epsilon\check{\underline{\rho}}_3 \\ &= \epsilon\check{\underline{\rho}}_3\check{\underline{G}} + \frac{i}{2}\,\check{\underline{\rho}}_3\partial_t\check{\underline{G}} - \check{\underline{G}}\epsilon\check{\underline{\rho}}_3 + \frac{i}{2}\,\partial_t\check{\underline{G}}\check{\underline{\rho}}_3 \\ &= \frac{i}{2}\left[\check{\underline{\rho}}_3, \partial_t\check{\underline{G}}\right]_+ + \left[\epsilon\check{\underline{\rho}}_3, \check{\underline{G}}\right]_- .\end{aligned} \tag{D.3.9}$$

Combining equations (D.3.8, D.3.9), moving the first term to the left and multiplying by i, we find

$$\begin{aligned}\frac{\hbar^2\boldsymbol{p}}{m}\cdot\left(\nabla_{\boldsymbol{r}}\check{\underline{G}} + ie\left[\check{\underline{\boldsymbol{A}}}\bullet\check{\underline{G}}\right]_-\right) = i\left[\epsilon\check{\underline{\rho}}_3 - q\check{\underline{\varphi}} - \check{\underline{V}}_{\text{imp}} - \check{\underline{V}}_{\text{sf}} - \check{\underline{V}}_{\mathbf{h}} - \check{\underline{\Delta}}\bullet\check{\underline{G}}\right]_- \\ - \frac{i\hbar^2e^2}{2m}\left[\check{\underline{\boldsymbol{A}}}^2\bullet\check{\underline{G}}\right]_- - \frac{\hbar^2e}{4m}\left[\nabla_{\boldsymbol{r}}\cdot\check{\underline{\boldsymbol{A}}} + \check{\underline{\boldsymbol{A}}}\cdot\nabla_{\boldsymbol{r}}\bullet\check{\underline{G}}\right]_+ .\end{aligned} \tag{D.3.10}$$

As we are more interested in the canonical momentum than in the kinetic momentum, it would be more appropriate to replace the spatial derivative $\nabla_{\boldsymbol{r}}$ that works on $\check{\underline{G}}$ with the covariant derivative $\tilde{\nabla}_{\boldsymbol{r}} = \nabla_{\boldsymbol{r}} + ie\check{\underline{\boldsymbol{A}}} = i\boldsymbol{p}/\hbar$. To see how this operator behaves when acting on the Green function, we take a closer look at the definitions of its components in equation (C.1.3). The spatial part of each component is contained by the expectation value of an (anti)commutator of field operators. Matrices can be brought inside the expectation bra-ket because as shown in equation (C.1.4). Similarly, operators in spacetime and energy-momentum space can be brought inside the expectation value, as the bra and ket states that the argument is placed between are defined in Fock space (rather than in Hilbert space). This means that

$$\tilde{\nabla}_{\boldsymbol{r}_\mu}\left\langle\left[\psi(\boldsymbol{r},t),\psi^\dagger(\boldsymbol{r}',t')\right]_\pm\right\rangle = \left\langle\tilde{\nabla}_{\boldsymbol{r}_\mu}\left(\psi(\boldsymbol{r},t)\psi^\dagger(\boldsymbol{r}',t')\pm\psi^\dagger(\boldsymbol{r}',t')\psi(\boldsymbol{r},t)\right)\right\rangle .$$

Using the result in equation (B.2.2), the right-hand side becomes

$$\left\langle\nabla_{\boldsymbol{r}_\mu}\left(\psi(\boldsymbol{r},t)\psi^\dagger(\boldsymbol{r}',t')\pm\psi^\dagger(\boldsymbol{r}',t')\psi(\boldsymbol{r},t)\right) + ie\left[\hat{\underline{\boldsymbol{A}}},\psi(\boldsymbol{r},t)\psi^\dagger(\boldsymbol{r}',t')\right]_-\right\rangle .$$

[1] Here we use the notation ∂_x^A for the differential operator ∂_x operating on A. For example, $\partial_x^A(AB) = (\partial_x A)B$ and $\partial_x^B(AB) = A(\partial_x B)$. The exponential function of the operator is defined by its power series $\exp(\partial_x^A) = \sum_{n=0}^{\infty}(\partial_x^A)^n/n!$.

As the product $\psi^\dagger\psi$ is diagonal and thus commutes with the vector potential, we are free to add or subtract this to the right-hand side of the commutator in the second term. We thus get to

$$\begin{aligned}\tilde{\nabla}_{\boldsymbol{r}_\mu}&\left\langle\left[\psi(\boldsymbol{r},t),\psi^\dagger(\boldsymbol{r}',t')\right]_\pm\right\rangle\\&=\left\langle\nabla_{\boldsymbol{r}_\mu}\left[\psi(\boldsymbol{r},t),\psi^\dagger(\boldsymbol{r}',t')\right]_\pm+ie\left[\underline{\hat{\boldsymbol{A}}},\left[\psi(\boldsymbol{r},t),\psi^\dagger(\boldsymbol{r}',t')\right]_\pm\right]_-\right\rangle,\end{aligned}$$

or, splitting this up and moving the derivative and vector potential back outside the braket, we have

$$\begin{aligned}\tilde{\nabla}_{\boldsymbol{r}_\mu}&\left\langle\left[\psi(\boldsymbol{r},t),\psi^\dagger(\boldsymbol{r}',t')\right]_\pm\right\rangle\\&=\nabla_{\boldsymbol{r}_\mu}\left\langle\left[\psi(\boldsymbol{r},t),\psi^\dagger(\boldsymbol{r}',t')\right]_\pm\right\rangle+ie\left[\underline{\hat{\boldsymbol{A}}},\left\langle\left[\psi(\boldsymbol{r},t),\psi^\dagger(\boldsymbol{r}',t')\right]_\pm\right\rangle\right]_-.\end{aligned}$$

In short, we conclude

$$\tilde{\nabla}_{\boldsymbol{r}}\check{\underline{G}}=\nabla_{\boldsymbol{r}}\check{\underline{G}}+ie\left[\check{\underline{\boldsymbol{A}}}\bullet,\check{\underline{G}}\right]_-. \tag{D.3.11}$$

Substituting this into equation (D.3.10), we can write it in the appreciable form

$$\begin{aligned}\frac{\hbar^2\boldsymbol{p}}{m}\cdot\tilde{\nabla}_{\boldsymbol{r}}\check{\underline{G}}=i\Big[\epsilon\check{\underline{\rho}}_3-q\underline{\check{\varphi}}-\underline{\check{V}}_{\text{imp}}-\underline{\check{V}}_{\text{sf}}-\underline{\check{V}}_{\mathbf{h}}-\underline{\check{\Delta}}\bullet,\check{\underline{G}}\Big]_-\\-\frac{i\hbar^2e^2}{2m}\left[\check{\underline{\boldsymbol{A}}}^2\bullet,\check{\underline{G}}\right]_--\frac{\hbar^2e}{4m}\left[\nabla_{\boldsymbol{r}}\cdot\check{\underline{\boldsymbol{A}}}+\check{\underline{\boldsymbol{A}}}\cdot\nabla_{\boldsymbol{r}}\bullet,\check{\underline{G}}\right]_+.\end{aligned} \tag{D.3.12}$$

D.3.1 The quasiclassical approximation

In the quasiclassical approximation, we assume that the quantities we are interested in vary over distances much larger than the Fermi wavelength [24]. We assume that the net transport of particles, charge and spin happens at the Fermi surface. This means that we can consider the momentum of the Green functions to be approximately equal to the Fermi momentum,

$$|\boldsymbol{p}|\approx p_F=\hbar k_F=\frac{2\pi\hbar}{\lambda_F}.$$

Simultaneously, we assume that both $\check{\underline{G}}$ and $\boldsymbol{A}$ depend on $\boldsymbol{r}$ on a scale comparable to the size of the system, which we will call L. Terms such as $\tilde{\nabla}_{\boldsymbol{r}}\check{\underline{G}}$, $\nabla_{\boldsymbol{r}}\check{\underline{G}}$ and $\nabla_{\boldsymbol{r}}\cdot\boldsymbol{A}$ will therefore be of order $1/L$. This means that whereas the left-hand side of equation (D.3.12) is of order $1/(\lambda_F L)$, the last term is of order $1/L^2$. Assuming now that $L\ll\lambda_F$, we can discard the last term on the right. The second-last term is gauge dependent, where we are free to choose a gauge such

that the average of $\boldsymbol{A}^2$ is zero, leaving just the local deviation from this average. As this variation is again of the order $1/L^2$, it also drops out.[2] This leaves the manageable Eilenberger equation

$$\frac{\hbar^2 \boldsymbol{p}}{m} \cdot \tilde{\nabla}_{\boldsymbol{r}} \underline{\check{G}} = i \left[\epsilon \underline{\check{\rho}}_3 - q\underline{\check{\varphi}} - \underline{\check{V}}_{\text{imp}} - \underline{\check{V}}_{\text{sf}} - \underline{\check{V}}_{\mathbf{h}} - \underline{\check{\Delta}} \bullet \underline{\check{G}} \right]_- ,$$

which upon replacing the Green functions with their quasiclassical counterparts becomes[3]

$$\boxed{\frac{\hbar^2 \boldsymbol{p}_F}{m} \cdot \tilde{\nabla}_{\boldsymbol{r}} \underline{\check{g}} = i \left[\epsilon \underline{\check{\rho}}_3 - q\underline{\check{\varphi}} - \underline{\check{V}}_{\text{imp}} - \underline{\check{V}}_{\text{sf}} - \underline{\check{V}}_{\mathbf{h}} - \underline{\check{\Delta}} \circ \underline{\check{g}} \right]_- .} \tag{D.3.13}$$

Since in the quasiclassical approximation the Green function is expected to be zero everywhere except on the Fermi surface, the products of position and momentum derivatives in the bullet product drop out, and we can replace it by a ring product (see appendix A.7).

D.4 The dirty limit and the Usadel equation

In the "dirty limit" we assume that impurity scattering self-energy dominates the Hamiltonian. In this case the rate of scattering is so high that the mean free path is much shorter than the phase coherence length, the electron will on average change its momentum direction many times before losing its phase coherence. This has as effect that the Green function becomes nearly isotropic. In terms of the involved physical quantities, which implies that [47]

$$|V_{\text{imp}}| \gg |\epsilon|, |q\varphi|, |\Delta|, |\boldsymbol{h}(\boldsymbol{r})|, \qquad \ell_e \ll \ell_\phi, \qquad \tau_{\text{imp}} \ll \tau_{\text{sf}}. \tag{D.4.1}$$

In this case we can expand the Green function in spherical harmonics and only keep the first two terms [23, 74]:

$$\underline{\check{g}} = \underline{\check{g}}_s + \hat{\boldsymbol{p}} \cdot \underline{\check{g}}_p,$$

where neither $\underline{\check{g}}_s$ nor $\underline{\check{g}}_p$ depends on the direction of the momentum. We are now only interested in the angular average of $\underline{\check{g}}$, which can be approximated as

$$\left\langle \underline{\check{g}}(\boldsymbol{r}, \hat{\boldsymbol{p}}, \epsilon) \right\rangle_{\hat{\boldsymbol{p}}} = \left\langle \underline{\check{g}}_s(\boldsymbol{r}, \epsilon) + \hat{\boldsymbol{p}} \cdot \underline{\check{g}}_p(\boldsymbol{r}, \epsilon) \right\rangle_{\hat{\boldsymbol{p}}} = \left\langle \underline{\check{g}}_s(\boldsymbol{r}, \epsilon) \right\rangle_{\hat{\boldsymbol{p}}} .$$

[2] This argument is based on section 4.4 in Ref. 75.

[3] See appendix C.2 or Ref. 47 for details on the quasiclassical Green function. The cited article also gives a very thorough introduction to the Green's function techniques used in this thesis.

We can now replace the scattering potentials with their corresponding self-energies.[4] In equation (D.3.13) we replace [20]

$$\underline{\check{V}}_{\text{imp}} \mapsto \sigma_{\text{imp}} = -\frac{i\hbar}{2\tau_{\text{imp}}}, \qquad \underline{\check{V}}_{\text{sf}} \mapsto \sigma_{\text{sf}} = -\frac{i\hbar}{2\tau_{\text{sf}}}\, \underline{\check{\rho}}_3 \underline{\check{g}}_s \underline{\check{\rho}}_3.$$

Upon substituting these for the scattering potentials in equation (D.3.13), the Eilenberger equation reads

$$\begin{aligned}
&\hbar^2 v_F\, \hat{\boldsymbol{p}} \cdot \tilde{\nabla}_{\boldsymbol{r}} \left(\underline{\check{g}}_s + \hat{\boldsymbol{p}} \cdot \underline{\check{g}}_p \right) \\
&\qquad = i \left[\epsilon \underline{\check{\rho}}_3 - q\underline{\check{\varphi}} + \frac{i\hbar}{2\tau_{\text{imp}}}\, \underline{\check{g}}_s + \frac{i\hbar}{2\tau_{\text{sf}}}\, \underline{\check{\rho}}_3 \underline{\check{g}}_s \underline{\check{\rho}}_3 + \underline{\hat{\boldsymbol{\sigma}}} \cdot \hat{\boldsymbol{h}}(\boldsymbol{r}) - \underline{\check{\Delta}} \circ \underline{\check{g}}_s + \hat{\boldsymbol{p}} \cdot \underline{\check{g}}_p \right]_- .
\end{aligned}$$

It is crucial to note that the terms odd in $\hat{\boldsymbol{p}}$ are independent of those even in $\hat{\boldsymbol{p}}$, which means that we can split the above into two decoupled equations

$$\begin{aligned}
&\hbar^2 v_F\, \hat{\boldsymbol{p}} \cdot \tilde{\nabla}_{\boldsymbol{r}} \underline{\check{g}}_s = \\
&\quad i \left[\epsilon \underline{\check{\rho}}_3 - q\underline{\check{\varphi}} + \frac{i\hbar}{2\tau_{\text{imp}}}\, \underline{\check{g}}_s + \frac{i\hbar}{2\tau_{\text{sf}}}\, \underline{\check{\rho}}_3 \underline{\check{g}}_s \underline{\check{\rho}}_3 + \underline{\hat{\boldsymbol{\sigma}}} \cdot \hat{\boldsymbol{h}}(\boldsymbol{r}) - \underline{\check{\Delta}} \circ \hat{\boldsymbol{p}} \cdot \underline{\check{g}}_p \right]_- , \\
&\hbar^2 v_F\, \hat{\boldsymbol{p}} \cdot \tilde{\nabla}_{\boldsymbol{r}} (\hat{\boldsymbol{p}} \cdot \underline{\check{g}}_p) = \\
&\quad i \left[\epsilon \underline{\check{\rho}}_3 - q\underline{\check{\varphi}} + \frac{i\hbar}{2\tau_{\text{imp}}}\, \underline{\check{g}}_s + \frac{i\hbar}{2\tau_{\text{sf}}}\, \underline{\check{\rho}}_3 \underline{\check{g}}_s \underline{\check{\rho}}_3 + \underline{\hat{\boldsymbol{\sigma}}} \cdot \hat{\boldsymbol{h}}(\boldsymbol{r}) - \underline{\check{\Delta}} \circ \underline{\check{g}}_s \right]_- .
\end{aligned} \tag{D.4.2}$$

Using the specifications in equation (D.4.1), the first term is approximated as

$$\hbar^2 v_F\, \tilde{\nabla}_{\boldsymbol{r}} \underline{\check{g}}_s = -\frac{1}{2\tau_{\text{imp}}} \left[\underline{\check{g}}_s \circ \underline{\check{g}}_p \right]_- , \tag{D.4.3}$$

where the $\hat{\boldsymbol{p}}$ left and right were dropped. Using the identity $\underline{\check{g}} \circ \underline{\check{g}} = \mathbb{1}^{8\times 8}$ [41], collecting terms odd and even in $\hat{\boldsymbol{p}}$ again and ignoring the terms quadratic in $\underline{\check{g}}_p$, the normalization conditions for $\underline{\check{g}}_s$ and $\underline{\check{g}}_p$ read

$$\underline{\check{g}}_s \circ \underline{\check{g}}_s \approx \mathbb{1}^{8\times 8}, \qquad \underline{\check{g}}_s \circ \underline{\check{g}}_p + \underline{\check{g}}_p \circ \underline{\check{g}}_s = 0. \tag{D.4.4}$$

The latter can be used to replace the commutator in equation (D.4.3) with a simple ring product:

$$\hbar^2 v_F\, \tilde{\nabla}_{\boldsymbol{r}} \underline{\check{g}}_s = -\frac{1}{\tau_{\text{imp}}} \underline{\check{g}}_s \circ \underline{\check{g}}_p, \tag{D.4.5}$$

[4] For details and more background on ensemble-averaging, self-energies, lifetimes and the Dyson equation, the reader is directed to Ref. 76, pp.147-59,226-31,300-40, Ref. 25 pp.211-25, and Ref. 26 pp.86-102.

or, multiplying with $\check{\underline{g}}_s$ from the left and using the commutativity of the ring product,

$$\check{\underline{g}}_s \circ (\check{\underline{g}}_s \circ \check{\underline{g}}_p) = (\check{\underline{g}}_s \circ \check{\underline{g}}_s) \circ \check{\underline{g}}_p = \boxed{\check{\underline{g}}_p = -\tau_{\mathrm{imp}} \hbar^2 v_F \, \check{\underline{g}}_s \circ \tilde{\nabla}_{\boldsymbol{r}} \check{\underline{g}}_s .} \tag{D.4.6}$$

Looking more closely at the second line in equation (D.4.2), we see that the third term in the commutator commutes, as $\left[\check{\underline{g}}_s, \check{\underline{g}}_s\right]_- = 0$, allowing us to simplify this to

$$\hbar^2 v_F \, \hat{\boldsymbol{p}} \cdot \tilde{\nabla}_{\boldsymbol{r}} (\hat{\boldsymbol{p}} \cdot \check{\underline{g}}_p) = i \left[\epsilon \check{\underline{\rho}}_3 - q \check{\underline{\varphi}} + \frac{i\hbar}{2\tau_{\mathrm{sf}}} \check{\underline{\rho}}_3 \check{\underline{g}}_s \check{\underline{\rho}}_3 + \hat{\underline{\boldsymbol{\sigma}}} \cdot \hat{\boldsymbol{h}}(\boldsymbol{r}) - \check{\underline{\Delta}} \, ; \check{\underline{g}}_s \right]_- .$$

Since we consider the diffusive case, we can extract just the isotropic information by taking the angular average. The right-hand side does not depend on the direction of the momentum, whereas the angular average of the left-hand side becomes

$$\left\langle \hat{\boldsymbol{p}} \cdot \tilde{\nabla}_{\boldsymbol{r}} (\hat{\boldsymbol{p}} \cdot \check{\underline{g}}_p) \right\rangle_{\hat{\boldsymbol{p}}} = \left\langle \hat{\boldsymbol{p}} \cdot \nabla_{\boldsymbol{r}} (\hat{\boldsymbol{p}} \cdot \check{\underline{g}}_p) \right\rangle_{\hat{\boldsymbol{p}}} + ie \left\langle (\hat{\boldsymbol{p}} \cdot \boldsymbol{A}) (\hat{\boldsymbol{p}} \cdot \check{\underline{g}}_p) \right\rangle_{\hat{\boldsymbol{p}}} .$$

Assessing these two terms separately,

$$\begin{aligned}
\left\langle \hat{\boldsymbol{p}} \cdot \nabla_{\boldsymbol{r}} (\hat{\boldsymbol{p}} \cdot \check{\underline{g}}_p) \right\rangle_{\hat{\boldsymbol{p}}} &= \frac{1}{4\pi} \underbrace{\int_0^{2\pi} \cos^2\phi \, d\phi}_{\pi} \underbrace{\int_0^{\pi} \sin^3\theta \, d\theta}_{4/3} \partial_x \check{\underline{g}}_{p,x} + (\cdots)_y + (\cdots)_z \\
&\quad + \frac{1}{4\pi} \underbrace{\int_0^{2\pi} \cos\phi \sin\phi \, d\phi}_{0} \int_0^{\pi} \sin^3\theta \, d\theta (\partial_x \check{\underline{g}}_{p,y} + \partial_y \check{\underline{g}}_{p,x}) \\
&\quad + (\cdots)_{xz} + (\cdots)_{yz} \\
&= \frac{1}{3} \nabla_{\boldsymbol{r}} \cdot \check{\underline{g}}_p ,
\end{aligned}$$

and similarly,

$$ie \left\langle (\hat{\boldsymbol{p}} \cdot \boldsymbol{A}) (\hat{\boldsymbol{p}} \cdot \check{\underline{g}}_p) \right\rangle_{\hat{\boldsymbol{p}}} = \frac{1}{3} \boldsymbol{A} \cdot \check{\underline{g}}_p .$$

This introduces a factor 1/3 by effectively dropping the crossterms:

$$\left\langle \hat{\boldsymbol{p}} \cdot \tilde{\nabla}_{\boldsymbol{r}} (\hat{\boldsymbol{p}} \cdot \check{\underline{g}}_p) \right\rangle_{\hat{\boldsymbol{p}}} = \frac{1}{3} \tilde{\nabla}_{\boldsymbol{r}} \cdot \check{\underline{g}}_p .$$

Combining this with equation (D.4.6), this gives

$$-\frac{\hbar^2 v_F^2 \tau_{\text{imp}}}{3}\,\tilde{\nabla}_{\boldsymbol{r}}\cdot(\check{\underline{g}}_s\circ\tilde{\nabla}_{\boldsymbol{r}}\check{\underline{g}}_s) = i\left[\epsilon\check{\underline{\rho}}_3 - q\check{\underline{\varphi}} + \frac{i\hbar}{2\tau_{\text{sf}}}\,\check{\underline{\rho}}_3\check{\underline{g}}_s\check{\underline{\rho}}_3 + \hat{\underline{\boldsymbol{\sigma}}}\cdot\hat{\boldsymbol{h}}(\boldsymbol{r}) - \check{\underline{\Delta}}\,\circ\!,\,\check{\underline{g}}_s\right]_-.$$

Note that the Fermi velocity — the average velocity — times the scattering time equals the mean free path, so we can write [23, 46]

$$\boxed{D \equiv \frac{\hbar^2 v_F^2 \tau_{\text{imp}}}{3} = \frac{\hbar^4}{3} v_F \ell_e,} \tag{D.4.7}$$

by which we arrive at the Usadel equation [17, 22]

$$\boxed{-D\tilde{\nabla}_{\boldsymbol{r}}\cdot(\check{\underline{g}}_s\circ\tilde{\nabla}_{\boldsymbol{r}}\check{\underline{g}}_s) = i\left[\epsilon\check{\underline{\rho}}_3 - q\check{\underline{\varphi}} + \frac{i\hbar}{2\tau_{\text{sf}}}\,\check{\underline{\rho}}_3\check{\underline{g}}_s\check{\underline{\rho}}_3 + \hat{\underline{\boldsymbol{\sigma}}}\cdot\hat{\boldsymbol{h}}(\boldsymbol{r}) - \check{\underline{\Delta}}\,\circ\!,\,\check{\underline{g}}_s\right]_-.} \tag{D.4.8}$$

By writing this out in components of $\check{\underline{g}}_s$, the chain of derivatives on the left becomes

$$\tilde{\nabla}_{\boldsymbol{r}}\cdot(\check{\underline{g}}_s\circ\tilde{\nabla}_{\boldsymbol{r}}\check{\underline{g}}_s) = \tilde{\nabla}_{\boldsymbol{r}}\cdot\begin{pmatrix}\hat{\underline{g}}_s^R\circ\tilde{\nabla}_{\boldsymbol{r}}\hat{\underline{g}}_s^R & \hat{\underline{g}}_s^R\circ\tilde{\nabla}_{\boldsymbol{r}}\hat{\underline{g}}_s^K + \hat{\underline{g}}_s^K\circ\tilde{\nabla}_{\boldsymbol{r}}\hat{\underline{g}}_s^A \\ 0 & \hat{\underline{g}}_s^A\circ\tilde{\nabla}_{\boldsymbol{r}}\hat{\underline{g}}_s^A\end{pmatrix},$$

which gives us the three equations

$$-D\tilde{\nabla}_{\boldsymbol{r}}\cdot\left(\hat{\underline{g}}_s^R\circ\tilde{\nabla}_{\boldsymbol{r}}\hat{\underline{g}}_s^R\right) = i\left[\epsilon\hat{\underline{\rho}}_3 - q\hat{\underline{\varphi}} + \frac{i\hbar}{2\tau_{\text{sf}}}\,\hat{\underline{\rho}}_3\hat{\underline{g}}_s^R\hat{\underline{\rho}}_3 + \hat{\underline{\boldsymbol{\sigma}}}\cdot\hat{\boldsymbol{h}}(\boldsymbol{r}) - \hat{\underline{\Delta}}\,\circ\!,\,\hat{\underline{g}}_s^R\right]_-, \tag{D.4.9a}$$

$$-D\tilde{\nabla}_{\boldsymbol{r}}\cdot\left(\hat{\underline{g}}_s^A\circ\tilde{\nabla}_{\boldsymbol{r}}\hat{\underline{g}}_s^A\right) = i\left[\epsilon\hat{\underline{\rho}}_3 - q\hat{\underline{\varphi}} + \frac{i\hbar}{2\tau_{\text{sf}}}\,\hat{\underline{\rho}}_3\hat{\underline{g}}_s^A\hat{\underline{\rho}}_3 + \hat{\underline{\boldsymbol{\sigma}}}\cdot\hat{\boldsymbol{h}}(\boldsymbol{r}) - \hat{\underline{\Delta}}\,\circ\!,\,\hat{\underline{g}}_s^A\right]_-, \tag{D.4.9b}$$

$$\begin{aligned}-D\tilde{\nabla}_{\boldsymbol{r}}\cdot\left(\hat{\underline{g}}_s^R\circ\tilde{\nabla}_{\boldsymbol{r}}\hat{\underline{g}}_s^K + \hat{\underline{g}}_s^K\circ\tilde{\nabla}_{\boldsymbol{r}}\hat{\underline{g}}_s^A\right) &= i\left[\epsilon\hat{\underline{\rho}}_3 - q\hat{\underline{\varphi}} + \hat{\underline{\boldsymbol{\sigma}}}\cdot\hat{\boldsymbol{h}}(\boldsymbol{r}) - \hat{\underline{\Delta}}\,\circ\!,\,\hat{\underline{g}}_s^K\right]_- \\ &\quad - \frac{\hbar}{2\tau_{\text{sf}}}\left(\hat{\underline{\rho}}_3\hat{\underline{g}}_s^R\hat{\underline{\rho}}_3\hat{\underline{g}}_s^K + \hat{\underline{g}}_s^K\hat{\underline{\rho}}_3\hat{\underline{g}}_s^A\hat{\underline{\rho}}_3 - \hat{\underline{g}}_s^R\hat{\underline{\rho}}_3\hat{\underline{g}}_s^K\hat{\underline{\rho}}_3 - \hat{\underline{\rho}}_3\hat{\underline{g}}_s^K\hat{\underline{\rho}}_3\hat{\underline{g}}_s^A\right).\end{aligned} \tag{D.4.9c}$$

D.5 Distribution functions in stationary systems

As the non-equilibrium information is contained by the Keldysh component, we would like to find an equation of motion that describes it. Using the normalization condition from equation (D.4.4), we find that $\hat{\underline{g}}_s^K$ is normalized in a way similar to $\hat{\underline{g}}^K$ (as stated in equation (C.2.6)):

$$\hat{\underline{g}}_s^R \circ \hat{\underline{g}}_s^K \approx -\hat{\underline{g}}_s^K \circ \hat{\underline{g}}_s^A,$$

which is accurate to first order in $\hat{\underline{g}}_p$. In order for the left-hand side to be equal to the right-hand side, $\hat{\underline{g}}_s^K$ needs to contain a term with $\hat{\underline{g}}_s^A$ on the right. Hence one way of writing $\hat{\underline{g}}_s^K$ is [46, 63]

$$\boxed{\hat{\underline{g}}_s^K = \hat{\underline{g}}_s^R \circ \hat{\underline{\hbar}} - \hat{\underline{\hbar}} \circ \hat{\underline{g}}_s^A,} \tag{D.5.1}$$

where we call $\hat{\underline{\hbar}}$ the *distribution function*, which is explored in more detail in section 2.2. Substituting this ansatz back into the normalization condition, we get $\hat{\underline{\hbar}} - \hat{\underline{g}}_s^R \circ \hat{\underline{\hbar}} \circ \hat{\underline{g}}_s^A$ on both sides.

Assuming now a stationary (i.e. time-independent) system, we can replace the ring products by ordinary products. Assuming also that the scalar potential is real, $\hat{\underline{\varphi}}$ commutes with the Green functions and drops out of the commutator. Making now the approximation that the contribution from spin-flip scattering is much smaller than the contributions from the other terms, the second line in equation (D.4.9c) drops out. With these approximations, we find

$$\begin{aligned} -D\tilde{\nabla}_{\boldsymbol{r}} \cdot \Big(\tilde{\nabla}_{\boldsymbol{r}} \hat{\underline{\hbar}} + \hat{\underline{g}}_s^R (\tilde{\nabla}_{\boldsymbol{r}} \hat{\underline{g}}_s^R) \hat{\underline{\hbar}} - \hat{\underline{g}}_s^R (\tilde{\nabla}_{\boldsymbol{r}} \hat{\underline{\hbar}}) \hat{\underline{g}}_s^A - \hat{\underline{\hbar}} \hat{\underline{g}}_s^A \tilde{\nabla}_{\boldsymbol{r}} \hat{\underline{g}}_s^A \Big) \\ = i \left[\epsilon \hat{\underline{\rho}}_3 + \hat{\boldsymbol{\sigma}} \cdot \hat{\boldsymbol{h}}(\boldsymbol{r}) - \hat{\underline{\Delta}}, \hat{\underline{g}}_s^R \hat{\underline{\hbar}} - \hat{\underline{\hbar}} \hat{\underline{g}}_s^A \right]_- . \end{aligned} \tag{D.5.2}$$

The terms $\hat{\underline{g}}_s^R (\tilde{\nabla}_{\boldsymbol{r}} \hat{\underline{g}}_s^R) \hat{\underline{\hbar}}$ on the left and $\hat{\underline{g}}_s^R \hat{\underline{\hbar}}$ on the right suggest we can simplify this by subtracting equation (D.4.9a) multiplied by $\hat{\underline{\hbar}}$ from the right. Similarly, the terms $-\hat{\underline{\hbar}} \hat{\underline{g}}_s^A \tilde{\nabla}_{\boldsymbol{r}} \hat{\underline{g}}_s^A$ on the left and $-\hat{\underline{\hbar}} \hat{\underline{g}}_s^A$ on the right suggest adding equation (D.4.9b) multiplied by $\hat{\underline{\hbar}}$ from the left. This gives

$$\boxed{-D\tilde{\nabla}_{\boldsymbol{r}} \cdot \Big(\tilde{\nabla}_{\boldsymbol{r}} \hat{\underline{\hbar}} - \hat{\underline{g}}_s^R (\tilde{\nabla}_{\boldsymbol{r}} \hat{\underline{\hbar}}) \hat{\underline{g}}_s^A \Big) = i \hat{\underline{g}}_s^R \left[\hat{\underline{E}}_{\hbar}, \hat{\underline{\hbar}} \right]_- - i \left[\hat{\underline{E}}_{\hbar}, \hat{\underline{\hbar}} \right]_- \hat{\underline{g}}_s^A,} \tag{D.5.3}$$

where

$$\hat{\underline{E}}_{\hbar} = \epsilon \hat{\underline{\rho}}_3 + \hat{\boldsymbol{\sigma}} \cdot \hat{\boldsymbol{h}}(\boldsymbol{r}) - \hat{\underline{\Delta}}. \tag{D.5.4}$$

This equation describes the diffusion of the distribution functions across the system, as function of both the local retarded and advanced Green functions and the available energy.

Appendix E

Full derivation of the current tensor

In the main text, chapter 2 is written without explicit derivations of the presented equations. This appendix describes the involved physics mathematics more thoroughly, and refers to the literature where necessary.

E.1 Velocity in quantum mechanics

From the quantum-mechanical definition of the expectation value, we calculate the expectation value of the velocity:

$$\langle \boldsymbol{v} \rangle = \partial_t \langle \boldsymbol{r} \rangle = \int_{\mathbb{R}} dV\, \boldsymbol{r} \partial_t |\psi|^2 = \int_{\mathbb{R}} dV\, \boldsymbol{r} \left(\psi^\dagger \partial_t \psi + (\partial_t \psi^\dagger)\psi \right). \tag{E.1.1}$$

Applying now Schrödinger's equation, we have

$$\partial_t \psi = \frac{i\hbar}{2m} \tilde{\nabla}^2_{\boldsymbol{r}} \psi - \frac{i}{\hbar} V\psi, \qquad \partial_t \psi^\dagger = -\frac{i\hbar}{2m} \tilde{\nabla}^2_{\boldsymbol{r}} \psi^\dagger + \frac{i}{\hbar} V\psi^\dagger, \tag{E.1.2}$$

which can be rewritten as

$$\begin{aligned} \langle \boldsymbol{v} \rangle &= \frac{i\hbar}{2m} \int_{\mathbb{R}} dV\, \boldsymbol{r} \left(\psi^\dagger \tilde{\nabla}^2_{\boldsymbol{r}} \psi - (\tilde{\nabla}^2_{\boldsymbol{r}} \psi^\dagger)\psi \right) \\ &= \frac{i\hbar}{2m} \int_{\mathbb{R}} dV\, \boldsymbol{r} \tilde{\nabla}_{\boldsymbol{r}} \left(\psi^\dagger \tilde{\nabla}_{\boldsymbol{r}} \psi - (\tilde{\nabla}_{\boldsymbol{r}} \psi^\dagger)\psi \right). \end{aligned} \tag{E.1.3}$$

Performing partial integration, it simplifies to

$$\langle \boldsymbol{v} \rangle = -\frac{i\hbar}{2m} \int_{\mathbb{R}} dV\, \left(\psi^\dagger \tilde{\nabla}_{\boldsymbol{r}} \psi - (\tilde{\nabla}_{\boldsymbol{r}} \psi^\dagger)\psi \right). \tag{E.1.4}$$

We can pull out the differential operators by ascribing different coordinates to the two wave functions:

$$\begin{aligned}\langle \boldsymbol{v} \rangle &= -\frac{i\hbar}{2m} \lim_{\boldsymbol{r}\to\boldsymbol{r}'} \int_{\mathbb{R}} \int_{\mathbb{R}'} dV dV' \left(\psi^\dagger(\boldsymbol{r}') \tilde{\nabla}_{\boldsymbol{r}} \psi(\boldsymbol{r}) - \tilde{\nabla}_{\boldsymbol{r}'} \psi^\dagger(\boldsymbol{r}') \psi(\boldsymbol{r}) \right) \\ &= -\frac{i\hbar}{2m} \lim_{\boldsymbol{r}\to\boldsymbol{r}'} \left\langle \left(\tilde{\nabla}_{\boldsymbol{r}} - \tilde{\nabla}_{\boldsymbol{r}'} \right) \psi^\dagger(\boldsymbol{r}') \psi(\boldsymbol{r}) \right\rangle .\end{aligned} \tag{E.1.5}$$

E.2 Relation to Green's functions

We found in section C.1 that for fermions

$$G^K_{\sigma,\sigma'}(\boldsymbol{r},t;\boldsymbol{r}',t') \equiv -i \left\langle \left[\psi_\sigma(\boldsymbol{r},t), \psi^\dagger_{\sigma'}(\boldsymbol{r}',t') \right]_- \right\rangle ,$$

which can be related to our expression for $\langle \boldsymbol{v} \rangle$ by extracting

$$\begin{aligned}\left\langle \psi^\dagger(\boldsymbol{r}')\psi(\boldsymbol{r}) \right\rangle &= \lim_{t\to t'} \left(\left\langle \psi(\boldsymbol{r},t)\psi^\dagger(\boldsymbol{r}',t') \right\rangle - \left\langle \left[\psi(\boldsymbol{r},t), \psi^\dagger(\boldsymbol{r}',t') \right]_- \right\rangle \right) \\ &= \lim_{t\to t'} \left(\delta(\boldsymbol{r},\boldsymbol{r}';t,t') - i \sum_\sigma G^K_{\sigma,\sigma}(\boldsymbol{r},t;\boldsymbol{r}',t') \right) .\end{aligned}$$

Since $(\tilde{\nabla}_{\boldsymbol{r}} - \tilde{\nabla}_{\boldsymbol{r}'})\delta(\boldsymbol{r},\boldsymbol{r}';t,t') = 0$,

$$\langle \boldsymbol{v} \rangle = \frac{\hbar}{2m} \lim_{\boldsymbol{r},t\to t',\boldsymbol{r}'} \left[\left(\tilde{\nabla}_{\boldsymbol{r}'} - \tilde{\nabla}_{\boldsymbol{r}} \right) \sum_\sigma G^K_{\sigma,\sigma}(\boldsymbol{r},t;\boldsymbol{r}',t') \right] .$$

To find our preferred component of the current density (for example $\boldsymbol{j}_{00}$ for the particle current, or $q\boldsymbol{j}_{30}$ for the electric current), we multiply with the corresponding Pauli matrices:

$$\begin{aligned}\boldsymbol{j}_{ij} &= \frac{\hbar}{2m} \lim_{\boldsymbol{r},t\to t',\boldsymbol{r}'} \left[\left(\tilde{\nabla}_{\boldsymbol{r}'} - \tilde{\nabla}_{\boldsymbol{r}} \right) \sum_\sigma \left(\hat{\tau}_i \underline{\sigma}_j \hat{\underline{G}}^K \right)_{\sigma,\sigma} (\boldsymbol{r},t;\boldsymbol{r}',t') \right] \\ &= \frac{\hbar}{2m} \lim_{\boldsymbol{r},t\to t',\boldsymbol{r}'} \left[\left(\tilde{\nabla}_{\boldsymbol{r}'} - \tilde{\nabla}_{\boldsymbol{r}} \right) \mathrm{Tr} \left\{ \hat{\tau}_i \underline{\sigma}_j \hat{\underline{G}}^K (\boldsymbol{r},t;\boldsymbol{r}',t') \right\} \right] .\end{aligned}$$

The particle current density is found by counting all diagonal components, and is therefore represented by $\boldsymbol{j}_{ij}$. To find the electric current density, we subtract the holes from the particles and multiply by the electron charge. Relating this to

the regular derivative, we need to note that the particles and holes have opposite charge[1]:

$$\tilde{\nabla}_{\boldsymbol{r}} = \nabla_{\boldsymbol{r}} - \frac{iq_h}{\hbar}\boldsymbol{A} = \nabla_{\boldsymbol{r}} + \frac{iq_p}{\hbar}\boldsymbol{A}, \qquad \tilde{\nabla}_{\boldsymbol{r}'} = \nabla_{\boldsymbol{r}'} - \frac{iq_p}{\hbar}\boldsymbol{A},$$

which allows us to write

$$\boldsymbol{j}_{ij} = \lim_{t\to t'}\lim_{\boldsymbol{r}\to\boldsymbol{r}'}\left[\frac{\hbar}{2m}\left(\nabla_{\boldsymbol{r}'} - \nabla_{\boldsymbol{r}} + \frac{2iq}{\hbar}\boldsymbol{A}\right)\mathrm{Tr}\left\{\hat{\tau}_i\underline{\sigma}_j\underline{G}^K(\boldsymbol{r},t;\boldsymbol{r}',t')\right\}\right],$$

which can be compared to Ref. [76, p. 316][2]. Introducing the average and relative spatial coordinates $\boldsymbol{r}_\mu$ and $\boldsymbol{r}_\delta$

$$\boldsymbol{r}_\mu = \frac{\boldsymbol{r}+\boldsymbol{r}'}{2}, \quad \boldsymbol{r}_\delta = \boldsymbol{r}-\boldsymbol{r}',$$

with the derivatives

$$\tilde{\nabla}_{\boldsymbol{r}} = \frac{1}{2}\tilde{\nabla}_{\boldsymbol{r}_\mu} + \tilde{\nabla}_{\boldsymbol{r}_\delta}, \quad \tilde{\nabla}_{\boldsymbol{r}'} = \frac{1}{2}\tilde{\nabla}_{\boldsymbol{r}_\mu} - \tilde{\nabla}_{\boldsymbol{r}_\delta},$$

we can write $\boldsymbol{j}_{ij}$ as

$$\boldsymbol{j}_{ij}(t,\boldsymbol{r}) = -\frac{\hbar q}{m}\lim_{\boldsymbol{r},t\to t',\boldsymbol{r}'}\left[\tilde{\nabla}_{\boldsymbol{r}_\delta}\,\mathrm{Tr}\left\{\hat{\tau}_i\underline{\sigma}_j\underline{G}^K(\boldsymbol{r},t;\boldsymbol{r}',t')\right\}\right].$$

Fourier transforming, we replace $\tilde{\nabla}_{\boldsymbol{r}_\delta} \to im\boldsymbol{v}\hbar$:

$$\boldsymbol{j}_{ij}(\varepsilon,\boldsymbol{p}) = -i\boldsymbol{v}\,\mathrm{Tr}\left[\hat{\tau}_i\underline{\sigma}_j\underline{G}^K(\varepsilon,\boldsymbol{p})\right].$$

Assuming now that the only significant contributions come from the Fermi surface, we can replace $\boldsymbol{v}$ with $v_F\hat{\boldsymbol{p}}$. The spectral current then becomes [40, 72]

$$\boxed{\boldsymbol{j}_{ij}(\varepsilon) = -iv_F\int\frac{d^3p}{(2\pi)^3}\,\hat{\boldsymbol{p}}\,\mathrm{Tr}\left[\hat{\tau}_i\underline{\sigma}_j\hat{\underline{G}}^K(\varepsilon,\boldsymbol{p})\right].} \tag{E.2.1}$$

To find the total current density, this expression can be integrated over energy.

E.3 The dirty limit

Replacing the momentum integral in equation (E.2.1) [46, 49],

$$\int\frac{d^3p}{(2\pi)^3} \quad\to\quad N_0\int d\xi\int\frac{d\Omega_{\boldsymbol{p}}}{4\pi}, \tag{E.3.1}$$

[1] To include the spin-orbit vector potential too, we just need to replace $q\boldsymbol{A} \mapsto \boldsymbol{\mathcal{A}}$.

[2] Datta specifically calculates the electric current here, hence the factor e.

where ξ is the kinetic energy, we get

$$\boldsymbol{j}_{ij}(\varepsilon) = -iv_F N_0 \int d\xi \int \frac{d\Omega_{\boldsymbol{p}}}{4\pi} \hat{\boldsymbol{p}} \operatorname{Tr}\left[\hat{\tau}_i \underline{\sigma}_j \hat{\underline{G}}^K(\varepsilon, \boldsymbol{p})\right]. \tag{E.3.2}$$

Introducing the quasiclassical Green function as defined in eq. (C.2.1),[3]

$$\begin{aligned} \boldsymbol{j}_{ij}(\varepsilon) &= -\frac{N_0 v_F}{2} \int \frac{d\Omega_{\boldsymbol{p}}}{4\pi} \hat{\boldsymbol{p}} \operatorname{Tr}\left[\hat{\tau}_i \underline{\sigma}_j \hat{\underline{g}}^K(\varepsilon, \boldsymbol{p})\right] \\ &= -\frac{v_F N_0}{2} \left\langle \hat{\boldsymbol{p}} \operatorname{Tr}\left[\hat{\tau}_i \underline{\sigma}_j \hat{\underline{g}}^K(\varepsilon, \boldsymbol{p})\right] \right\rangle_{\boldsymbol{p}}. \end{aligned} \tag{E.3.3}$$

To find the total current density we integrate the partial current density over energy:

$$\boxed{\boldsymbol{I}_{ij} = -\frac{N_0 v_F}{2} \int d\varepsilon \left\langle \hat{\boldsymbol{p}} \operatorname{Tr}\left[\hat{\tau}_i \underline{\sigma}_j \hat{\underline{g}}^K(\varepsilon, \boldsymbol{p})\right] \right\rangle_{\boldsymbol{p}}.} \tag{E.3.4}$$

This can be compared to Ref. [47, p. 336].[4] In the dirty, or *diffusive* limit, the elastic scattering energy is much greater than all other energy terms in the Eilenberger equation:

$$V_{\text{imp}}| \gg |\epsilon|, |q\varphi|, |\Delta|, \qquad \ell_e \ll \ell_\phi, \qquad \tau_{\text{imp}} \ll \tau_{\text{sf}}.$$

This means that the mean free path is much shorter than the system dimensions, and the Green functions approach isotropy. In this case we can expand the Green function in spherical harmonics and only keep the first two terms:

$$\check{\underline{g}} = \check{\underline{g}}_s + \hat{\boldsymbol{p}} \cdot \check{\underline{\boldsymbol{g}}}_p,$$

where neither $\check{\underline{g}}_s$ or $\check{\underline{g}}_p$ depends on the direction of the momentum. Hence the angular average of $\check{\underline{g}}$ can be approximated as

$$\begin{aligned} \left\langle \check{\underline{g}}(\boldsymbol{r}, \hat{\boldsymbol{p}}, \epsilon) \right\rangle_{\hat{\boldsymbol{p}}} &= \left\langle \check{\underline{g}}_s(\boldsymbol{r}, \epsilon) + \hat{\boldsymbol{p}} \cdot \check{\underline{g}}_p(\boldsymbol{r}, \epsilon) \right\rangle_{\hat{\boldsymbol{p}}} \\ &= \left\langle \check{\underline{g}}_s(\boldsymbol{r}, \epsilon) \right\rangle_{\hat{\boldsymbol{p}}} + \left\langle \hat{\boldsymbol{p}} \cdot \check{\underline{g}}_p(\boldsymbol{r}, \epsilon) \right\rangle_{\hat{\boldsymbol{p}}} = \left\langle \check{\underline{g}}_s(\boldsymbol{r}, \epsilon) \right\rangle_{\hat{\boldsymbol{p}}}. \end{aligned}$$

[3] Note the factor $1/2\pi$ that comes from the Fourier transformation.

[4] Ref. [47, p. 7] includes $\operatorname{Tr}\hat{\tau}_3$ to select the electric current from the matrix expression, but differs by a factor two. Equation (3.30) in Ref. [46] omits the trace and Pauli matrices, but presents the correct factor $-qN_0/2$ (remember that $\boldsymbol{I}_e = q\boldsymbol{I}_{ij}$).

We can now calculate the angular average in equation (E.3.4). We find

$$\left\langle \hat{\boldsymbol{p}} \operatorname{Tr}\left(\hat{\tau}_i \underline{\sigma}_j \underline{\hat{g}}^K\right)\right\rangle_{\hat{\boldsymbol{p}}} = \left\langle \operatorname{Tr}\left(\hat{\tau}_i \underline{\sigma}_j \left[\hat{\boldsymbol{p}}\, \underline{\hat{g}}_s^K + \hat{\boldsymbol{p}}\,(\hat{\boldsymbol{p}}\cdot \underline{\hat{\boldsymbol{g}}}_p^K)\right]\right)\right\rangle_{\hat{\boldsymbol{p}}}$$

$$= \operatorname{Tr}\left(\hat{\tau}_i \underline{\sigma}_j \left\langle \hat{\boldsymbol{p}}\,(\hat{\boldsymbol{p}}\cdot \underline{\hat{\boldsymbol{g}}}_p^K)\right\rangle_{\hat{\boldsymbol{p}}}\right).$$

As described in appendix D.4, by applying these approximations to the Usadel equation (where we drop the ring product by assuming time independence),

$$\underline{\check{\boldsymbol{g}}}_p = -\tau_{\mathrm{imp}}\hbar^2 v_F\, \underline{\check{g}}_s \circ \tilde{\nabla}_{\boldsymbol{r}} \underline{\check{g}}_s = -\tau_{\mathrm{imp}}\hbar^2 v_F\, \underline{\check{g}}_s \tilde{\nabla}_{\boldsymbol{r}} \underline{\check{g}}_s,$$

and thus, using that $\left\langle \hat{\boldsymbol{p}}\,(\hat{\boldsymbol{p}}\cdot \underline{\hat{\boldsymbol{g}}}_p^K)\right\rangle_{\hat{\boldsymbol{p}}} = \underline{\hat{\boldsymbol{g}}}_p^K/3$, equation (E.3.4) cna be expressed as

$$\boldsymbol{I}_{ij} = -\frac{N_0 v_F}{6}\int d\varepsilon \operatorname{Tr}\left(-\hat{\tau}_i \underline{\sigma}_j \tau_{\mathrm{imp}}\hbar^2 v_F \left[\underline{\check{g}}_s \tilde{\nabla}_{\boldsymbol{r}} \underline{\check{g}}_s\right]^K\right). \tag{E.3.5}$$

Introducing again the diffusion constant D from equation (D.4.7), this is more simply expressed as [42]

$$\boxed{\boldsymbol{I}_{ij} = \frac{N_0 D}{2}\int d\varepsilon \operatorname{Tr}\left(\hat{\tau}_i \underline{\sigma}_j \left[\underline{\check{g}}_s \tilde{\nabla}_{\boldsymbol{r}} \underline{\check{g}}_s\right]^K\right).} \tag{E.3.6}$$

This is the expression for the current tensor we use in the discussion in the main text.

Appendix F

Parametrization

Throughout the thesis different parametrizations have been used, depending on what is most convenient in that context. To assist the reader in converting between these different notations, both the definitions of the parametrizatins and the transformations between them have been provided here.

F.1 Theta parametrization

We can parametrize the Green functions as [47]

$$\boxed{\underline{\hat{G}}^R(\epsilon, \boldsymbol{r}) = \begin{pmatrix} \underline{G} & \underline{F} \\ -\underline{\tilde{F}} & -\underline{\tilde{G}} \end{pmatrix} = \begin{pmatrix} \cosh\theta & i\underline{\sigma}_2 \sinh\theta\, e^{i\chi} \\ i\underline{\sigma}_2 \sinh\theta\, e^{-i\chi} & -\cosh\theta \end{pmatrix},} \tag{F.1.1}$$

with the following identities for conjugation:

$$\tilde{\theta}(\epsilon) = \theta^*(-\epsilon) = -\theta(\epsilon), \qquad \tilde{\chi}(\epsilon) = \chi^*(-\epsilon) = \chi(\epsilon).$$

The SNS boundary value problem is given by

$$D\partial_x\theta = -2i\epsilon \sinh\theta = \frac{D}{2}\left(\partial_x\chi\right)^2 \sinh(2\theta),$$

with the boundary conditions

$$\text{left:} \quad \theta = \operatorname{atanh}\left(\frac{\Delta}{\epsilon}\right),\ \chi = 0, \qquad \text{right:} \quad \theta = \operatorname{atanh}\left(\frac{\Delta}{\epsilon}\right),\ \chi = \phi_0.$$

F.2 Gamma parametrization

The Riccati parametrization is given by [39, 40]

$$\boxed{\begin{aligned}\hat{\underline{G}}^{R.A} &= \begin{pmatrix} \underline{G} & \underline{F} \\ -\underline{\tilde{F}} & -\underline{\tilde{G}} \end{pmatrix} = \begin{pmatrix} \underline{N} & 0 \\ 0 & -\underline{\tilde{N}} \end{pmatrix} \begin{pmatrix} 1+\underline{\gamma}\underline{\tilde{\gamma}} & 2\underline{\gamma} \\ 2\underline{\tilde{\gamma}} & 1+\underline{\tilde{\gamma}}\underline{\gamma} \end{pmatrix} \\ &= \begin{pmatrix} 2\underline{N}-1 & 2\underline{N}\underline{\gamma} \\ -2\underline{\tilde{N}}\underline{\tilde{\gamma}} & 1-2\underline{\tilde{N}} \end{pmatrix},\end{aligned}} \tag{F.2.1}$$

where

$$\underline{N} = (1-\underline{\gamma}\underline{\tilde{\gamma}})^{-1}, \qquad \underline{\tilde{N}} = (1-\underline{\tilde{\gamma}}\underline{\gamma})^{-1}.$$

The tilde $\sim$ denotes *tilde conjugation*, which is a combination of complex conjugation and energy inversion:

$$\boxed{\tilde{f}(\varepsilon) = f^\star(-\varepsilon).} \tag{F.2.2}$$

The retarded and advanced gamma functions are related through [42, 63]

$$\boxed{\underline{\gamma}^A = (\underline{\tilde{\gamma}}^R)^\dagger = -(\underline{\tilde{\gamma}}^R)^\star.} \tag{F.2.3}$$

The following identities apply:

$$(\underline{N}\underline{\gamma})^{-1} = \underline{\gamma}^{-1} - \underline{\tilde{\gamma}} = (\underline{\gamma}\underline{\tilde{N}})^{-1}, \qquad (\underline{\tilde{N}}\underline{\tilde{\gamma}})^{-1} = \underline{\tilde{\gamma}}^{-1} - \underline{\gamma} = (\underline{\tilde{\gamma}}\underline{N})^{-1},$$

which directly implies that

$$\underline{N}\underline{\gamma} = \underline{\gamma}\underline{\tilde{N}}, \qquad \underline{\tilde{N}}\underline{\tilde{\gamma}} = \underline{\tilde{\gamma}}\underline{N}. \tag{F.2.4}$$

Using the matrix identity [77]

$$\partial_x A^{-1} = -A^{-1}(\partial_x A)A^{-1},$$

the derivative of $\underline{N}$ is

$$\partial_x \underline{N} = \partial_x (1-\underline{\gamma}\underline{\tilde{\gamma}})^{-1} = -\underline{N}\partial_x(1-\underline{\gamma}\underline{\tilde{\gamma}})\underline{N} = \underline{N}(\underline{\gamma}'\underline{\tilde{\gamma}} + \underline{\gamma}\underline{\tilde{\gamma}}')\underline{N}, \tag{F.2.5a}$$

where the prime indicates derivation with respect to x. Conjugating gives us the corresponding equation for $\underline{\tilde{N}}$:

$$\partial_x \underline{\tilde{N}} = \underline{\tilde{N}}(\underline{\tilde{\gamma}}'\underline{\gamma} + \underline{\tilde{\gamma}}\underline{\gamma}')\underline{\tilde{N}}. \tag{F.2.5b}$$

F.3 Parametrization of the Usadel equation

The Usadel equation will be easier to solve numerically if we exploit the symmetries present in the Green functions to reduce the number of components that need to be calculated. In order to be able to use the rules given in equation (F.2.4), we need to replace the ring products by normal products. This means looking at the time-independent case.

F.3.1 The retarded component in a system with isotropy along two axes

We defined in equation (D.4.9a) the Usadel equation for the retarded component of the Green function,

$$-D\tilde{\nabla}_{\boldsymbol{r}} \cdot \left(\underline{\hat{g}}_s^R \circ \tilde{\nabla}_{\boldsymbol{r}} \underline{\hat{g}}_s^R\right) = i\left[\epsilon \underline{\hat{\rho}}_3 - q\underline{\hat{\varphi}} + \frac{i}{2\tau_{\mathrm{sf}}} \underline{\hat{\rho}}_3 \underline{\hat{g}}_s^R \underline{\hat{\rho}}_3 + \underline{\hat{\boldsymbol{\sigma}}} \cdot \hat{\boldsymbol{h}}(\boldsymbol{r}) - \underline{\hat{\Delta}}, \underline{\hat{g}}_s^R\right]_-.$$

Assuming time independence, the scalar terms drop out:

$$-D\tilde{\nabla}_{\boldsymbol{r}} \cdot \left(\underline{\hat{g}}_s^R \tilde{\nabla}_{\boldsymbol{r}} \underline{\hat{g}}_s^R\right) = i\left[\epsilon \underline{\hat{\rho}}_3 + \frac{i}{2\tau_{\mathrm{sf}}} \underline{\hat{\rho}}_3 \underline{\hat{g}}_s^R \underline{\hat{\rho}}_3 + \underline{\hat{\boldsymbol{\sigma}}} \cdot \hat{\boldsymbol{h}}(\boldsymbol{r}) - \underline{\hat{\Delta}}, \underline{\hat{g}}_s^R\right]_-. \tag{F.3.1}$$

The covariant derivatives on the left-hand side need to be expanded in spatial derivatives and vector fields in order to be able to use equations (F.2.5). Using the result derived in equation (D.3.11),

$$\tilde{\nabla}_{\boldsymbol{r}} \underline{\check{G}} = \nabla_{\boldsymbol{r}} \underline{\check{G}} + i\left[\underline{\check{\boldsymbol{A}}} \overset{\bullet}{,} \underline{\check{G}}\right]_- \qquad \Rightarrow \qquad \tilde{\nabla}_{\boldsymbol{r}} \underline{\hat{g}}_s^R = \nabla_{\boldsymbol{r}} \underline{\hat{g}}_s^R + i\left[\underline{\hat{\boldsymbol{A}}}, \underline{\hat{g}}_s^R\right]_-,$$

the expansion becomes

$$\begin{aligned}\tilde{\nabla}_{\boldsymbol{r}} \cdot \left(\underline{\hat{g}}_s^R \tilde{\nabla}_{\boldsymbol{r}} \underline{\hat{g}}_s^R\right) = \nabla_{\boldsymbol{r}} \cdot \left(\underline{\hat{g}}_s^R \nabla_{\boldsymbol{r}} \underline{\hat{g}}_s^R\right) + i\nabla_{\boldsymbol{r}} \cdot \left(\underline{\hat{g}}_s^R \left[\underline{\hat{\boldsymbol{A}}}, \underline{\hat{g}}_s^R\right]_-\right) \\ + i\left[\underline{\hat{\boldsymbol{A}}}, \underline{\hat{g}}_s^R \nabla_{\boldsymbol{r}} \underline{\hat{g}}_s^R\right]_- - \left[\underline{\hat{\boldsymbol{A}}}, \underline{\hat{g}}_s^R \left[\underline{\hat{\boldsymbol{A}}}, \underline{\hat{g}}_s^R\right]_-\right]_-.\end{aligned}$$

This can be simplified somewhat by considering isotropy in two directions (which we will choose to be $\hat{\boldsymbol{e}}_x$ and $\hat{\boldsymbol{e}}_y$) and that $(\underline{\hat{g}}_s^R)^2 \approx 1$. The former allows us to assume that

$$\partial_y \underline{\hat{g}}_s^R = \partial_z \underline{\hat{g}}_s^R = 0,$$

whereas the latter simplifies

$$\nabla_{\boldsymbol{r}} \cdot \left(\underline{\hat{g}}_s^R \left[\underline{\hat{\boldsymbol{A}}}, \underline{\hat{g}}_s^R\right]_-\right) = \nabla_{\boldsymbol{r}} \cdot \left(\underline{\hat{g}}_s^R \underline{\hat{\boldsymbol{A}}} \underline{\hat{g}}_s^R - \underline{\hat{\boldsymbol{A}}}\right) = \nabla_{\boldsymbol{r}} \cdot \left(\underline{\hat{g}}_s^R \underline{\hat{\boldsymbol{A}}} \underline{\hat{g}}_s^R\right)$$

and

$$\left[\underline{\hat{\boldsymbol{A}}}, \underline{\hat{g}}_s^R \left[\underline{\hat{\boldsymbol{A}}}, \underline{\hat{g}}_s^R\right]_-\right]_- = \underline{\hat{\boldsymbol{A}}}\underline{\hat{g}}_s^R\underline{\hat{\boldsymbol{A}}}\underline{\hat{g}}_s^R - \underline{\hat{g}}_s^R\underline{\hat{\boldsymbol{A}}}\underline{\hat{g}}_s^R\underline{\hat{\boldsymbol{A}}} = \left[\underline{\hat{\boldsymbol{A}}}, \underline{\hat{g}}_s^R\underline{\hat{\boldsymbol{A}}}\underline{\hat{g}}_s^R\right]_- .$$

Here we assumed that the spatial derivatives of the vector potential are negligible. We will now assume that the system is isotropic in two directions, and focus on the direction in which it is not, which we choose to be $\hat{\boldsymbol{e}}_z$. Looking at the covariant derivative in this direction, we find[1]

$$\begin{aligned}\tilde{\nabla}_{\boldsymbol{r}} \cdot \left(\underline{\hat{g}}_s^R \tilde{\nabla}_{\boldsymbol{r}} \underline{\hat{g}}_s^R\right) = \partial_z \left(\underline{\hat{g}}_s^R \partial_z \underline{\hat{g}}_s^R\right) + i\partial_z \left(\underline{\hat{g}}_s^R \underline{\hat{\boldsymbol{A}}}_z \underline{\hat{g}}_s^R\right) \\ + i\left[\underline{\hat{\boldsymbol{A}}}_z, \underline{\hat{g}}_s^R \partial_z \underline{\hat{g}}_s^R\right]_- - \left[\underline{\hat{\boldsymbol{A}}}, \underline{\hat{g}}_s^R \underline{\hat{\boldsymbol{A}}} \underline{\hat{g}}_s^R\right]_- .\end{aligned} \tag{F.3.2}$$

Using the parametrization in equation (F.2.1),

$$\underline{\hat{g}}_s^R = \begin{pmatrix} 2\underline{N} - 1 & 2\underline{N}\underline{\gamma} \\ -2\underline{\tilde{N}}\underline{\tilde{\gamma}} & 1 - 2\underline{\tilde{N}} \end{pmatrix},$$

we can write this in terms of γ and N. Since the bottom row of the $\underline{\hat{g}}_s^R$ on the right-hand side of equation (F.3.1) is just minus the conjugated top row, the latter contains all the information we need. We thus focus on the top row on the left-hand side as well. There are some repeating terms, which we can simplify by using equations (F.2.4, F.2.5).

$$\begin{aligned}\left(\underline{\hat{g}}_s^R \partial_z \underline{\hat{g}}_s^R\right)^{(1,1)} &= (2\underline{N} - 1)\partial_z(2\underline{N} - 1) - (2\underline{N}\underline{\gamma})\partial_z(2\underline{\tilde{N}}\underline{\tilde{\gamma}}) \\ &= 2\underline{N}(\underline{\gamma}'\underline{\tilde{\gamma}} - \underline{\gamma}\underline{\tilde{\gamma}}')\underline{N}, \\ \left(\underline{\hat{g}}_s^R \partial_z \underline{\hat{g}}_s^R\right)^{(1,2)} &= (2\underline{N} - 1)\partial_z(2\underline{N}\underline{\gamma}) + (2\underline{N}\underline{\gamma})\partial_z(1 - 2\underline{\tilde{N}}) \\ &= 2\underline{N}(\underline{\gamma}' - \underline{\gamma}\underline{\tilde{\gamma}}'\underline{\gamma})\underline{\tilde{N}}.\end{aligned}$$

Similarly, to find the second term on the right of equation (F.3.2) we calculate

$$\begin{aligned}\left(\underline{\hat{g}}_s^R \underline{\hat{\boldsymbol{A}}} \underline{\hat{g}}_s^R\right)^{(1,1)} &= (2\underline{N} - 1)\underline{\boldsymbol{A}}(2\underline{N} - 1) + 4\underline{N}\underline{\gamma}\underline{\boldsymbol{A}}^\star \underline{\tilde{N}}\underline{\tilde{\gamma}}, \\ \left(\underline{\hat{g}}_s^R \underline{\hat{\boldsymbol{A}}} \underline{\hat{g}}_s^R\right)^{(1,2)} &= (4\underline{N} - 2)\underline{\boldsymbol{A}}\underline{N}\underline{\gamma} + 2\underline{N}\underline{\gamma}\underline{\boldsymbol{A}}^\star(2\underline{\tilde{N}} - 1).\end{aligned}$$

[1] Note that because of the dot product on the left, only $\underline{\boldsymbol{A}}_z$ enters in the second and third term on the right.

Note that the diagonality in spin space is an approximation in itself, neglecting general spin-orbit coupling [30]. With this approximation, the last two terms in equation (F.3.2) drop out. Calculating the top row of the first term, we find

$$\begin{aligned}
\left[\partial_z\left(\underline{\hat{g}}_s^R\partial_z\underline{\hat{g}}_s^R\right)\right]^{(1,1)} &= \partial_z\left[2\underline{N}(\underline{\gamma}'\underline{\tilde{\gamma}}-\underline{\gamma}\underline{\tilde{\gamma}}')\underline{N}\right]\\
&= 2\underline{N}(\underline{\gamma}''+2\underline{\gamma}'\underline{\tilde{N}}\underline{\tilde{\gamma}}\underline{\gamma}')\underline{\tilde{\gamma}}\underline{N}-2\underline{N}\underline{\gamma}(\underline{\tilde{\gamma}}''+2\underline{\tilde{\gamma}}'\underline{N}\underline{\gamma}\underline{\tilde{\gamma}}')\underline{N}.\\
\left[\partial_z\left(\underline{\hat{g}}_s^R\partial_z\underline{\hat{g}}_s^R\right)\right]^{(1,2)} &= \partial_z\left[2\underline{N}(\underline{\gamma}'-\underline{\gamma}\underline{\tilde{\gamma}}'\underline{\gamma})\underline{\tilde{N}}\right]\\
&= 2\underline{N}(\underline{\gamma}''+2\underline{\gamma}'\underline{\tilde{N}}\underline{\tilde{\gamma}}\underline{\gamma}')\underline{\tilde{N}}-2\underline{N}\underline{\gamma}(\underline{\tilde{\gamma}}''+2\underline{\tilde{\gamma}}'\underline{N}\underline{\gamma}\underline{\tilde{\gamma}}')\underline{\gamma}\underline{\tilde{N}}.
\end{aligned}$$

Similarly, the top row of the second term becomes

$$\begin{aligned}
\left[\partial_z\left(\underline{\hat{g}}_s^R\underline{\hat{\boldsymbol{A}}}_z\underline{\hat{g}}_s^R\right)\right]^{(1,1)} &= 2\underline{N}\Big[(1+\underline{\gamma}\underline{\tilde{\gamma}})\underline{\boldsymbol{A}}_z\underline{N}(\underline{\gamma}\underline{\tilde{\gamma}}'+\underline{\gamma}'\underline{\tilde{\gamma}})\\
&\quad+(\underline{\gamma}\underline{\tilde{\gamma}}'+\underline{\gamma}'\underline{\tilde{\gamma}})\underline{N}\underline{\boldsymbol{A}}_z(1+\underline{\gamma}\underline{\tilde{\gamma}})\Big]\underline{N}\\
&\quad+4\underline{N}\left[\underline{\gamma}\underline{\boldsymbol{A}}_z^\star\underline{\tilde{N}}(\underline{\tilde{\gamma}}'+\underline{\tilde{\gamma}}\underline{\gamma}'\underline{\tilde{\gamma}})+(\underline{\gamma}'+\underline{\gamma}\underline{\tilde{\gamma}}'\underline{\gamma})\underline{\tilde{N}}\underline{\boldsymbol{A}}_z^\star\underline{\tilde{\gamma}}\right]\underline{N},\\
\left[\partial_z\left(\underline{\hat{g}}_s^R\underline{\hat{\boldsymbol{A}}}_z\underline{\hat{g}}_s^R\right)\right]^{(1,2)} &= 2\underline{N}\Big[(1+\underline{\gamma}\underline{\tilde{\gamma}})\underline{\boldsymbol{A}}_z\underline{N}(\underline{\gamma}'+\underline{\gamma}\underline{\tilde{\gamma}}'\underline{\tilde{\gamma}})\\
&\quad+(\underline{\gamma}'+\underline{\gamma}\underline{\tilde{\gamma}}'\underline{\gamma})\underline{\tilde{N}}\underline{\boldsymbol{A}}_z(1+\underline{\tilde{\gamma}}\underline{\gamma})\Big]\underline{\tilde{N}}\\
&\quad+4\underline{N}\left[\underline{\gamma}\underline{\boldsymbol{A}}_z^\star\underline{\tilde{N}}(\underline{\tilde{\gamma}}\underline{\gamma}'+\underline{\tilde{\gamma}}'\underline{\gamma})+(\underline{\gamma}\underline{\tilde{\gamma}}'+\underline{\gamma}'\underline{\tilde{\gamma}})\underline{N}\underline{\boldsymbol{A}}_z^\star\underline{\tilde{\gamma}}\right]\underline{\tilde{N}}.
\end{aligned}\tag{F.3.3}$$

Multiplying the top-left component by $\underline{\gamma}$ from the right, using equation (F.2.4), subtracting the result from the top-right component and multiplying by $\underline{N}^{-1}/2D$ from the left, we find an expression for $\underline{\gamma}''$:

$$\begin{aligned}
\underline{\gamma}'' = \frac{\underline{N}^{-1}}{2D}\Bigg(&\left[\tilde{\nabla}_{\boldsymbol{r}}\cdot\left(\underline{\hat{g}}_s^R\tilde{\nabla}_{\boldsymbol{r}}\underline{\hat{g}}_s^R\right)\right]^{(1,2)}-\left[\tilde{\nabla}_{\boldsymbol{r}}\cdot\left(\underline{\hat{g}}_s^R\tilde{\nabla}_{\boldsymbol{r}}\underline{\hat{g}}_s^R\right)\right]^{(1,1)}\underline{\gamma}\Bigg)\\
&-2\underline{\gamma}'\underline{\tilde{N}}\underline{\tilde{\gamma}}\underline{\gamma}'+2i\left[(\underline{\boldsymbol{A}}_z+\underline{\gamma}\underline{\boldsymbol{A}}_z^\star\underline{\tilde{\gamma}})\underline{N}\underline{\gamma}'+\underline{\gamma}'\underline{\tilde{N}}(\underline{\boldsymbol{A}}_z^\star+\underline{\tilde{\gamma}}\underline{\boldsymbol{A}}_z\underline{\gamma})\right]\\
&+2(\underline{\boldsymbol{A}}\underline{\gamma}+\underline{\gamma}\underline{\boldsymbol{A}}^\star)\underline{\tilde{N}}(\underline{\boldsymbol{A}}^\star+\underline{\tilde{\gamma}}\underline{\boldsymbol{A}}\underline{\gamma})+\underline{\boldsymbol{A}}^2\underline{\gamma}-\underline{\gamma}(\underline{\boldsymbol{A}}^\star)^2.
\end{aligned}\tag{F.3.4}$$

Calculating now also the top row of the right-hand side of equation (F.3.1) using the definitions in equation (D.3.7),

$$\left(\left[\epsilon\hat{\underline{\rho}}_3 + \frac{i}{2\tau_{\rm sf}}\,\hat{\underline{\rho}}_3\hat{\underline{g}}_s^R\hat{\underline{\rho}}_3 + \hat{\underline{\boldsymbol{\sigma}}}\cdot\hat{\boldsymbol{h}}(\boldsymbol{r}) - \hat{\underline{\Delta}}, \hat{\underline{g}}_s^R\right]_-\right)^{(1,1)} = 2\boldsymbol{h}\cdot(\boldsymbol{\sigma}\underline{N} - \underline{N}\boldsymbol{\sigma})$$
$$-2i\underline{\sigma}_2\Delta\,\underline{\tilde{N}}\underline{\tilde{\gamma}} - 2N\underline{\gamma}\,[i\underline{\sigma}_2\Delta]^\dagger\,,$$

$$\left(\left[\epsilon\hat{\underline{\rho}}_3 + \frac{i}{2\tau_{\rm sf}}\,\hat{\underline{\rho}}_3\hat{\underline{g}}_s^R\hat{\underline{\rho}}_3 + \hat{\underline{\boldsymbol{\sigma}}}\cdot\hat{\boldsymbol{h}}(\boldsymbol{r}) - \hat{\underline{\Delta}}, \hat{\underline{g}}_s^R\right]_-\right)^{(1,2)} = 2\boldsymbol{h}\cdot(\boldsymbol{\sigma}\underline{N}\underline{\gamma} - \underline{N}\underline{\gamma}\boldsymbol{\sigma}^\star)$$
$$4\epsilon\,\underline{N}\underline{\gamma} + i\underline{\sigma}_2\Delta(1-2\underline{\tilde{N}}) + (1-2\underline{N})i\underline{\sigma}_2\Delta$$
$$+\frac{2i}{\tau_{\rm sf}}\left[(2\underline{N}-1)\underline{N}\underline{\gamma} - \underline{N}\underline{\gamma}(1-2\underline{\tilde{N}})\right],$$

we can write (assuming $\Delta = \Delta^\dagger$) [30]

$$\begin{aligned}
D\underline{\gamma}'' = {} & -2i\epsilon\,\underline{\gamma} - i\boldsymbol{h}\cdot(\underline{\boldsymbol{\sigma}}\underline{\gamma} - \underline{\gamma}\boldsymbol{\sigma}^\star) - \Delta(\underline{\sigma}_2 - \underline{\gamma}\underline{\sigma}_2\underline{\gamma}) \\
& + \frac{1}{\tau_{\rm sf}}\left[(2\underline{N}-1)\underline{\gamma} - \underline{\gamma}(1-2\underline{\tilde{N}})\right] + D\Big\{ - 2\underline{\gamma}'\underline{\tilde{N}}\underline{\tilde{\gamma}}\underline{\gamma}' \\
& + 2i\left[(\underline{\boldsymbol{A}}_z + \underline{\gamma}\underline{\boldsymbol{A}}_z^\star\underline{\tilde{\gamma}})\underline{N}\underline{\gamma}' + \underline{\gamma}'\underline{\tilde{N}}(\underline{\boldsymbol{A}}_z^\star + \underline{\tilde{\gamma}}\underline{\boldsymbol{A}}_z\underline{\gamma})\right] \\
& + 2(\underline{\boldsymbol{A}}\underline{\gamma} + \underline{\gamma}\underline{\boldsymbol{A}}^\star)\underline{\tilde{N}}(\underline{\boldsymbol{A}}^\star + \underline{\tilde{\gamma}}\underline{\boldsymbol{A}}\underline{\gamma}) + \underline{\boldsymbol{A}}^2\underline{\gamma} - \underline{\gamma}(\underline{\boldsymbol{A}}^\star)^2\Big\}.
\end{aligned} \tag{F.3.5}$$

The corresponding expression for $\underline{\tilde{\gamma}}''$ is found through tilde conjugation (see equation (F.2.2)).

F.4 Pauli decomposition

Any 2×2 matrix $\underline{A}$ in spin space can be built up from the four Pauli matrices:

$$\underline{A} = \sum_i A_i^{\mathcal{P}}\underline{\sigma}_i.$$

To find the coefficients $A_i^{\mathcal{P}}$, we first define a flat mapping or "flatmap" that simply lists the elements of A row by row:

$$\text{flatmap } f: \quad A \to \vec{A}, \quad \begin{pmatrix} A_{11} & A_{12} \\ A_{21} & A_{22} \end{pmatrix} \mapsto \begin{pmatrix} A_{11} \\ A_{12} \\ A_{21} \\ A_{22} \end{pmatrix}.$$

By simply writing out the expression $\vec{A} = \underline{\mathcal{P}}\vec{A}^{\mathcal{P}}$ we find

$$\underline{\mathcal{P}} = \begin{pmatrix} 1 & 0 & 0 & 1 \\ 0 & 1 & -i & 0 \\ 0 & 1 & i & 0 \\ 1 & 0 & 0 & -1 \end{pmatrix}, \quad \underline{\mathcal{P}}^{-1} = \begin{pmatrix} 1/2 & 0 & 0 & 1/2 \\ 0 & 1/2 & 1/2 & 0 \\ 0 & i/2 & -i/2 & 0 \\ 1/2 & 0 & 0 & -1/2 \end{pmatrix}.$$

We can now find the Pauli coefficients $A_i^{\mathcal{P}}$ with the operation

$$\vec{A}^{\mathcal{P}} = \underline{\mathcal{P}}^{-1} f \underline{A}.$$

In this thesis we also write out the distribution function $\hat{\underline{h}}$ in its Pauli components, in which we account for the simpler structure in Nambu space (only $\hat{\tau}_0$ and $\hat{\tau}_3$ are involved) by only listing eight coefficients. Accounting for the empty top-right and bottom-left quarters, we define the distribution function-specific flatmap as

$$\text{flatmap } f_{\hat{\underline{h}}}: \quad \hat{\underline{h}} = \begin{pmatrix} \underline{x} & \\ 0 & -\underline{\tilde{x}} \end{pmatrix} \mapsto \begin{pmatrix} x_{11} \\ \vdots \\ x_{22} \\ -\tilde{x}_{11} \\ \vdots \\ -\tilde{x}_{22} \end{pmatrix} = \vec{x}.$$

The Pauli decomposition that decomposes $\vec{x}$ into its Pauli matrix components $\vec{h} = h_{kl}$ is then represented by the matrix $\hat{\underline{\mathcal{P}}}^{-1}$ such that

$$\vec{x} = \hat{\underline{\mathcal{P}}}\vec{h}, \quad \vec{h} = \hat{\underline{\mathcal{P}}}^{-1}\vec{x}, \quad \text{where} \quad \hat{\underline{\mathcal{P}}} = \begin{pmatrix} \underline{\mathcal{P}} & \underline{\mathcal{P}} \\ \underline{\mathcal{P}} & -\underline{\mathcal{P}} \end{pmatrix}.$$

Combining the two operations, the 4×4 matrix $\hat{\underline{h}}$ and the Pauli decomposition h_{kl} can be related by

$$h_{kl} = \hat{\underline{\mathcal{P}}}^{-1} f \hat{\underline{h}}, \qquad \hat{\underline{h}} = f^{-1} \hat{\underline{\mathcal{P}}} h_{kl}.$$

F.5 Mapping between parametrizations

Suppose an 8×8 matrix $A^{8\times 8}$ maps the vector $\vec{x}$ (equivalent to $\hat{\underline{h}}$) to another vector $\vec{x}'$ (equivalent to $\hat{\underline{h}}'$), then there should exist a 4×4 matrix $B^{4\times 4}$ that, when operating on $\hat{\underline{h}}$, creates $\hat{\underline{h}}'$. Writing out $A^{8\times 8}\vec{x} = \vec{x}'$, we find that the top-left component of $\hat{\underline{h}}'$ is equal to $\sum_i A_{1i}x_i$. We see that the first column of $\hat{\underline{h}}'$ contains elements of all columns of $\hat{\underline{h}}$, which per matrix multiplication is impossible unless $A_{12}, A_{14} \ldots A_{18}$, $A_{21}, A_{23}, A_{25} \ldots A_{28}$, $A_{32}, A_{34} \ldots A_{38}$, etc. are zero. Keeping 48 of the 64 elements of $A^{8\times 8}$ zero is a simple way to ensure that the pairing of $B^{4\times 4}$ and $A^{8\times 8}$ is a bijection. The matrix $B^{4\times 4}$ would then be

$$B^{4\times 4} = \begin{pmatrix} A_{11} & A_{13} & 0 & 0 \\ A_{31} & A_{33} & 0 & 0 \\ 0 & 0 & A_{55} & A_{57} \\ 0 & 0 & A_{75} & A_{77} \end{pmatrix} = \begin{pmatrix} A_{22} & A_{24} & 0 & 0 \\ A_{42} & A_{44} & 0 & 0 \\ 0 & 0 & A_{66} & A_{68} \\ 0 & 0 & A_{86} & A_{88} \end{pmatrix}. \tag{F.5.1}$$

Similarly, from B we can find A:

$$A^{8\times 8} = \begin{pmatrix} B_{11} & 0 & B_{12} & 0 & 0 & 0 & 0 & 0 \\ 0 & B_{11} & 0 & B_{12} & 0 & 0 & 0 & 0 \\ B_{21} & 0 & B_{22} & 0 & 0 & 0 & 0 & 0 \\ 0 & B_{21} & 0 & B_{22} & 0 & 0 & 0 & 0 \\ 0 & 0 & 0 & 0 & B_{33} & 0 & B_{34} & 0 \\ 0 & 0 & 0 & 0 & 0 & B_{33} & 0 & B_{34} \\ 0 & 0 & 0 & 0 & B_{43} & 0 & B_{44} & 0 \\ 0 & 0 & 0 & 0 & 0 & B_{43} & 0 & B_{44} \end{pmatrix},$$

where we see the extra restriction that each even row of $A^{8\times 8}$ must be equal to the row above it, shifted by one position to the right.

If the result of the operation on the distribution function is *not* another distribution function, and has nonzero elements in the top-right and bottom-left quadrant, it cannot be represented by a square matrix when operating on the Pauli decomposed function. A square matrix B with nonzero elements in all quadrants will not have a square but a 16×8 representation when acting on the

Pauli decomposition:

$$A^{16\times 8} = \begin{pmatrix} B_{11} & 0 & B_{12} & 0 & 0 & 0 & 0 & 0 \\ 0 & B_{11} & 0 & B_{12} & 0 & 0 & 0 & 0 \\ 0 & 0 & 0 & 0 & B_{13} & 0 & B_{14} & 0 \\ 0 & 0 & 0 & 0 & 0 & B_{13} & 0 & B_{14} \\ B_{21} & 0 & B_{22} & 0 & 0 & 0 & 0 & 0 \\ 0 & B_{21} & 0 & B_{22} & 0 & 0 & 0 & 0 \\ 0 & 0 & 0 & 0 & B_{23} & 0 & B_{24} & 0 \\ 0 & 0 & 0 & 0 & 0 & B_{23} & 0 & B_{24} \\ B_{31} & 0 & B_{32} & 0 & 0 & 0 & 0 & 0 \\ 0 & B_{31} & 0 & B_{32} & 0 & 0 & 0 & 0 \\ 0 & 0 & 0 & 0 & B_{33} & 0 & B_{34} & 0 \\ 0 & 0 & 0 & 0 & 0 & B_{33} & 0 & B_{34} \\ B_{41} & 0 & B_{42} & 0 & 0 & 0 & 0 & 0 \\ 0 & B_{41} & 0 & B_{42} & 0 & 0 & 0 & 0 \\ 0 & 0 & 0 & 0 & B_{43} & 0 & B_{44} & 0 \\ 0 & 0 & 0 & 0 & 0 & B_{43} & 0 & B_{44} \end{pmatrix},$$

which has the inverse

$$B^{4\times 4} = \begin{pmatrix} A_{11} & A_{13} & A_{35} & A_{37} \\ A_{51} & A_{53} & A_{75} & A_{77} \\ A_{91} & A_{93} & A_{11,5} & A_{11,7} \\ A_{13,1} & A_{13,3} & A_{15,5} & A_{15,7} \end{pmatrix} = \begin{pmatrix} A_{22} & A_{24} & A_{46} & A_{48} \\ A_{62} & A_{64} & A_{86} & A_{88} \\ A_{10,2} & A_{10,4} & A_{12,6} & A_{12,8} \\ A_{14,2} & A_{14,4} & A_{16,6} & A_{16,8} \end{pmatrix}.$$

Quite often, one encounters an expression where $\underline{\hat{\hbar}}$ is operated on both from the left and the right. For example, in section 2.8 we twice find the expression

$$A\underline{\hat{\hbar}} + \underline{\hat{\hbar}}B = C.$$

Note that in the more general expression $A\underline{\hat{\hbar}}B = C$ (from which we can construct expressions like those above by choosing either A or B to be the identity), the elements are given by

$$(A\underline{\hat{\hbar}}B)_{ij} = \sum_{k,l} A_{ik}\underline{\hat{\hbar}}_{kl}B_{lj}.$$

We introduce the function $\mathcal{F}_{\underline{\hat{\hbar}}}$ that operates on the flatmapped distribution function,

$$\mathcal{F}_{\underline{\hat{\hbar}}}(A,B)\mathit{f}X = \mathcal{F}_{\underline{\hat{\hbar}}}(A,B)\vec{x} = \mathit{f}C,$$

where element C_{ij} of C, equivalent to row $(i-1)*\dim(C)+j$ of $\mathit{f}C$, is given by

$$C_{ij} = \sum_{k,l} A_{ik}X_{kl}B_{lj}.$$

In flatmapped notation row i then equals

$$\sum_{k=1:8} A_{\lceil i/4\rceil,\lceil k/2\rceil}\vec{x}_k B_{k-2\lceil k/2\rceil+2\lceil k/4\rceil,i+4-4\lceil i/4\rceil},$$

so element i,j of $\mathcal{F}_{\underline{\hat{H}}}$ is

$$\boxed{(\mathcal{F}_{\underline{\hat{H}}})_{ij}(A,B) = A_{\lceil i/4\rceil,\lceil j/2\rceil}B_{j-2\lceil j/2\rceil+2\lceil j/4\rceil,i+4-4\lceil i/4\rceil}.} \tag{F.5.2}$$

This operation allows us to quickly find the ordinary differential equations and boundary conditions for the distribution functions in section 2.8.

Bibliography

[1] Dirk Van Delft and Peter Kes. "The discovery of superconductivity". In: *Physics Today* 63.9 (2010), pp. 38–43.

[2] Y-H Tang. "Josephson Voltage Metrology for Watt Balance Experiments at NIST". In: *Measurement Automation Monitoring* 62 (2016).

[3] L DiCarlo et al. "Demonstration of two-qubit algorithms with a superconducting quantum processor". In: *Nature* 460.7252 (2009), pp. 240–244.

[4] Erik Lucero et al. "Computing prime factors with a Josephson phase qubit quantum processor". In: *Nature Physics* 8.10 (2012), pp. 719–723.

[5] Yutaka Terao, Masaki Sekino, and Hiroyuki Ohsaki. "Electromagnetic design of 10 MW class fully superconducting wind turbine generators". In: *IEEE Transactions on Applied Superconductivity* 22.3 (2012), pp. 5201904–5201904.

[6] VS Vysotsky et al. "Hybrid Energy Transfer Line With Liquid Hydrogen and Superconducting Cable—First Experimental Proof of Concept". In: *IEEE Transactions on Applied Superconductivity* 23.3 (2013), pp. 5400906–5400906.

[7] Jacob Linder and Jason WA Robinson. "Superconducting spintronics". In: *Nature Physics* 11.4 (2015), pp. 307–315.

[8] JWA Robinson, JDS Witt, and MG Blamire. "Controlled injection of spin-triplet supercurrents into a strong ferromagnet". In: *Science* 329.5987 (2010), pp. 59–61.

[9] LR Tagirov. "Low-field superconducting spin switch based on a superconductor/ferromagnet multilayer". In: *Physical review letters* 83.10 (1999), p. 2058.

[10] S Takahashi, H Imamura, and S Maekawa. "Spin imbalance and magnetoresistance in ferromagnet/superconductor/ferromagnet double tunnel junctions". In: *Physical review letters* 82.19 (1999), p. 3911.

[11] Jabir Ali Ouassou et al. “Electric control of superconducting transition through a spin-orbit coupled interface”. In: *arXiv preprint arXiv:1601.07176* (2016).

[12] John Bardeen, Leon N Cooper, and J Robert Schrieffer. “Theory of superconductivity”. In: *Physical Review* 108.5 (1957), p. 1175.

[13] BT Matthias, H Suhl, and E Corenzwit. “Spin exchange in superconductors”. In: *Physical Review Letters* 1.3 (1958), p. 92.

[14] Bernd Matthias et al. “Ferromagnetic solutes in superconductors”. In: *Physical Review* 115.6 (1959), p. 1597.

[15] VL Ginzburg. “Ferromagnetic superconductors”. In: *Soviet Physics Jetp-Ussr* 4.2 (1957), pp. 153–160.

[16] Alexandre I Buzdin. “Proximity effects in superconductor-ferromagnet heterostructures”. In: *Reviews of modern physics* 77.3 (2005), p. 935.

[17] FS Bergeret and IV Tokatly. “Spin-orbit coupling as a source of long-range triplet proximity effect in superconductor-ferromagnet hybrid structures”. In: *Physical Review B* 89.13 (2014), p. 134517.

[18] Matthias Eschrig. “Spin-polarized supercurrents for spintronics”. In: *Phys. Today* 64.1 (2011), p. 43.

[19] FS Bergeret, AF Volkov, and KB Efetov. “Long-range proximity effects in superconductor-ferromagnet structures”. In: *Physical review letters* 86.18 (2001), p. 4096.

[20] FS Bergeret, AF Volkov, and KB Efetov. “Odd triplet superconductivity and related phenomena in superconductor-ferromagnet structures”. In: *Reviews of modern physics* 77.4 (2005), p. 1321.

[21] Matthias Eschrig et al. “Singlet-triplet mixing in superconductor-ferromagnet hybrid devices”. In: *Advances in Solid State Physics*. Springer, 2004, pp. 533–545.

[22] FS Bergeret and IV Tokatly. “Singlet-triplet conversion and the long-range proximity effect in superconductor-ferromagnet structures with generic spin dependent fields”. In: *Physical review letters* 110.11 (2013), p. 117003.

[23] Klaus D Usadel. “Generalized diffusion equation for superconducting alloys”. In: *Physical Review Letters* 25.8 (1970), p. 507.

[24] AI Larkin and Yu N Ovchinnikov. “Quasiclassical method in the theory of superconductivity”. In: *Soviet Journal of Experimental and Theoretical Physics* 28 (1969), p. 1200.

[25] Henrik Bruus and Karsten Flensberg. *Many-body quantum theory in condensed matter physics: an introduction*. Oxford University Press, 2004.

[26] GD Mahan. *Many-Particle Physics, 3nd.* 2000.

[27] Jacob Linder, Takehito Yokoyama, and Asle Sudbø. "Theory of superconducting and magnetic proximity effect in S/F structures with inhomogeneous magnetization textures and spin-active interfaces". In: *Physical Review B* 79.5 (2009), p. 054523.

[28] K Fossheim and Asle Sudbø. *Superconductivity: physics and applications.* English. Chichester, West Sussex, England; Hoboken, NJ: Wiley, 2004. ISBN: 9780470844526.

[29] A. C Rose-Innes and E. H Rhoderick. *Introduction to superconductivity.* English. Oxford: Pergamon Press, 1978. ISBN: 9780080216522.

[30] Sol H Jacobsen, Jabir Ali Ouassou, and Jacob Linder. "Critical temperature and tunneling spectroscopy of superconductor-ferromagnet hybrids with intrinsic Rashba-Dresselhaus spin-orbit coupling". In: *Physical Review B* 92.2 (2015), p. 024510.

[31] EI Rashba. "Properties of semiconductors with an extremum loop. 1. Cyclotron and combinational resonance in a magnetic field perpendicular to the plane of the loop". In: *Sov. Phys. Solid State* 2 (1960), pp. 1109–1122.

[32] G Dresselhaus. "Spin-orbit coupling effects in zinc blende structures". In: *Physical Review* 100.2 (1955), p. 580.

[33] EG Mishchenko and BI Halperin. "Transport equations for a two-dimensional electron gas with spin-orbit interaction". In: *Physical Review B* 68.4 (2003), p. 045317.

[34] Aurelien Manchon et al. "New perspectives for Rashba spin-orbit coupling". In: *Nature materials* 14.9 (2015), pp. 871–882.

[35] CL Romano, SE Ulloa, and PI Tamborenea. "Level structure and spin-orbit effects in quasi-one-dimensional semiconductor nanostructures". In: *Physical Review B* 71.3 (2005), p. 035336. URL: `http://journals.aps.org/prb/abstract/10.1103/PhysRevB.71.035336`.

[36] V Fallahi and M Ghanaatshoar. "Ballistic transport through a semiconducting magnetic nanocontact in the presence of Rashba and Dresselhaus spin–orbit interactions". In: *physica status solidi (b)* 249.5 (2012), pp. 1077–1082.

[37] Michael Tinkham. *Introduction to superconductivity.* English. Mineola, N.Y.: Dover Publications, 2004. ISBN: 9780486435039.

[38] Alexander Altland, Yuval Gefen, and Gilles Montambaux. "What is the Thouless energy for ballistic systems?" In: *Physical review letters* 76.7 (1996), p. 1130.

[39] Nils Schopohl. “Transformation of the Eilenberger equations of superconductivity to a scalar Riccati equation”. In: *arXiv preprint cond-mat/9804064* (1998).

[40] Matthias Eschrig. “Distribution functions in nonequilibrium theory of superconductivity and Andreev spectroscopy in unconventional superconductors”. In: *Physical Review B* 61.13 (2000), p. 9061.

[41] AV Zaitsev. “Quasiclassical equations of the theory of superconductivity for contiguous metals and the properties of constricted microcontacts”. In: *Zh. Eksp. Teor. Fiz* 86 (1984), pp. 1742–1758.

[42] JC Hammer et al. “Density of states and supercurrent in diffusive SNS junctions: Roles of nonideal interfaces and spin-flip scattering”. In: *Physical Review B* 76.6 (2007), p. 064514.

[43] Yuli V Nazarov. “Novel circuit theory of Andreev reflection”. In: *arXiv preprint cond-mat/9811155* (1998).

[44] Yuli V Nazarov. “Circuit theory of non-equilibrium superconductivity”. In: *Physica C: Superconductivity* 352.1 (2001), pp. 19–24.

[45] M Yu Kuprianov and VF Lukichev. “Influence of boundary transparency on the critical current of dirty SS’S structures”. In: *Zh. Eksp. Teor. Fiz* 94 (1988), p. 149.

[46] Jørgen Rammer and H Smith. “Quantum field-theoretical methods in transport theory of metals”. In: *Reviews of modern physics* 58.2 (1986), p. 323.

[47] Wolfgang Belzig et al. “Quasiclassical Green’s function approach to mesoscopic superconductivity”. In: *Superlattices and microstructures* 25.5 (1999), pp. 1251–1288.

[48] DA Ivanov and Ya V Fominov. “Minigap in superconductor-ferromagnet junctions with inhomogeneous magnetization”. In: *Physical Review B* 73.21 (2006), p. 214524.

[49] Venkat Chandrasekhar. “An introduction to the quasiclassical theory of superconductivity for diffusive proximity-coupled systems”. In: *arXiv: cond-mat* 312507 (2003).

[50] P Townsend and J Sutton. “Investigation by electron tunneling of the superconducting energy gaps in nb, ta, sn, and pb”. In: *Physical Review* 128.2 (1962), p. 591.

[51] Ivar Giaever and Karl Megerle. “Study of superconductors by electron tunneling”. In: *Physical Review* 122.4 (1961), p. 1101.

[52] Ph B Allen and RC Dynes. “Transition temperature of strong-coupled superconductors reanalyzed”. In: *Physical Review B* 12.3 (1975), p. 905.

[53] Rosario Fazio and Carlo Lucheroni. “Local density of states in superconductor-ferromagnetic hybrid systems”. In: *EPL (Europhysics Letters)* 45.6 (1999), p. 707.

[54] Ulrich Eckern and Albert Schmid. “Quasiclassical Green’s function in the BCS pairing theory”. In: *Journal of Low Temperature Physics* 45.1-2 (1981), pp. 137–166.

[55] Mihail Silaev et al. “Long-range spin accumulation from heat injection in mesoscopic superconductors with zeeman splitting”. In: *Physical review letters* 114.16 (2015), p. 167002.

[56] Mihail Silaev et al. “Spin Hanle effect in mesoscopic superconductors”. In: *Physical Review B* 91.2 (2015), p. 024506.

[57] Andreas Moor, Anatoly F Volkov, and Konstantin B Efetov. “Excess current in ferromagnet-superconductor structures with fully polarized triplet component”. In: *Physical Review B* 93.17 (2016), p. 174510.

[58] Albert Schmid and Gerd Schön. “Linearized kinetic equations and relaxation processes of a superconductor near T c”. In: *Journal of Low Temperature Physics* 20.1-2 (1975), pp. 207–227.

[59] Sergey Nikolaevich Artemenko, AF Volkov, and AV Zaitsev. “On the excess current in microbridges ScS and ScN”. In: *Solid State Communications* 30.12 (1979), pp. 771–773.

[60] Junren Shi et al. “Proper definition of spin current in spin-orbit coupled systems”. In: *Physical review letters* 96.7 (2006), p. 076604.

[61] AF Volkov, AV Zaitsev, and TM Klapwijk. “Proximity effect under nonequilibrium conditions in double-barrier superconducting junctions”. In: *Physica C: Superconductivity* 210.1 (1993), pp. 21–34.

[62] Y Tanaka, AA Golubov, and S Kashiwaya. “Theory of charge transport in diffusive normal metal/conventional superconductor point contacts”. In: *Physical Review B* 68.5 (2003), p. 054513.

[63] Matthias Eschrig. “Scattering problem in nonequilibrium quasiclassical theory of metals and superconductors: General boundary conditions and applications”. In: *Physical Review B* 80.13 (2009), p. 134511.

[64] D.J. Griffiths. *Introduction to Quantum Mechanics*. Pearson international edition. Pearson Prentice Hall, 2005. ISBN: 9780131118928. URL: `https://books.google.no/books?id=z4fwAAAAMAAJ`.

[65] AF Andreev. “The thermal conductivity of the intermediate state in superconductors”. In: *Sov. Phys. JETP* 19.5 (1964), pp. 1228–1231.

[66] BJ Van Wees et al. “Excess conductance of superconductor-semiconductor interfaces due to phase conjugation between electrons and holes”. In: *Physical review letters* 69.3 (1992), p. 510.

[67] FWJ Hekking and Yu V Nazarov. “Interference of two electrons entering a superconductor”. In: *Physical review letters* 71.10 (1993), p. 1625.

[68] Gary A Prinz. “Magnetoelectronics”. In: *Science* 282.5394 (1998), pp. 1660–1663.

[69] Jacob Linder and Asle Sudbø. “Triplet supercurrent due to spin-active zones in a Josephson junction”. In: *Physical Review B* 82.2 (2010), p. 020512.

[70] Wolfgang Pauli. “Relativistic field theories of elementary particles”. In: *Reviews of Modern Physics* 13.3 (1941), p. 203.

[71] Leonid V Keldysh. “Diagram technique for nonequilibrium processes”. In: *Sov. Phys. JETP* 20.4 (1965), pp. 1018–1026.

[72] Francois Konschelle. “Transport equations for superconductors in the presence of spin interaction”. In: *The European Physical Journal B* 87.5 (2014), pp. 1–19.

[73] Gert Eilenberger. “Transformation of Gorkov’s equation for type II superconductors into transport-like equations”. In: *Zeitschrift für Physik* 214.2 (1968), pp. 195–213.

[74] AI Larkin and Yu N Ovchinnikov. *Nonlinear conductivity of superconductors in the mixed state*. Tech. rep. Inst. of Theoretical Physics, Moscow, 1975.

[75] Jabir Ali Ouassou. *Full Proximity Effect in Spin-Textured Superconductor—Ferromagnet Bilayers*. 2015. URL: `http://www.pvv.org/~jabirali/academic/master/project.pdf`.

[76] Supriyo Datta. *Electronic transport in mesoscopic systems*. Cambridge university press, 1997.

[77] Kaare Brandt Petersen, Michael Syskind Pedersen, et al. “The matrix cookbook”. In: *Technical University of Denmark* 7 (2008), p. 15.